Tunable Synthesis and Characterization of Oleo-Furan Sulfonate Surfactants from Renewable Furan and Fatty Acids

A DISSERTATION
SUBMITTED TO THE FACULTY OF
UNIVERSITY OF MINNESOTA
BY

Kristeen Esther Joseph

IN PARTIAL FULFILLMENT OF THE REQUIREMENTS
FOR THE DEGREE OF
DOCTOR OF PHILOSOPHY

Paul J. Dauenhauer

May 2018

Acknowledgements

First and foremost, I would like to thank my advisor, Paul Dauenhauer, for providing mentorship and opportunity to pursue my interests in science and research engineering. His guidance and motivation has helped me develop over the last five years, a publishable and fruitful research project. Paul's ambitious approach to research, passion and continual motivation are qualities that make him a great advisor, something that I have tried to learn from and hope to extend into the next phase of my life. I have thoroughly enjoyed working with Paul and cannot emphasize enough, the role he has played in my professional development.

I am thankful for the mentorship from Dr. Dae Sung Park, for all the skills that I have acquired from him and without whom this project would not be possible. He has been a patient teacher and a colleague at the same time and I am truly indebted to him for his guidance. I am also thankful for Dr. Omar Ali Abdelrahman and Dr. Anargyros Chatzidimitriou for their constant guidance and research aid during critical times.

I am thankful for all the advice and mentorship I have received over the years from Prof. Dionisios G. Vlachos, Prof. Raul Lobo, Prof. Michael Tsapatsis and Prof. Wei Fan. I am especially thankful for the research assistance provided by Dr Limin Ren, Dr Xiaobing Zuo, Dr. Byeongdu Lee, and Meera Shete.

I am thankful for my senior lab mates throughout my Ph.D.; Dr. Andrew Teixeira, Dr. Christoph Krumm, Dr. Cheng Zhu, and Dr. Alex Paulsen, who have provided technical insight, professional advice and in a lot of cases sighs of relief. I also had the pleasure to work with Katherine Vinter, Saurabh Maduskar, Gregory Facas, Choongsze Lee, Yutong Pang, Costas Papageorgiou, Jonathan Damen, Connor Beech, Deepak Kumar Ojha and Casey Stephenson. I am grateful to them for all the technical discussions, group meetings, lab lunches and milkshake breaks we did together. I

would especially like to thank my lab peers, Katherine Vinter and Saurabh Maduskar, who have been my technical soundboards, my first brainstorming stop and for always offering to help.

I would like to thank all my friends, especially Sajna Hameed, Manjiri Moharir, Meera Shete, Cheng Zhu, and Ashwin Dev for being my extracurricular support, my cooking buddies, my lunch break distractions, my fellow movie geeks and for playing countless other roles in my life outside the lab. Without them, surviving this journey would have been tough.

I would like to thank my parents, M.C Joseph and Anne Joseph, for believing in me and for their continuing support and love throughout my graduate studies and life, and for making everything that I am today possible. I would like to thank my husband, Zubin John for undertaking all the endless trips to be my constant source of encouragement and mental support as well as his family for coming into my life and supporting me in every way possible, to achieve my academic goal and to push myself to be successful.

Finally, I am thankful to the Almighty for providing me with the opportunity and the strength to persevere.

Dedication

This thesis is dedicated to all my friends and family for the constant love, support, and encouragement I received every day without which this would be an unfulfilled dream.

“It is our choices that show what we truly are, far more than our abilities.”

--Albus Dumbledore

Abstract

An important advance in fluid surface control was the amphiphilic surfactant composed of coupled molecular structures (i.e., hydrophilic and hydrophobic) to reduce surface tension between two distinct fluid phases. Surfactants are widely used in household detergents, cleaners, emulsifiers, foaming agents, and personal care products. Anionic surfactants constitute 50% of the $30 billion global surfactant industry and are widely used in household detergents, and personal care products. Linear alkylbenzene sulfonates (LAS) are widely used due to their low cost and high detergency. Current LAS production methods rely on toxic catalysts and petrochemical-based constituents, such as benzene and long chain hydrocarbons. The reaction has low selectivity to the prescribed linear structure thereby rendering minimal control over the desired composition and properties. Additionally, implementation of simple surfactants such as LAS has been hindered by the broad range of applications in water containing alkaline earth metals (i.e., hard water), which disrupt surfactant function and require extensive use of undesirable and expensive chelating additives. Despite growing demand for sustainable cleaning products, most large-volume surfactants are still produced from petrochemical sources, while efforts to make renewable surfactants are primarily focused on synthesizing existing surfactant structures from renewable resources.

In this work, we introduce a new class of surfactants based on the natural structure and chemistry of plant-based oils and sugars with superior function and suitability as a replacement to petrochemicals. Renewable feedstocks such as furans obtained from the sugar, xylose, in biomass and fatty acids obtained from the hydrolysis of triglycerides found in natural oils such as coconut and soybean oil are primarily used for the synthesis. The key chemistry enables selective, single-step acylation of furan with lauric acid or anhydride in the presence of a homogenous co-reactant such as trifluoroacetic anhydride or a heterogenous catalyst such as a zeolite SPP. Fatty acid anhydride which are obtained from the dehydration of fatty acids can also be used as acylating

agents. The results obtained for the reaction of lauric anhydride, based on a C_{12} fatty acid, with furan indicate varying acylation activity results from different pore size, structure, and acidity within zeolites. Brønsted acid zeolites, particularly hierarchical self-pillared pentasil (SPP) was found to be the most active for heterogenous acylation resulting in 91% yield. Preliminary kinetic studies of the indirect acylation using anhydrides provide insight into reaction orders and product inhibition resulting in lowering of catalytic activity. In the second synthesis step following acylation, alkylfuran can be upgraded via several independent and sequential chemistries including hydrogenation, aldol condensation and dehydration and finally subjected to sulfonation to yield surfactant molecules referred to as “oleo-furan sulfonates” (OFS) in high yield. The synthesis of these oleo-furan molecules is highly tunable, where surfactant properties can be selected by using different sources of triglycerides and by coupling various chemistries to obtain a wide range of surfactants possessing different chemical functionalities. It is also selective where the number of carbon atoms in the linear or branched chain can be readily varied without compromising on reaction yields to achieve desired surfactant properties. Evaluation of surfactant performance of three subclasses of OFS revealed linear OFS molecules and OFS mixtures possess hundredfold better detergency and stability in hard water conditions in comparison with petroleum-derived counterparts thereby bypassing the need for chelants. These alkylfuran surfactants independently suppress the effects of hard water while simultaneously permitting broad tunability of size, structure, and function, which can be optimized for superior capability for forming micelles and solubilizing in water.

Contents

List of Tables

List of Figures

List of Schemes

Chapter 1 Introduction

Most chemicals and products are synthesized from petroleum, a limited and soon-depleting resource. Hence, there is an ever increasing need to find a renewable alternative to replace petroleum. One such resource is biomass, a rich source for various organic molecules as precursors to several commodity chemicals such as plastics (**Figure 1-1**).[1,2] Utilization for fuels, products, and power is recognized as a critical component in a nation's strategic plan to address our continued dependence on volatile supplies and prices of imported oil.[3] Production of chemicals from biomass offers a promising opportunity to reduce the dependence on oil as well as to improve overall economics and sustainability. Even though the production of chemicals constitutes only 15% of the entire oil consumption, it accounts for nearly 50% of the profits. More importantly, the chemical industry accounts for 30% of the global industrial energy demand and is responsible for 20% of the industrial greenhouse gas emissions.[4] Therefore, there are clear opportunities to positively impact overall sustainability and economics by targeting bio-derived chemicals.[5] Bio-based chemicals have been increasingly displacing petroleum derived products and currently they displace about 300 million gallons of petroleum each year equivalent to taking 200,000 cars off the road. The biochemical market is projected to reach 19.7 billion USD by 2030.[6] A major incentive in using biomass as a chemical resource is the value upgradation in converting a cheap resource like biomass ($0.10/$lb_m$-carbon) to a high volume-commodity chemical such as plastics ($0.50/$lb_m$-carbon) or specialty chemicals such as surfactants ($0.90/$lb_m$-carbon).

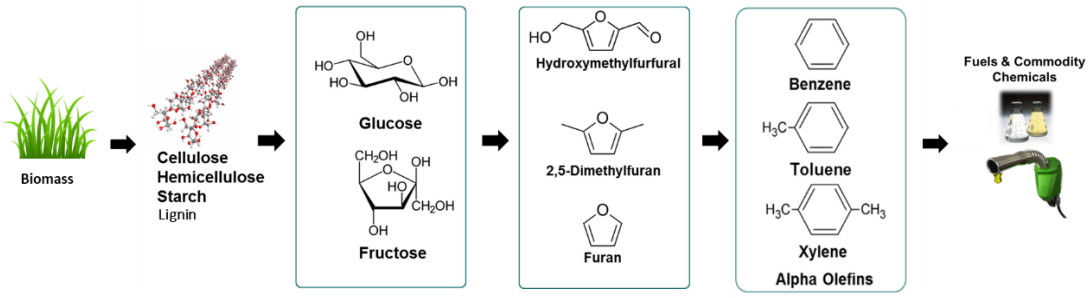

Figure 1-1. Biomass conversion to fuels and chemicals via molecule upgradation

Surfactant chemicals are widely used in cleaning products, oil spill remediation, and even agricultural products, with precise structures tuned for each application.[7] Despite years of technology development, most large-volume surfactants are made from petrochemical sources, while efforts to make renewable surfactants are focused on making existing surfactant structures from renewable sources. More recently, a new surfactant based on the natural structure and chemistry of plant-based oils and sugars has demonstrated superior function and suitability as a replacement to petrochemicals.[8] The word "surfactant" is derived from the term "Surface Active Agent." The unique molecular structure of a surfactant, which consists of a hydrophobic chain coupled to a hydrophilic moiety, enables reduction in surface or interfacial tension and imparts detergency, wetting, emulsifying, dispersing, and foaming properties to liquids.[9] This makes surfactants a key ingredient in laundry detergents, cleaning products, cosmetics, personal care products, industrial solvents, and agrochemicals.[10] In detergents and cleaning products, their function is to remove soil (oil, grease, dust etc.) from solid surfaces and to keep it in suspension in the wash solution, preventing re-deposition. Household detergents primarily comprised of surfactants like linear alkylbenzene sulfonate (LAS) constitute over 50% of the global surfactant market, which is currently estimated at $30 billion.[11–13] This market is projected to reach $40 billion and 22,800 kilo tons by 2020 at a growth rate of 2.5% (**Figure 1-2**). Specifically, in the US, this number is estimated to be around 5000 kilo tons and $14.4 billion. 83-87% utilization of LAS is in

the household detergent industry.[14] Heavy duty laundry liquids dominated the global LAS market and accounted for over 32.7% of the total demand in 2013.[15]

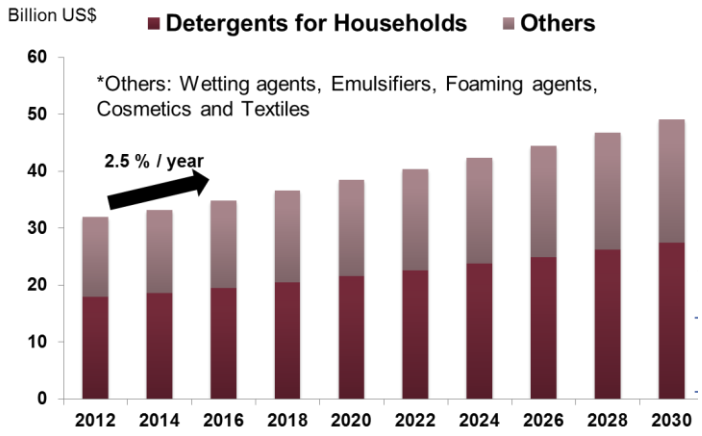

Figure 1-2. Growth of detergents market within the surfactant industry

Current high-volume surfactant molecules are commonly made from petrochemical carbon sources such as benzene, alpha-olefins, and ethylene. Efforts to reduce reliance on fossil fuels have resulted in oleochemical analogues, which primarily use coconut oil, palm kernel oil, or algal oils for surfactant synthesis. The growing emphasis on products made from renewable carbon sources is evidenced by the development of programs such as the US Department of Agriculture Bio-preferred Product award and the US Environmental Protection Agency Design for the Environment certification. Still, cost is a major limitation for plant-based surfactants. Nearly all green products come with a premium price tag. As a result, green cleaners have managed only 3% market penetration, even though over 95% of consumers say they would purchase green products if they were cheaper, according to Packaged Facts.[16] The challenge for oleochemical surfactants to compete with petrochemicals is further increased by their performance market.[17] LAS is commercially made via sulfonation of linear alkylbenzene (LAB) with SO_3-air or SO_3 in sulfuric acid mixtures.[18–20] Linear alkylbenzene (LAB), a key monomer of LAS, relies on petrochemical routes and is industrially produced via alkylation of benzene with alpha-olefins, particularly 1-

dodecene, over corrosive and toxic acid catalysts such as HF or $AlCl_3$ catalyst. Alkylation chemistry used in commercial surfactant production yields a broad distribution of structures, which limits the application-specific engineering of surfactant molecules to achieve desired properties. The reaction is not selective towards the desired product rendering minimal control over desired surfactant properties. During alkylation of benzene, isomers ranging from 2-phenyl to 6-phenyl LAB are produced except for 1-phenyl LAB due to formation of a carbonium cation on the beta position in alpha-olefins by protonation from acid catalysts.[21–23] Among the isomers, 2-phenyl LAB is the most biodegradable and exhibits the highest detergency.[24,25] As a result, a major research focus has been to improve selectivity toward the desired 2-phenyl LAB product and to transition production methods from homogeneous catalysts to solid acid catalysts.[22,26] Though selective production of 2-phenyl LAB is desirable, a major drawback of this surfactant is its high Krafft temperature, making it only moderately soluble in hard and cold water.[27] The 2-phenyl isomer exhibits a high packing factor in a crystal lattice due to the terminal-located phenyl group in the straight alkyl chain. This leads to strong interaction between molecules, resulting in a high Krafft temperature.[25,28] For this reason, 2-phenyl LAB needs a lot of builders, such as, phosphate, sodium carbonate and sodium silicate to increase its solubility; an increase in usage of the builders directly affects the price and efficiency of the detergents.

Additionally, large-volume oleochemical surfactants, such as sodium lauryl sulfate (SLS) have limited performance compared with petrochemical analogues, such as LAS, especially in hard water conditions; calcium and magnesium ions in hard water bind to the surfactant causing it to precipitate from the solution. About 85% of the water in the United States is hard (>200 ppm of Ca^{2+}) and unsuitable for direct use with surfactants (**Figure 1-3**).[29] As a result, formulators of detergents incorporate costly co-formulated chelating agents (phosphates, ethylenediaminetetraacetic acid, among others) that preferentially bind to the ions to mitigate the

effects of hard water and improve performance.[30] This drawback necessitates the use of chelants as additives when using LAS in a formulation, as the chelants trap ions in hard water to ensure minimal interference of Ca^{2+} in surfactant performance. In a conventional detergent formulation, 10-30% of the bulk is comprised of surfactant and 6-22% consists of chelating agents thus constituting a major chunk. Such chelants are expensive, and many are banned due to their detrimental impact on the environment.[31,32]

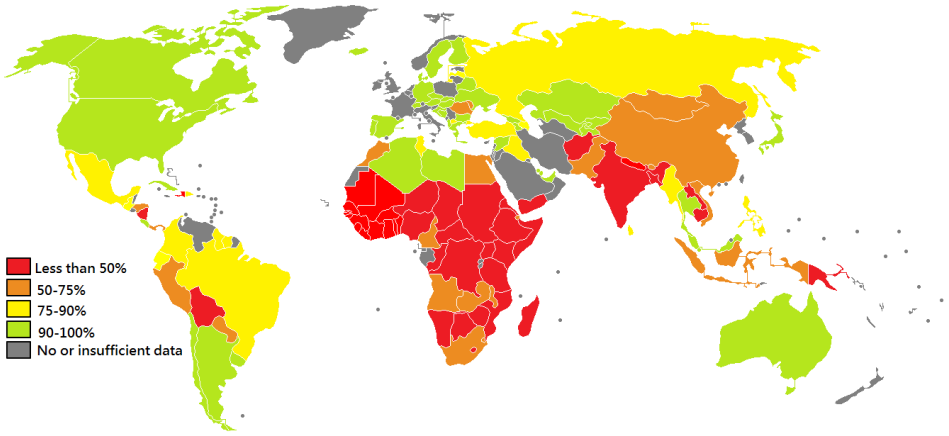

Figure 1-3. Global hard water treatment capabilities[29]

Petroleum dependence, limited selectivity and tunability of commercial surfactants, coupled with the use of expensive and toxic chelating agents drive the need to find bio-renewable surfactants with improved properties. It is imperative for surfactant manufacturers to phase out petroleum-based surfactants and look for cleaner, superior renewable alternatives.

Chapter 2 Thesis Scope and Objectives

There have been growing concerns about the environmental impact of the existing surfactant technology and additives used in detergent formulations. To address drawbacks associated with the commercial LAS surfactant, we propose a sustainable technology for producing benign, bio-renewable oleo-furan surfactants (OFS) with improved detergency, solubility, and exceptional stability in hard water conditions. The global trend has shown inclination towards products that possess improved efficiency, greater safety, sustainability and multifunctionality. This trend will favor superior specialty products that are derived from biomass at the expense of commodity products such as LAS.[25] The driving force for synthetic, petroleum-derived surfactants is their ready availability and low price, whereas the market for bio-based surfactants is driven by increasing consumer awareness of ecological benefits, and the availability of a wide variety of raw materials.[33,34] Governments and regulatory bodies are promoting bio-products through subsidies. Consumers are ready to incur extra cost to get 'green' products. To make significant progress, the goal should be to develop superior products through economic and sustainable routes. Superior bio-products will incentivize further development efforts to make these sustainable products economically viable and competitive against existing fossil-based commercial products.[35]

The bio-based detergent and cleaners market is currently at 3% of the total global retail market.[36] A study from Packaged Facts showed that, globally, the sale of bio-cleaners doubled from $303 million in 2007 to $640 million in 2017.[37] Another study by Frost & Sullivan in 2014 showed that in Asia-Pacific, synthetic, petroleum-derived surfactants dominated the total surfactant market by 70.1% while the remaining 29.9% comprised of bio-surfactants.[38] This market revenue is expected to grow at a CAGR of 8.9% from 2011 to 2018 emphasizing on the potential for a huge market growth. **Figure 2-1** demonstrates the market share of various surfactants based on the source of raw material, 50% of this market is captured by molecules that are entirely made from petroleum

while only 7% of the surfactants are truly 'green' or in other words entirely renewably sourced.[39] This low market share is explained by the fact that current biomass-based surfactants fail to compete in performance when compared to their petrochemical counterparts.[40–42] Although renewable surfactants made from oleochemical feedstock have been developed and are used in household detergents, their capacity is still too low to be utilized in the large market of detergents due to their high cost and low detergency.[43] Commercially available bio-based detergents, despite being sustainable have certain limitations. Sodium Lauryl Sulfate (SLS) is a common surfactant used in bio-detergents.[44,45] While SLS has good low temperature solubility, it has a critical micelle concentration (CMC) value 3-4 times higher than that of LAS necessitating the use of four times the amount of surfactant in the same detergent formulation.[8] SLS was also found to possess extremely poor hard water stability (**Chapter 4**). The high CMC values and poor hard water stability for SLS makes the bio-based green alternatives barely efficient when compared to LAS.

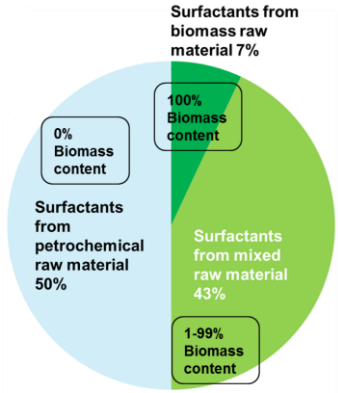

Figure 2-1. Surfactants based on the types of raw materials (% market volume)[39]

Recently, attempts have been made toward developing a furan-based surfactant.[46–48] Furan-based surfactants have more hydrophilicity and solubility than benzene due to the oxygen atom in aromatic ring. We propose a sustainable technology for producing benign, bio-renewable oleo-furan surfactants (OFS). We design a new renewable pathway to produce surfactants made from biomass-derived feedstocks, such as furan and fatty acids such as lauric acid. Furan is a five-

membered aromatic heterocycle that can be produced from the decarbonylation of furfural. Furfural is a biomass-derived chemical, which is produced from the acid-catalyzed dehydration of xylose, a hydrolysis product from the hemi cellulosic component of biomass. Lauric acid is a saturated fatty acid, which is produced via the hydrolysis of biomass-derived triglycerides in palm-kernel oil and coconut oil. The reaction platform consists of a highly selective furan acylation reaction as an alternative to benzene alkylation. The furan acylation reaction bonds a selected hydrophobic alkyl moiety to a furan molecule. This is followed by additional reactions such as hydrogenation and aldol condensation which can be subsequently functionalized with a hydrophilic group to form a surfactant. This work reveals a new renewable surfactant that boasts hundred times greater hard water stability, eliminating the need for chelating agents.[8,49] The result could make bio-renewable detergent formulations even cheaper than their petrochemical counterparts. OFS provide advanced properties made possible through the molecular structure of biomass-derived chemicals. They were developed to replace conventional detergent molecules like LAS, which combine hydrophilic sulfonate functionality with a hydrophobic alkyl chain using a benzene linker. Alternatively, the OFS structure utilizes a polar furan linker, which changes the characteristics of the sulfonate and stabilizes the formation of micelles relative to conventional LAS.

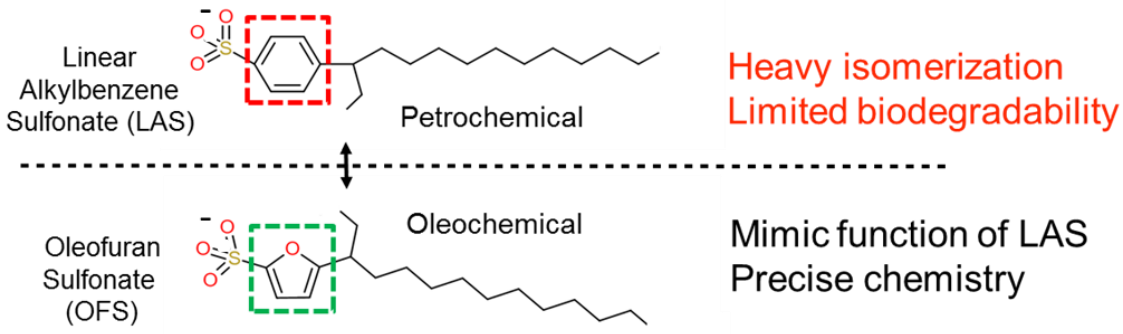

Figure 2-2. Comparison of conventional LAS surfactants and biomass-derived OFS surfactants

The molecular structure of a surfactant determines its efficacy and drives its properties; addition of carbons or branching in the linear hydrophobic chain can have dramatic effects on surfactant performance. Incorporation of functionalities or additional substituents greatly affect properties and hence final applications (**Figure 2-3**). For example, adding or removing a carbon atom in the long hydrophobic tail can positively influence a surfactant property such as critical micelle concentration while negatively affecting another such as Krafft point.

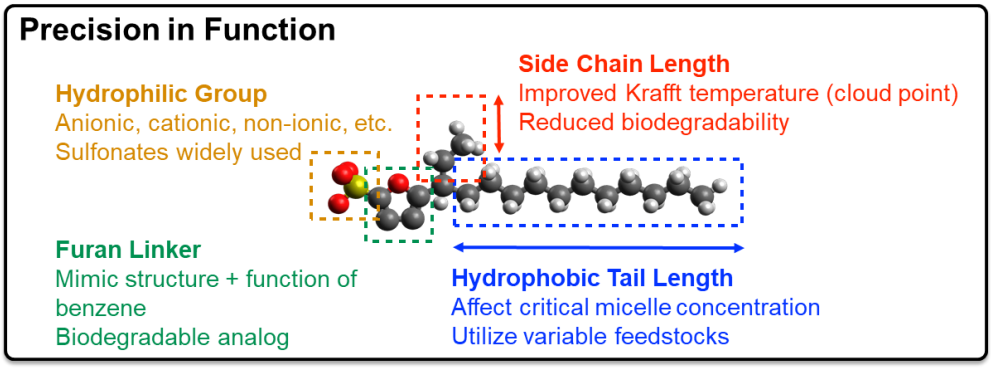

Figure 2-3. Structure-Property relationships of oleo-furan surfactants

Chapter 4 of this thesis undertakes the study of evaluation of structure-property relationships of surfactants synthesized via acylation of furans. We also look at dehydration chemistries that allow synthesis of potential surfactant precursors for gemini surfactants in Chapter 5. The OFS platform enables synthesis of renewable surfactants with superior properties using a plethora of catalytic chemistries. We propose the synthesis of a renewable LAS substitute with enhanced stability in hard water, overcoming the need for toxic and expensive chelating agents via the coupling of reaction chemistries and performance evaluation.

Chapter 3 Renewable Furan & Fatty Acids to OFS Surfactants

3.1 Introduction

The surface energy of droplets, bubbles, and foams determines the efficacy of applications in food,[50] agriculture, cleaning,[51] and drug delivery[52,53] and can be optimized for each use by chemical surfactants. Many approaches to surfactant design have utilized commodity chemicals to provide both hydrophilic (water engaging) and hydrophobic (oil engaging) functionality from low-cost feedstocks. The use of surfactants with eight to eighteen saturated carbon atoms combined with a polar function has been particularly useful within aqueous systems,[51] as the carbon chains aggregate into micelles that can trap oils or stabilize active ingredients within water. This approach has worked in soap and detergent technologies for over a century, but modern variations of these surfactants based on fossil fuel precursors exhibit performance limitations inherent to their molecular structure.[27,54] The largest volume surfactant for aqueous applications such as detergency remains linear alkylbenzene sulfonate (LAS). LAS chemicals are composed of a benzene ring connecting polar functionality (e.g., $Na^+SO_3^-$) with branched alkyl chains (eight to fourteen carbons). These surfactants are produced by alkylation of benzene with alpha olefins such as 1-dodecene; by this method, acid catalysts protonate the olefin leading to double bond migration and various alkylbenzene isomers such as 2-phenyl- to 6-phenyldodecane.[11,55–57] The surfactant is then prepared by reacting alkylbenzene precursors with SO_3–air or SO_3 in sulfuric acid mixtures.[18] In this work[8,58,59], we replace the benzene moiety of LAS with biomass-derived furans[60] to link polar and hydrophobic alkyl chains from the fatty acids of natural oils[61] to form new oleo furan sulfonate (OFS) surfactants, shown in **Figure 3-1**. Furan and its derivatives can be synthesized from the xylose, a monomer found in the hemi cellulosic component of biomass while fatty acids are obtained in abundance

from the hydrolysis of triglycerides found in natural oils. Surfactant synthesis occurs by precise furan acylation using heterogeneous catalysts and systematic tuning of the molecular structure via incorporation of branching, polarity, and variable chain length.

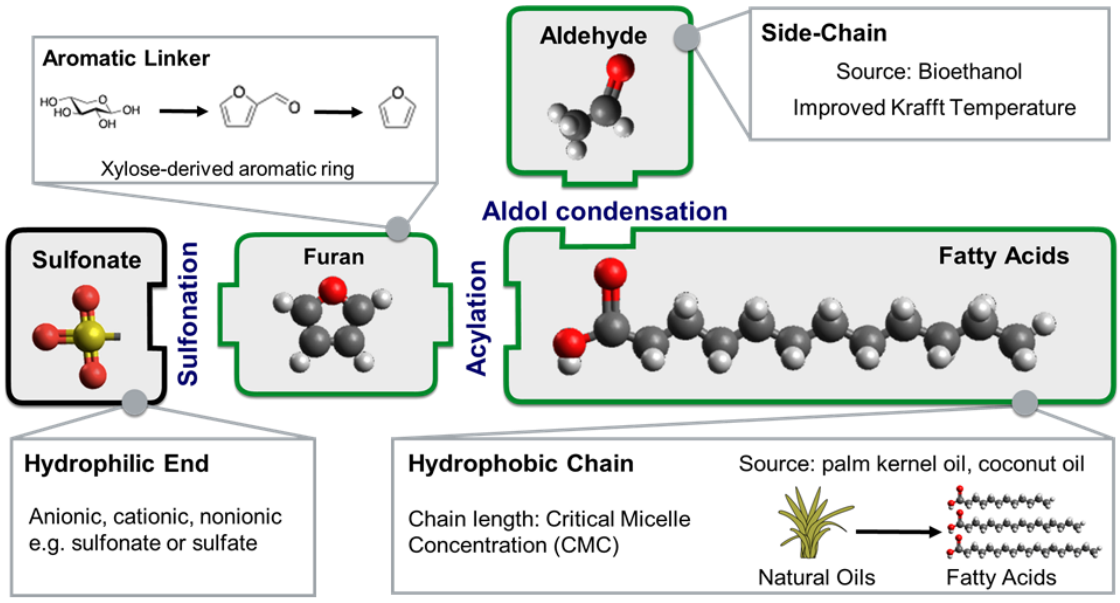

Figure 3-1. Preparation of OFS utilizes selective addition of hydrophobic alkyl-chain tails with or without added branching to furan linkers connected to hydrophilic heads such as sulfonates

3.2 Materials and Methods

3.2.1 Chemicals

Hexane (95 %), Furan (99 %), and Trifluoroacetic anhydride (99 %) were purchased from Sigma-Aldrich. The saturated fatty acids, lauric acid (C_{12}, 99 %, Acros), myristic acid (C_{14}, 99 %, Sigma-Aldrich), stearic acid (C_{18}, 95 %, Sigma-Aldrich), and cocinic acid (mixture of fatty acids, C_8~C_{18}, BOC Sciences) were used in furan acylation for the first step in overall reaction pathway. The reference standards, 2-n-heptylfuran (98 %) and 2-n-dodecylfuran (95 %) were purchased from Alfa Aesar and MP Biomedical, respectively. Lauric anhydride (98 %, TCI Chemicals) was also used for furan acylation with solid acid

catalysts. H-BEA catalyst (CP814E, SiO_2/Al_2O_3 = 25) and copper chromite catalyst were obtained from Zeolyst and Sigma-Aldrich, respectively. The H-BEA was calcined at 550 ℃ for 12 h at the rate of 1 ℃ min^{-1} in a tube furnace under air flow. The reduction of copper chromite was carried out at 300 ℃ for 3 h under 10 % H_2/Argon flow.

3.2.2 Zeolite Synthesis Methods[1]

Several types of self-pillared zeolites, Al/Sn-SPP and Al/Sn-MWW were used as catalysts in furan acylation with anhydride after calcination at 500 ºC for 4 h.

a. Sn-MWW synthesis. Sn-MWW was synthesized by modifying an existing literature method.[62] First, B-MWW precursor was de-boronated by 6M HNO_3 (1 g zeolite/ 50 ml HNO_3) at 100 °C under reflux for 1 day, this procedure was performed twice. Then 2.5 g of the de-boronated sample was mixed with 30 g of distilled water and 3.549 g of piperidine (99 %, Aldrich). After stirring for 1 hour, 0.146 g of tin tetrachloride pentahydrate ($SnCl_4 \cdot 5H_2O$, 98 %, Aldrich) was added into the above mixture and stirred for 2 hours. Then the final gel with chemical composition $1SiO_2$: 0.01 SnO_2: 1.0 piperidine: 40 H_2O was transferred to an autoclave and hydrothermally treated in a rotation oven at 170 °C for 14 days. The products were separated and fully washed by filtration and then dried at 70 °C overnight. Calcination of this sample was performed in static air at 580 °C for 10 hours.

b. Sn-SPP synthesis. First, 0.129 g of tin tetrachloride pentahydrate ($SnCl_4 \cdot 5H_2O$, 98 %, Sigma-Aldrich) was dissolved into 7.35 g of tetra(n-butyl)phosphonium hydroxide (TBPOH, 40 wt%, TCI America) followed by the addition of 7.5 g of tetraethyl orthosilicate (TEOS, 98 %, Sigma-Aldrich). After hydrolysis, 3.2 g of deionized water

[1] Performed by Dr. Limin Ren

was added to the mixture. The mixture was stirred overnight, and a clear sol was obtained. The composition of the final sol was: 1.0 SiO_2 : 0.03 TBPOH : 4.0 EtOH : 30H_2O : 0.01SnO_2. The sol was sealed in a Teflon-lined stainless-steel autoclave and hydrothermally treated in a pre-heated static oven at 115 °C for 5 days. The solid products were centrifuged, washed with distilled water, and then dried at 70 °C overnight and calcined at 550 °C for 6 h in air under static conditions. The calcined samples were washed again with water, dried at 70 °C overnight and calcined at 550 °C for 6 h in air under static conditions and this process was repeated to ensure removal of P_2O_5.

c. **Al-MWW synthesis.** Al-MWW was synthesized according to a literature method.[63] First, 0.72 g of sodium aluminate (MP Biomedicals, USA) and 2.48 g of sodium hydroxide (98.5 %, Sigma-Aldrich) were dissolved in 311 g of distilled water. Then, 19.1 g of hexamethyleneimine (HMI) (Aldrich) was added to the mixture and stirred for 30 min. Subsequently 23.6 g of fumed silica (Cab-o-sil M5) was added to the mixture and stirred overnight. The homogeneous gel was sealed in Teflon-lined stainless-steel autoclaves and heated at 135 °C for 11 days. The products were separated and fully washed by filtration followed by drying at 70 °C overnight, then calcined at 580 °C in static air for 10 hours.

d. **Al-SPP synthesis.** 0.098 g of Aluminum isopropoxide (Sigma-Aldrich) was mixed with 3.23 g of distilled water and 7.35 g of tetra(n-butyl)phosphonium hydroxide solution (TBPOH, 40wt %, TCI America). The mixture was added to 7.5 g of tetraethyl orthosilicate (TEOS, Sigma-Aldrich) and stirred overnight. The sol was sealed in a Teflon-lined stainless-steel autoclave and hydrothermally treated in a pre-heated static oven at 115 °C for 5 days. The solid products were centrifuged, washed with distilled

water and then dried at 70 °C overnight and calcined at 550 °C for 6 h in air under static conditions.

e. **Ion exchange to obtain the proton form Al-zeolites.** Typically, ion exchange was performed by stirring Al-zeolites with 1M ammonium nitrate (NH_4NO_3, Sigma-Aldrich) solution (1g zeolite + 100 ml NH_4NO_3 solution) at 80 °C for 5h. After the stirring, zeolites products were centrifuged, washed with distilled water and then dried at 70 °C overnight and calcined at 500 °C for 4 h in air under static conditions. The whole procedure was performed twice for complete ion exchange.

f. **Mg-Zr-O synthesis.** The mixed oxide, Mg-Zr-O, catalyst was synthesized by sol-gel method. 0.01 mol of magnesium nitrate (Sigma-Aldrich, 99 %) and 0.009 mol of zirconyl nitrate (Sigma-Aldrich, 99 %) were mixed in DI water at room temperature. NaOH was added to the mixtures until the pH was 10, and the slurry was aged at room temperature for 72 h. The slurry was filtered and washed with DI water, and then, dried at 110 ^oC for 24 h. The catalyst was then calcined at 600 ^oC for 3h before being used for aldol-condensation reaction.[64]

g. **K-BEA and K-Y synthesis.** K-BEA and K-Y zeolites were prepared by typical ion-exchange method. 2.5 g of zeolite (H-BEA or H-Y) was added to 0.6 M solution of KNO_3 (Sigma-Aldrich, 99 %). The mixture was aged at 70 ^oC for 10 h with vigorous stirring in a round bottom flask connected with a condenser. After filtration and washing with DI water, the powder was dried at 100 ^oC for 24 h and calcined at 500 ^oC for 4 h.[65]

3.2.3 Oleo-Furan Sulfonate Synthesis Methods

a. Preparation of OFS-n-1/O: Acylation

The acylation of furan to produce 1-(furan-2-yl)alkan-1-one can be done in multiple ways using fatty acids or fatty acid anhydrides as the acylating agent along with homogenous and/or heterogenous catalysts and co-reactants at varying temperature and pressure conditions. In one set of experiments, trifluoroacetic anhydride was used as a co-reactant/catalyst along with Al-BEA. In a typical reaction, a 1:1:2 molar ratio of furan (0.014 mol) to fatty acid to TFAA was dissolved in 10 ml n-hexane to which 0.2 g of Al-BEA zeolite was added. A twelve-carbon fatty acid, namely lauric acid was used as the acylating agents for these experiments. The reaction was carried out in a 100 ml, high pressure, high temperature Parr benchtop reactor (model 4598HTHP with a 4848-temperature controller). The reactor was sealed and purged with nitrogen twice to remove any residual of air and then pressurized to 200 psi using nitrogen. The temperature was varied from 25 – 150 ℃ (298 – 423K) with a stirring of ~1000 rpm across multiple experiments with a reaction time of 6 h. Tridecane (0.002 mol) was used as an internal standard to enable reactant and product concentration quantification in a Gas Chromatogram.

In another set of experiments, acylation was conducted at room temperature (25 ℃, 298K) and atmospheric pressure in a 20 ml glass scintillation vial containing furan, fatty acid and TFAA in 6 ml n-hexane (**Scheme 3-1**). Fatty acids containing twelve, fourteen and eighteen carbons (lauric, myristic and stearic acid, respectively) as well as a mixture of eight to eighteen carbon atom fatty acids, namely cocinic acid (see **Figure 3-2**) were used for acylation. The ratio of furan to fatty acid to TFAA was varied to achieve the highest yield. Acylation using this method was also performed

on 2-methylfuran and 2,5-dimethylfuran using a furan derivative to lauric acid to TFAA ratio of 1:1.3:1.

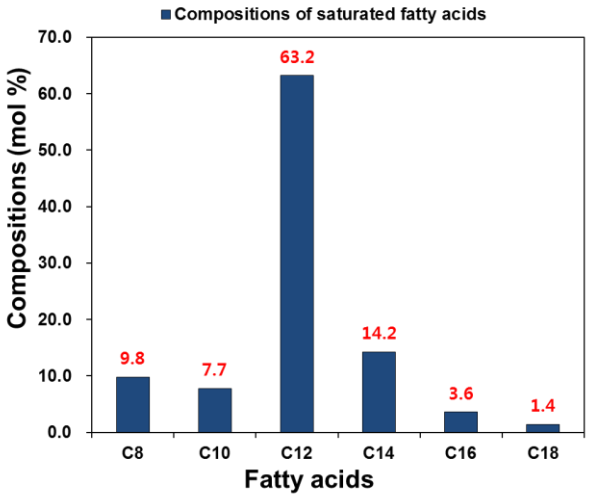

Figure 3-2. Composition of the saturated fatty acids in standard cocinic acid quantified by GC-FID, unsaturated C_{18} fatty acid : < 3 mol %

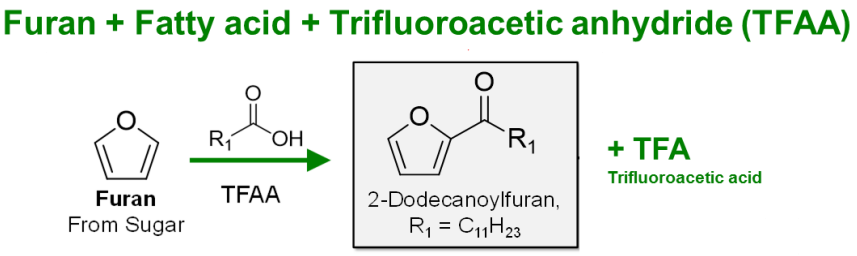

Scheme 3-1. Homogenous acylation reaction between furan and lauric acid using trifluoroacetic anhydride (TFAA)

Alternatively, acylation was carried out using fatty acid anhydride (lauric anhydride) as the acylating agent (**Scheme 3-2**). In a typical experiment, the Parr reactor was charged with a 1:1 mixture of furan to fatty acid anhydride (0.014 mol), 0.002 mol tridecane (internal standard) in 15 ml of hexane as the solvent and 0.2 g of the catalyst was loaded into a 100 ml Parr reactor. The sealed reactor was purged with nitrogen twice to remove the residual air in the reactor and then pressurized to 200 psi to keep the reactants in the liquid phase. Various Lewis and Brønsted acid zeolites such as Al-

BEA, Al-MWW, Al-SPP, Sn-BEA, Sn-MWW and Sn-SPP were tested for their activity at 180℃ (453K) over a period of 5 h under a vigorous stirring of ~ 1000 rpm. At the end of 5 h, the reactor was cooled to room temperature and the gas in the head space was vented before sampling.

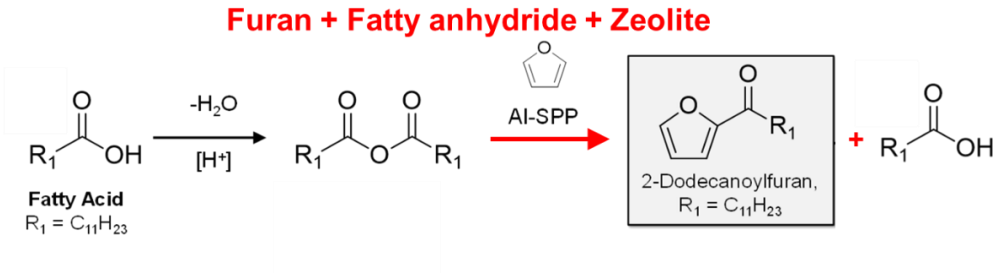

Scheme 3-2. Heterogenous acylation reaction between furan and lauric anhydride using solid acid zeolites such as Al-SPP

The selectivity of 1-(furan-2-yl)alkan-1-one was calculated by dividing the moles of 1-(furan-2-yl)alkan-1-one produced with the moles of furan reacted. The final surfactant OFS-n-1/O was prepared according to the method detailed in (**d**) which can be found later in this Section.

b. Preparation of OFS-n: Hydrodeoxygenation

2-Alkylfuran was synthesized from 1-(furan-2-yl)alkan-1-one via hydrodeoxygenation in a 100 ml Parr reactor charged with 1-(furan-2-yl)alkan-1-one (reactant, 2ml), n-tridecane (internal standard, 0.5 ml), hexane (solvent, 30 ml), and 0.5 g of $2CuO.Cr_2O_3$ (copper chromite) catalyst (**Scheme 3-3**). In certain experiments, the catalyst was pre-reduced in a hydrogen atmosphere (10% H_2 in Ar) at 300 ℃ for 3 h followed by passivation using 5% Oxygen/Helium at 35 ℃ for half an hour. The reactor was sealed and purged twice using nitrogen to remove any residual air followed by a hydrogen purge. The reactor was then pressurized using hydrogen pressures between 100 – 350 psi at the desired reaction temperature (180 – 220 ℃) under vigorous stirring of 1000

rpm. Time on-stream data was collected using the double-valve sampling block connected to the Parr reactor. At the end of the reaction time (3 - 5 h), the reactor was finally cooled and vented before taking the final time sample. The selectivity of 2-alkylfuran was calculated by dividing the moles of 2-n-alkylfuran formed by the moles of 1-(furan-2-yl)alkan-1-one reacted. The final surfactant OFS-n was prepared according to the method detailed in (**d**) which can be found later in this Section.

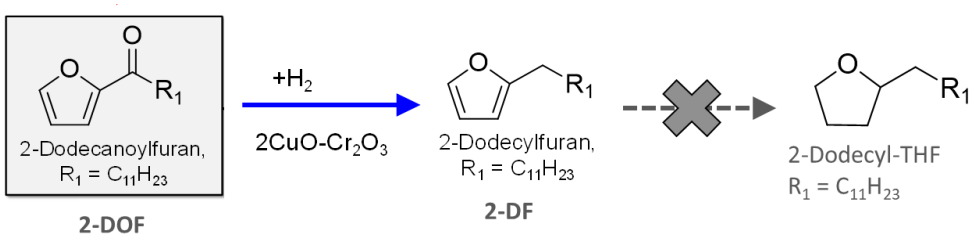

Scheme 3-3. Hydrodeoxygenation of 1-(furan-2-yl)dodecan-1-one i.e. 2-dodecanoylfuran to form 2-dodecylfuran

c. Preparation of OFS-12-2/C2H5: Aldol Condensation & Hydrogenation

The twelve carbon 1-(furan-2-yl)alkan-1-one, 2-dodecanoylfuran (DOF) was reacted with acetaldehyde via the aldol condensation reaction followed by hydrodeoxygenation and hydrogenation to synthesize the mono-ethyl branched surfactant monomer (m-DF, **Scheme 3-4**). A 100 ml Parr reactor was charged with DOF (reactant, 0.0054 – 0.01 mol), acetaldehyde (reactant, 0.0054 – 0.054 mol), hexane (solvent, 20 ml) and 0.2 g of solid acid/base catalysts. For the purposes of quantification, tridecane (0.02 mol) was used as an internal standard. The reactor was sealed and purged with nitrogen to remove any residual air and pressurized to 200 psi to minimize vaporization of acetaldehyde and heated to temperatures between 180 – 220 ℃ under vigorous stirring (1000 rpm). At the end of the reaction time (6 - 48 h), the reactor was cooled and vented before taking the final time sample. Post

purification, the mixture of unreacted DOF and aldol-product (Al-DOF) was then subject to hydrogenation and hydrodeoxygenation to m-DF. The reduction of the ketone and the double bond was achieved in a 100 ml Parr reactor at 220 ℃ and 100 psi of hydrogen for 7 h using unreduced $2CuO.Cr_2O_3$ (copper chromite) as the catalyst to produce m-DF. The reactor was fed with the reactant mixture (DOF + Al-DOF, 2ml) and hexane (solvent, 30 ml), sealed and purged twice using nitrogen to remove any residual air followed by a hydrogen purge. Time on-stream data was collected using the double-valve sampling block connected to the Parr reactor. The final surfactant OFS-12/C2H5 was prepared according to the method detailed in (**d**) which can be found later in this Section.

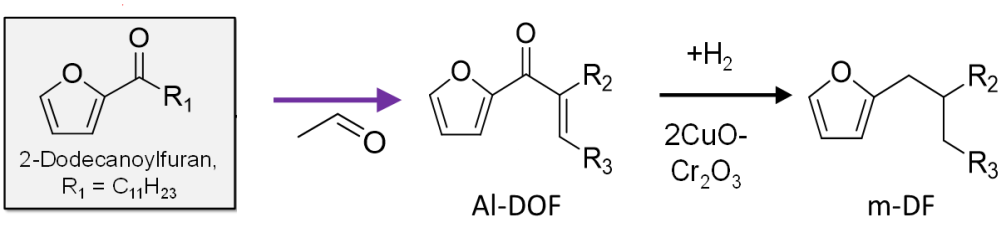

Scheme 3-4. Sequential aldol condensation and hydrogenation/hydrodeoxygenation of 2-dodecanoylfuran to form m-DF ($R_1 = R_2$ + C (carbon), $R_3 = CH_3$ for acetaldehyde)

d. Sulfonation

All surfactant precursors synthesized under **Section 3.2.3**, **(a)-(c)**, namely, 1-(furan-2-yl)alkan-1-one, 2-alkylfuran, Al-DOF, and reference standards such as 2-n-heptylfuran, were sulfonated and neutralized to make oleo-furan sulfonate surfactants (OFS-n, OFS-n-1/O, OFS-12-2/C2H5) by combining two existing methods as listed below.[47,66,67] The synthesized precursor (13 mmol) was added to a slurry of sulfur trioxide-pyridine complex (13 mmol) in anhydrous acetonitrile (12 ml). The mixture was stirred at room temperature for 3 days in a glass beaker sealed with aluminum foil.

At the end of 72 h, 40 ml of water at 70 ℃ was introduced to the slurry, and the slurry was stirred for 1 h. The slurry was then fed to a separatory funnel for phase separation and left for 24 h. The aqueous phase was then separated using a separatory funnel, and the aqueous solution was neutralized by using sodium carbonate till the pH of the solution was 7.0. The water was then evaporated off and the crystalline phase was collected by filtration and washed five times using 50 ml iso-propanol for each wash at 60 ℃.

3.2.4 Separation and Purification Methods

a. Separation of 1-(furan-2-yl)alkan-1-one

1-(Furan-2-yl)alkan-1-one (lauric, myristic, stearic and cocinic) synthesized via the TFAA method at room temperature (**Section 3.2.3 (a)**) was purified using a rotary evaporator for use in other reactions. A Hei-VAP/G5 Heidolph rotary evaporator equipped with a liquid nitrogen/dry ice condenser was used for concentration and purification of the reaction mixture. The boiling points of the various compounds used or produced in the reaction using lauric acid as the acylating agent are listed in **Table 3-1**. To enable ease of separation, the ratio of furan to fatty acid to TFAA was 1:0.8:1.3 such that lauric acid becomes the limiting reagent to enable ease of separation during purification. Several batch reactions were conducted without the internal standard chemical (n-tridecane) to collect the product mixture. The rotary evaporator was operated at room temperature for 30 min under high vacuum to remove the light molecules (hexane, furan, trifluoroacetic anhydride and trifluoroacetic acid). The remaining mixture was further concentrated at 70 ℃ for 2h under high vacuum and then left on a hot plate at 100 ℃ overnight before use.

Table 3-1 Boiling points at 1 atm of various compounds used and generated in the acylation reaction employing TFAA and lauric acid

Compound	Boiling Point (°C)
Furan	31.3
Trifluoroacetic anhydride (TFAA)	39.2
Hexane	68.0
Trifluoroacetic acid (TFA)	72.4
Lauric acid	298.8
2-Dodecanoylfuran	>300.0

b. Separation and purification of 2-alkylfuran

The catalyst was first separated from the reaction mixture by filtering the mixture using a syringe filter (Millipore-Millex-FG hydrophobic PTFE, 0.2 μm). The products obtained after hydrodeoxygenation were then concentrated by using a rotary evaporator (Hei-VAP/G5 Heidolph) followed by flash chromatography. The rotary evaporator was operated at 50 °C for 1 h under vacuum to evaporate the solvent hexane and other light molecules. Further purification was done by flash chromatography[68,69] using a 12-inch length and 1-inch diameter column (CG-1189-07) packed with silica gel (230-400 mesh, particle size 40-63 μm). Hexane was used as the mobile phase to separate 2-dodecylfuran (2-DF, **Scheme 3-3**) from the product mixture, and a 50% acetone in hexane solution was used as the eluent to remove undesired products (e.g. 2-dodecyl-THF, **Scheme 3-3**). The eluent hexane was then removed, and the purified 2-DF was concentrated at 70 °C for 2 h under high vacuum.

c. Separation and purification of Al-DOF

Post filtration to aid catalyst removal, unreacted 2-dodecanoylfuran (2-DOF) and aldol-product (Al-DOF), were concentrated from the reaction mixture using a rotary evaporator (Hei-VAP/G5 Heidolph) equipped with a liquid nitrogen condenser at 50 °C for 1 h under vacuum to evaporate the solvent hexane and other light molecules.

The mixture of 2-DOF and Al-DOF was further purified via flash chromatography using a 1-inch diameter glass column, and 1,2-dichloroethane as the eluent to separate the desired products (DOF and Al-DOF) from all other impurities present. The eluent was then removed, and the purified mixture was concentrated at 70 ℃ for 2h under high vacuum and was thereafter left on a hot plate at 100 ℃ overnight.

During the process of separation and purification, the ratio of unreacted 2-DOF to Al-DOF changed from 77:23 to 70:30 due to losses during flash chromatography.

d. Separation and purification of m-DF

After removing the catalyst by filtration, the products obtained after hydrogenation/hydrodeoxygenation were first concentrated by using a rotary evaporator (Hei-VAP/G5 Heidolph) followed by flash chromatography. The rotary evaporator was operated at 50 ^{o}C for 1 h under vacuum to evaporate the solvent hexane and other light molecules. Further purification was done by flash chromatography using a 12-inch length and 1-inch diameter column (CG-1189-07) packed with silica gel (230-400 mesh, particle size 40-63 μm). Hexane was used as the mobile phase to separate the mixture of 2-DF and m-DF from other heavy impurities present (**Scheme 3-3** and **Scheme 3-4**) in the product mixture. The eluent was then removed, and the purified mixture was concentrated at 70 ℃ for 2 h under high vacuum and was thereafter left on a hot plate at 100 ℃ overnight.

While the reactant feed had a ratio of 70:30 for 2-DOF to Al-DOF, the ratio of the two products (2-DF:m-DF) changed to 66:34 which further reduced to ~60:40 post purification.

3.2.5 Product Quantification and Identification

a. Gas Chromatogram – Mass Spectrometer (GC-MS)

The products formed in the reactions were identified by a GC-MS (Agilent 7890A connected with Triple-Axis MS detector, Agilent 5975C) and quantified by a GC (Agilent 7890A) equipped with an HP-5 column and a flame ionization detector.

b. Nuclear Magnetic Resonance Spectroscopy (NMR)

The synthesized surfactant precursors (1-(furan-2-yl)alkan-1-one, 2-alkylfuran, m-DF) and oleo-furan sulfonate surfactants (OFS-n, OFS-n-1/O, OFS-12-2/C2H5) were analyzed by NMR spectroscopy[70] (Bruker AX400, 400 MHz). The ^{1}H and ^{13}C NMR of the surfactant precursors was performed by dissolving ~20 μL of the compound in $CDCl_3$ containing 5 mM of tetramethylsilane (TMS) as an internal standard. The oleo-furan surfactants were also identified by NMR using DMSO-d_6 as the solvent.

3.3 Results and Discussion

For the purposes of acylation, fatty acids can be converted to their corresponding anhydride by various existing methods reported in literature such as heating the acid with a dehydrating agent like acetic anhydride whereby the carboxylic acid gets dehydrated to the anhydride and the acetic anhydride gets hydrated to the acid form.[71,72] One way this has been achieved in literature is by passing excess amounts of acetic anhydride vapor through molten fatty acid.[71] Fatty acid anhydride can also be produced by heating the acid with liquid acetic anhydride in the presence of an organic solvent like toluene, ethylbenzene or tetrachloroethylene which forms an azeotrope with acetic anhydride.[73] This method has reported good yields of fatty acid anhydrides using lesser amounts of acetic anhydride as compared to the previous vapor method.[72] In this method, a mixture of fatty acid, acetic anhydride and the azeotropic agent (solvent) is heated to 120 °C at atmospheric pressure. As the reaction occurs, the azeotropic

mixture of acetic acid and solvent is distilled off and any vaporized acetic anhydride is condensed and returned to the reaction vessel. An increase in the temperature of the reaction mixture marks the completion of reaction. A third method reported in literature for the synthesis of fatty acid anhydrides makes use of metal salts such as salts of cobalt, manganese, palladium, copper, nickel, chromium, rhodium, thorium and iron.[74,75] The reaction is carried out between 140 – 220 °C in an inert atmosphere. Water produced during the dehydration of fatty acid is removed as an azeotrope with a hydrocarbon solvent such as linear alkanes, toluene etc.[73] Examples of metal salts that can be used as catalysts include $Co(OAc)_2 \cdot 4H_2O$, $Pd(OAc)_2$, $Cr(OAc)_3$, $Mn(OAc)_2 \cdot 4H_2O$, $Th(NO_3)_4 \cdot 4H_2O$, Rh_2O_3, $Cu(OAc)_2$ and $Fe(OAc)_3$.[75]

3.3.1 Acylation

Acylation of aromatics such as benzene and toluene have been frequently carried out and reported in literature[76–78] using homogenous and heterogenous catalysts such as aluminum trichloride, heteropolyacids and solid acid catalysts such as Nafion, Amberlyst, and zeolites.[79–81] Common acylating agents include acyl chlorides and anhydrides that relatively easily acylate aromatic substrates to form alkyl aromatic ketones.[82] Friedel Crafts acylation is a highly selective reaction as opposed to alkylation reaction due to the inhibitive effect of the carbonyl substituent on the aromatic substrate. The results of acylation employing lauric acid, TFAA and Al-BEA at varying temperatures are given in **Table 3-2**.

Table 3-2. Acylation of furan with lauric acid. Reaction Conditions: 200 psi (N_2), 0.014 mol of furan, 0.018 mol of lauric acid, and 0.028 mol of TFAA in hexane (10 ml), Al-BEA 0.2 g, 6 h in Parr reactor.

Temperature	Conversion (%)			Selectivity (%)
	Furan	Lauric Acid	TFAA	2-Dodecanoylfuran
25 °C [a]	100	100	51.1	87.0
25 °C	100	100	71.6	81.3
50 °C	100	100	70.2	75.6
100 °C	100	100	27.4	27.4
150 °C	100	95.6	100	43.9
180 °C	100	78.3	100	13.5
150 °C [b]	53.9	91.2	100	20.1

[a]no solid acid catalyst (Al-BEA) [b]tetrahydrofuran used as solvent

The conversion of furan and lauric acid were approximately 100% in a range of temperatures from room temperature (25 ℃) to 100 ℃. It is observed that higher temperatures lower the selectivity to 2-dodecanoylfuran (reported with respect to furan) while the conversion of furan remains high. This indicates that there is potential polymerization (coking) of furan in the presence of solid acid Al-BEA catalyst at higher temperatures which has also been reported in literature.[83] Above 150 ℃, the lauric acid conversion slightly decreased. With decreasing reaction temperature, the selectivity of 2-dodecanoylfuran (2-DOF) sharply increased up to 87 % at room temperature without the Al-BEA catalyst. In the use of THF (tetrahydrofuran) solvent, acylation was not significantly observed due to high reactivity of THF with trifluoroacetic anhydride. Lower selectivities at high conversions of lauric acid can be explained as follows: lauric acid forms a mixed anhydride with TFAA which effectively acts as the acylating agent hence forming a second product apart from 2-dodecanoylfuran (**Scheme 3-6**). Furthermore, the selectivity to 2-DOF was lower at high reaction temperatures, because acylation is a

reversible reaction in the presence of trifluoroacetic anhydride. The data in **Figure 3-3** shows the change in concentration of 2-dodecanoylfuran (A) and lauric acid (B), respectively, during a reaction. After the addition of trifluoroacetic anhydride, 2-DOF was rapidly produced with about 90 – 95 % selectivity within a few minutes. However, the produced 2-DOF gradually decreases with continued reaction. The decreasing rate of selectivity was faster at high temperatures. Above 150 ℃, conversion of lauric acid was reversed. The best conversions and selectivities obtained was at 25 ℃. The solid acid catalyst, Al-BEA was found to adversely affect selectivities when compared to the pure TFAA system due to the potential formation of coke on these acid sites.

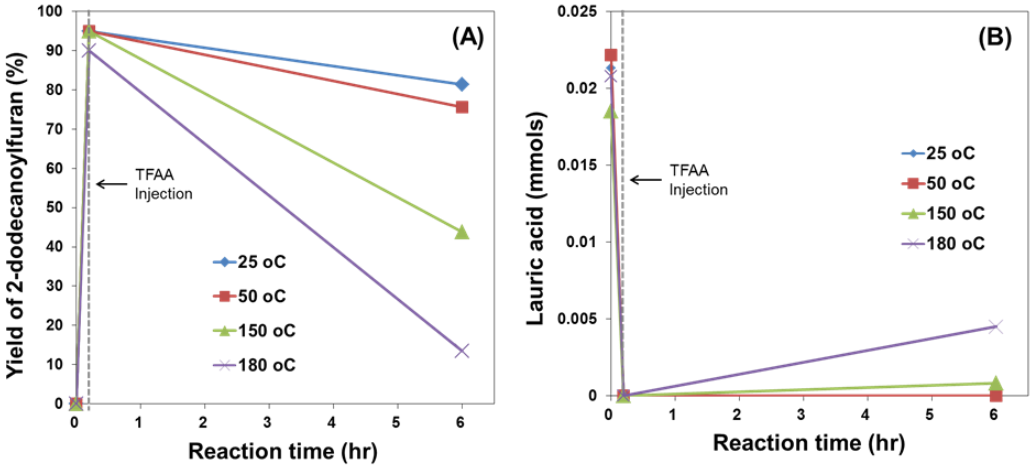

Figure 3-3. The change in the yield of **A.** 2-dodecanoylfuran and, **B.** lauric acid concentration during a reaction. Reaction Conditions: 200 psi (N_2), 0.014 mol furan, 0.018 mol lauric acid, and 0.028 mol of TFAA in hexane (10 ml), Al-BEA 0.2 g, 6 h

As a consequence of the results obtained from the above experiments, acylation was further conducted in the absence of Al-BEA at 25 ℃ and atmospheric pressure.[84] The ratio of furan to lauric acid to TFAA was varied and the results obtained are shown in **Figure 3-4**.

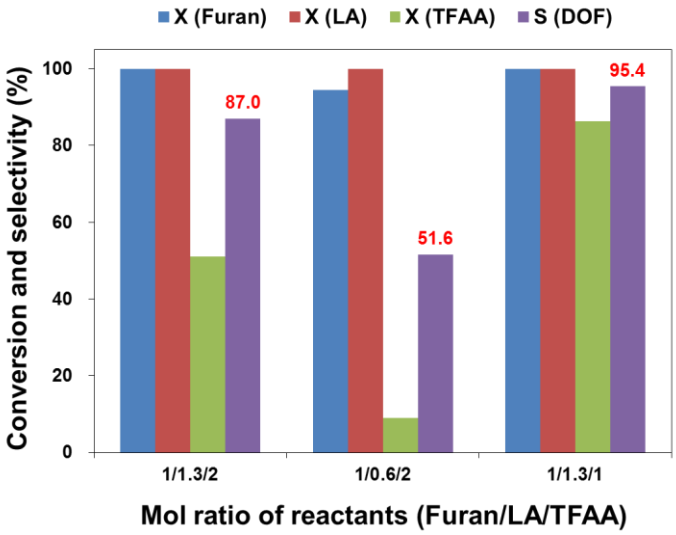

Figure 3-4. Results for the acylation of furan and lauric acid at different mole ratios of reactants. LA: Lauric acid, TFAA: Trifluoroacetic anhydride, Mole ratio (1/1.3/1): 0.014 mol of furan / 0.018 mol of lauric acid / 0.014 mol of TFAA

We see that a ratio of 1:1.3:1 results in the highest selectivity of 95.4% at ~100% conversion of both furan and lauric acid (LA). When TFAA is used in excess such as in the case of a molar ratio of 1:1.3:2, the selectivity is lowered to 87%. This is because, during the reaction, excess TFAA reacts with the furan to form the acylated product, 2,2,2-trifluoro-1-(furan-2-yl)ethan-1-one (observed in GC chromatogram). At lower amounts of fatty acid, such as in the case of a 1:0.6:2 ratio, the selectivity is significantly lowered to 51.6% due to the lack of sufficient fatty acid. **Figure 3-5** and **Figure 3-6** show the time on-stream data and conversion for a 1:1.3:1 ratio of furan : lauric acid : TFAA at 25 ℃ and 1 atm in 10 ml hexane. We see that the reaction is complete in under one hour to yield >95% yield. The images in **Figure 3-6** depict the rapid reaction progression with time due to the change in the color of the reacting mixture in the vial. Time zero corresponds to the point of addition of TFAA to the mixture that contains furan, solvent and fatty acid and we see that the reaction progresses rapidly and is complete in under 5 min.

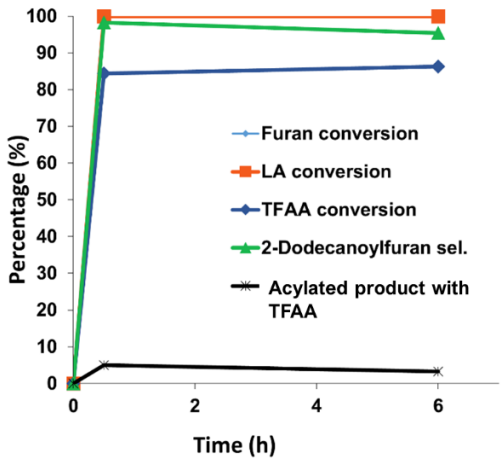

Figure 3-5. Time on-stream conversion and selectivity data. Reaction Conditions: 1 atm, 25°C, Furan: LA: TFAA = 1:1.3:1 in 10 ml n-hexane, 6 h.

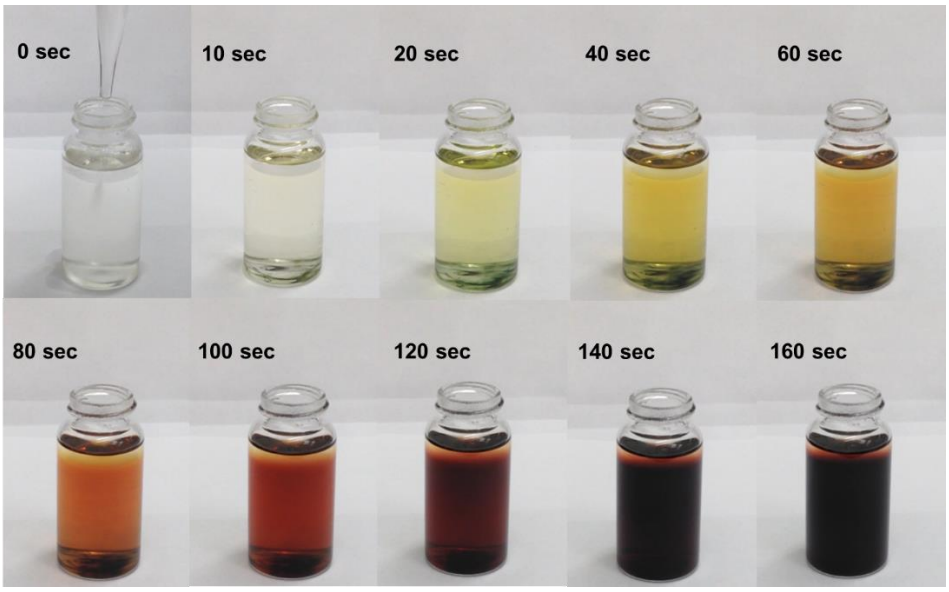

Figure 3-6. Reaction progression of acylation of furan with lauric acid using TFAA with time. Zero seconds corresponds to the point of addition of TFAA to a reaction mixture containing hexane, furan and lauric acid

The effect of using various fatty acids (twelve, fourteen and eighteen carbon atoms) as acylating agents was also studied. As shown in **Table 3-3**, it was found that using fatty acids of different chain lengths does not significantly affect the conversion or selectivity

of the reaction. Different substituted furans as acylating substrates were also found to not influence conversions and selectivities.

Table 3-3. Results for acylation using different furanics as acylating substrates and various fatty acids as acylating agents

Reactant	**Fatty Acid**	**Conversion (%)**		**Product Selectivity (%)**
		Furan	Fatty Acid	
Furan	C_{12}	100	100	95.4
	C_{14}	99.8	99.2	91.6
	$C_{18\ (saturated)}$	99.5	99.6	94.2
	$C_{18\ (unsaturated)}$	99.6	99.3	93.3
2-Methylfuran	C_{12}	100	98.9	96
2,5-Dimethylfuran	C_{12}	99.1	98	96.5

Acylation is a highly selective reaction which stops after a single selective addition at the C2 position of the furan ring (**Scheme 3-5**). This is because of the deactivating effect of the carbonyl group attached directly to the aromatic ring of furan. Carbonyl groups deactivate the ring due to inductive effect of the electron withdrawing carbonyl group leading to withdrawal of electrons away from the ring.[85] In the case of 2-methylfuran, the electrophilic substitution of the acyl group occurs at the C5 position dominantly since the C2 position is blocked by a methyl group. 2,5-Dimethylfuran has both C2 and C5 positions blocked by a methyl group each and hence the substitution occurs at the C3 position in high yield. We could exploit this feature of the acylation reaction to make molecules of different sizes and structures in the future.

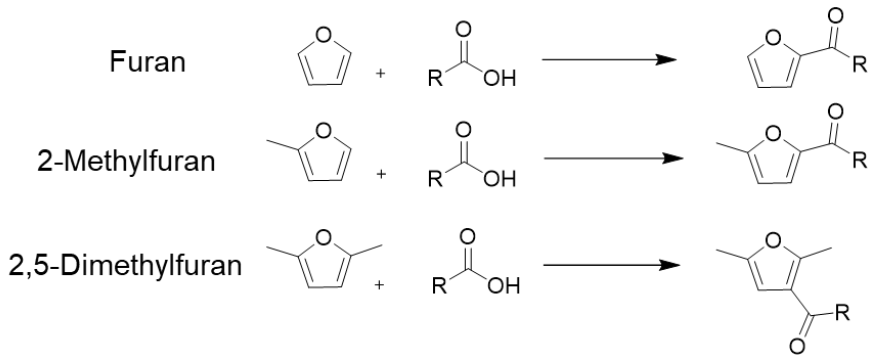

Scheme 3-5. Reaction between different substituted furans with fatty acids

Finally, from the results obtained so far, the mechanism shown in **Scheme 3-6** can be proposed. Trifluoroacetic anhydride (TFAA) forms a mixed anhydride with fatty acid to form a mixed anhydride (CF3-FA). The strong electrophilic nature of the fluorine group in the molecule creates an electron deficiency on the carbonyl carbon of the fatty acid group in the mixed anhydride leading to a +δ charge. The nucleophilic furan ring donates electrons to form the acylated product, 1-(furan-2-yl)alkan-1-one followed by a proton abstraction by the trifluoro carboxylate anion to form trifluoroacetic acid (TFA). TFAA could be regenerated from TFA using a dehydrating agent such as phosphorus pentoxide.[86,87]

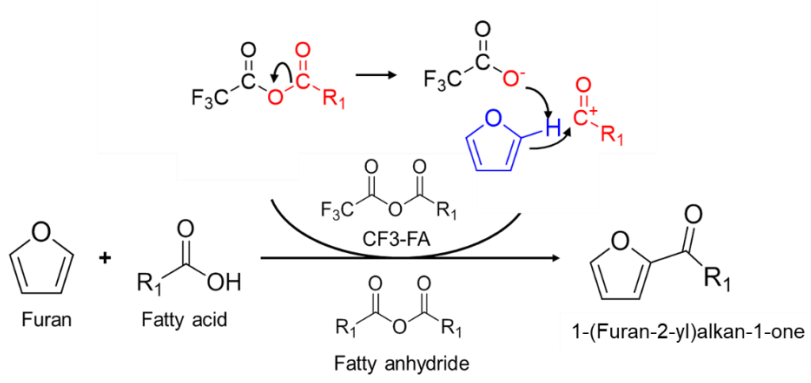

Scheme 3-6. Mechanism of acylation between furan and fatty acid to form 1-(furan-2-yl)alkan-1-one vi the formation of a mixed anhydride (CF_3-FA)

For most reactions, solid acids are preferable because of easy separation.[88] Heterogenous acylation of furan using lauric anhydride and various Lewis and Brønsted acid zeolites yielded interesting results. Acidity, pore size and zeolitic framework were found to have varying effects on acylation activity. As shown in **Figure 3-7**, the reaction of lauric anhydride with furan on either Lewis acid zeolites (such as Sn-BEA, Sn-MWW, or Sn-SPP) or Brønsted acid zeolites (such as Al-BEA or Al-SPP) exhibited varying activity for acylation. Acylation of furan occurs with varying activity on Sn and H+ sites as well as large and small pore structures. Lewis acid zeolites were found to possess low activity (<11%) for the acylation reaction when compared to Brønsted acid zeolites signifying the importance of a Brønsted proton in catalyzing the reaction. A microporous Brønsted acid zeolite like Al-BEA gave a lower yield of 75% when compared to the hierarchical SPP (89%) that contains both micro and mesopores.

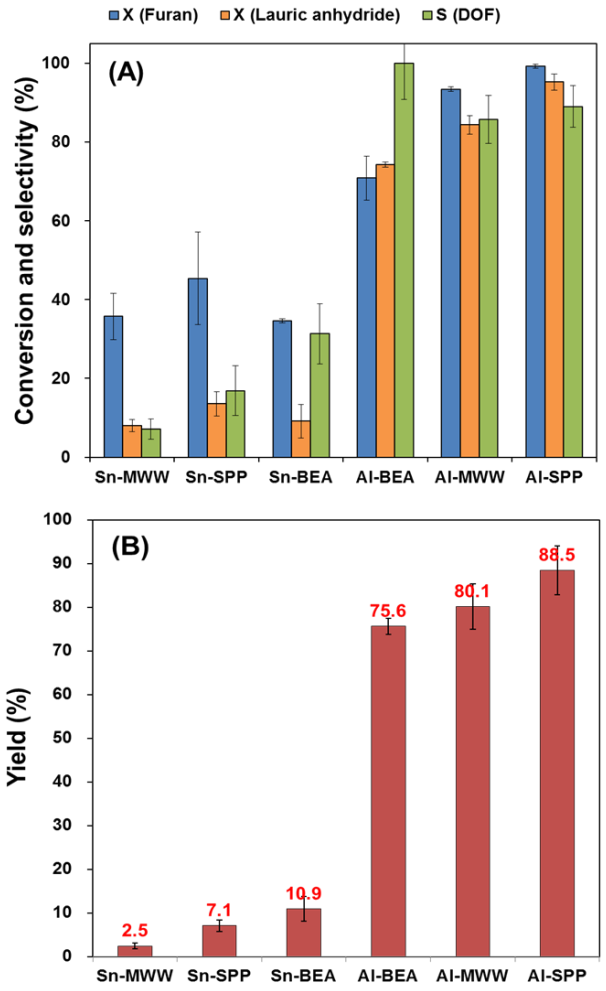

Figure 3-7. Results for **A.** conversion and selectivity and **B.** yield in furan acylation with lauric anhydride over various solid acid catalysts (Reaction conditions: 180 °C, 200 psi N_2, 5 h, 0.014 mol furan, 0.014 mol lauric anhydride in 15 ml hexane).

For the purposes of product collection, the TFAA method was employed. After concentration and purification using a rotary evaporator, the product was separated from the rest of the reaction mixture at 98.2% purity as shown in the Gas chromatogram (GC) profile in **Figure 3-8**. GC-MS and ^{1}H and ^{13}C NMR (**Figure 3-9** and **Figure 3-10**) analysis results of 2-dodecanoylfuran post purification confirm the formation of the desired product.

GC-MS (EI) m/z (relative intensity): 151 (3.4), 123 (20.1), 111 (10.9), 110 (99.9), 95 (31.6), 81 (2.6), 55 (5.5), 43 (4.4), 41 (6.2), 39 (3.6)

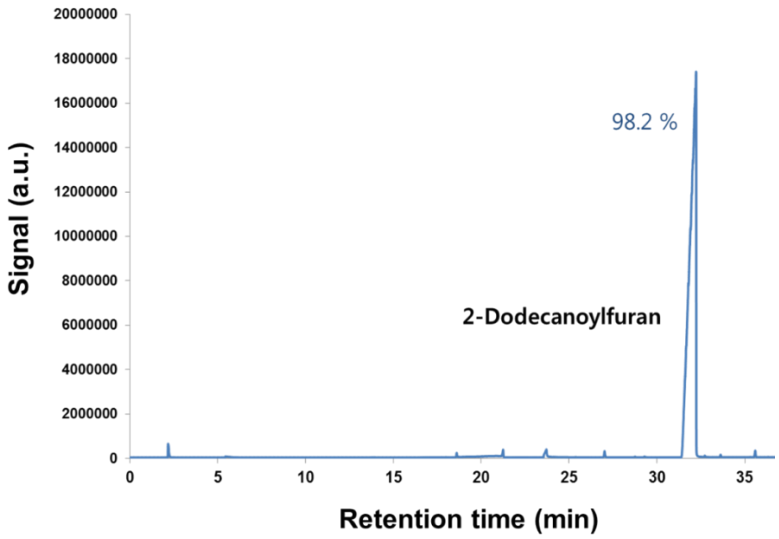

Figure 3-8. Typical GC profile post purification of 2-dodecanoylfuran by rotary evaporator.

^{1}H-NMR (400 MHz, CDCl3) δ 0.86-0.90 (t, 3H), 1.25 (brm, 16H), 1.67-1.75 (m, 2H), 2.80-2.84 (t, 2H), 6.53-6.54 (q, 1H), 7.20-7.21 (q, 1H), 7.58-7.59 (q, 1H) ppm.

^{13}C-NMR (100 MHz, CDCl3) δ 14.11, 22.68, 24.50, 29.32, 29.37, 29.46, 29.60, 31.90, 38.52, 112.27, 117.49, 146.55, 152.69, 190.68 ppm.

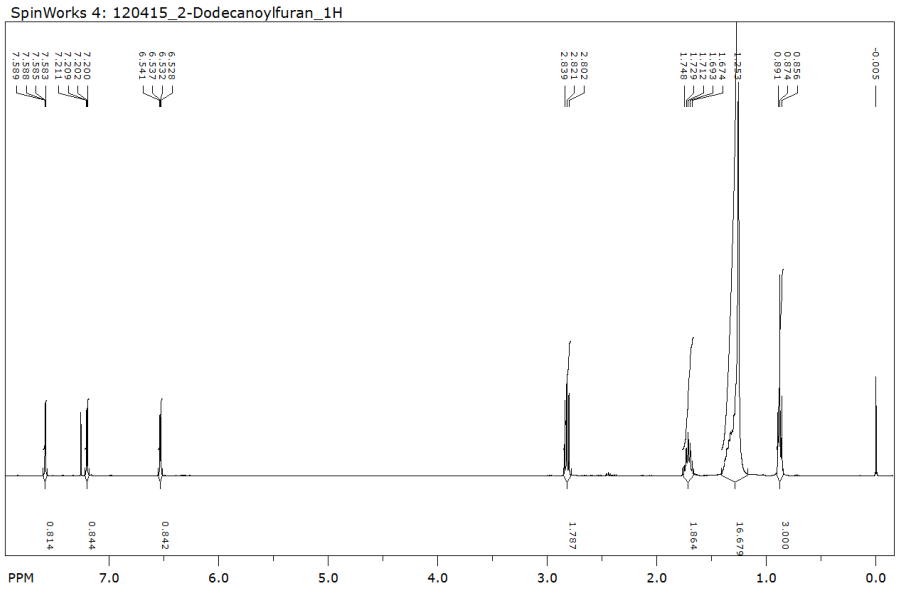

Figure 3-9. ^{1}H NMR of 2-dodecanoylfuran (1-(furan-2-yl)dodecan-1one) in $CDCl_3$

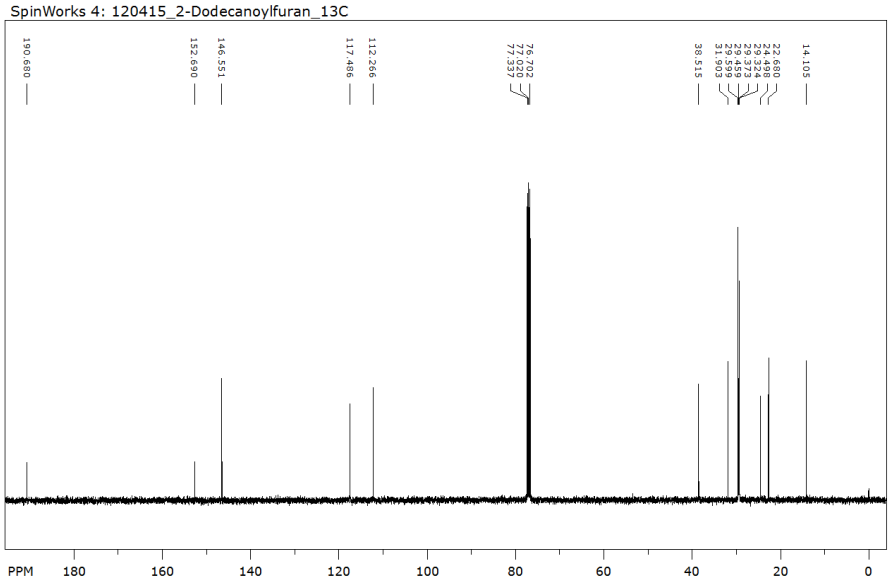

Figure 3-10. ^{13}C NMR of 2-dodecanoylfuran (1-(furan-2-yl)dodecan-1one) in $CDCl_3$

3.3.2 Hydrodeoxygenation

Long chain furan ketones such as 2-dodecanoylfuran (2-DOF) prepared by acylation provide the key capability for producing tunable surfactant chemicals. Hydrodeoxygenation will result in removal of the oxygen atom in the carbonyl group resulting in linear alkyl furan molecules. Depending on the catalyst and reaction conditions (hydrogen pressure, temperature), it is possible to over hydrogenate the molecule leading to loss of aromaticity of the furan ring[89,90] to form tetrahydrofuran (THF) derivatives and other unknown products. Retention of furan aromaticity is essential for surfactant synthesis; sulfonation occurs only on the aromatic ring. Common hydrogenation/hydrodeoxygenation catalysts such as platinum, palladium or nickel tend to over hydrogenate forming the THF molecule.[89] However, as shown in **Scheme 3-3**, the carbonyl functionality can be eliminated by catalytic reduction with copper chromite ($2CuO{-}Cr_2O_3$) catalyst without hydrogenation of the furan ring by tuning hydrogen pressures and reaction temperatures. As shown in **Table 3-4**, varying hydrogen pressures have a significant effect on the selectivity/yield of 2-dodecylfuran (2-DF). At high hydrogen pressures of 350 psi, less than 1% yield was observed towards the desired 2-DF molecule while more than 99% of the product composition was composed of the THF derivative and another unidentified compound. The yield improved from under 1% to ~92% by lowering the hydrogen pressure to 100 psi. It was also found that pre-reducing the copper chromite catalyst ex-situ increased the hydrogenation activity leading to higher amounts of over hydrogenated THF species i.e. at 250 psi hydrogen, the unreduced copper chromite resulted in a yield of 54.8% which dropped down to 18.3% upon using the reduced catalyst.

Table 3-4. Summarized results for the hydrodeoxygenation of 2-dodecanoylfuran over copper chromite at varying hydrogen pressures

Pressure (psi)	Conversion (%) 2-DOF	Selectivity (%)		
		2-Dodecylfuran	2-Dodecyl-THF	Other
100	100	91.6	7.3	1.1
150	100	59.5	12.3	28.2
250	100	54.8	18.3	26.9
250 [a]	99.6	18.3	74.9	6.9
350	100	0.9	47.6	51.5

[a] pre-reduced $2CuO\text{-}Cr_2O_3$
Reaction Conditions: 220 ℃, 0.0077 mol of 2-dodecanoylfuran (2-DOF) in hexane (30 ml), copper chromite 0.5 g, 5 h.

The effect of temperature on this reaction was also studied and was found to be less significant when compared to the effects of hydrogen pressure. Increasing the temperature from 180-220 ℃ improved the yield from 79% to 91% as shown in **Figure 3-11**.

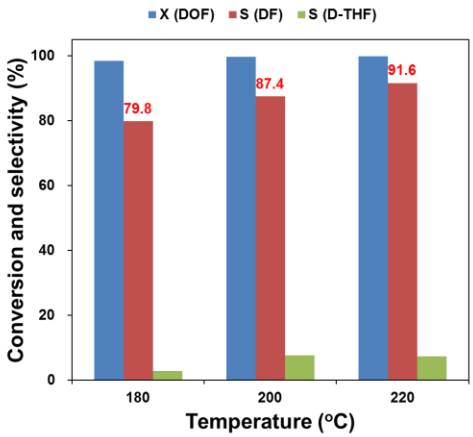

Figure 3-11. Results for the hydrodeoxygenation of 2-dodecanoylfuran (2-DOF) at 180 – 220 ℃. Reaction Conditions: 100 psi H_2, 0.0077 mol of 2-dodecanoylfuran in hexane (30 ml), copper chromite 0.5 g, 5 h. *Note: Selectivities of other unknown hydrogenated compounds are not depicted in the graph.*

The time on-stream conversion and yield data for the reactant and two products is shown in **Figure 3-12** and we see that, with time, the conversion of the reactant increases and so does the yield for 2-DF. However, as we cross the three-hour mark, we slowly start forming

the THF-derivative molecule and five hours was chosen as the optimum reaction time for product collection.

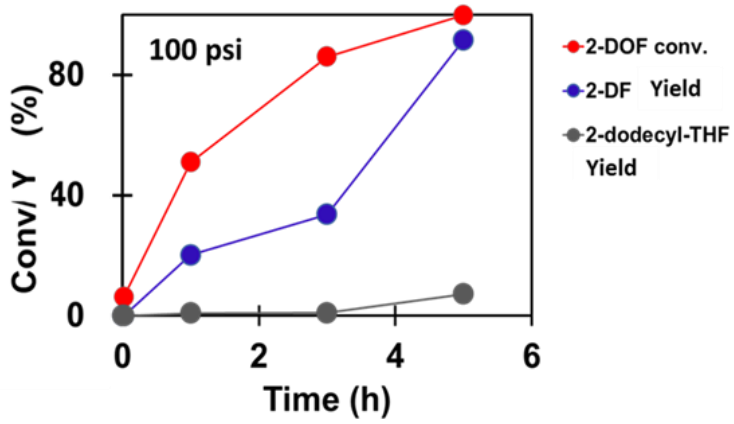

Figure 3-12. Time-on-stream results (conversion of 2-dodecanoylfuran, red (2-DOF) and yields (Y) of 2-dodecylfuran, blue (2-DF) and 2-dodecyl-tetrahydrofuran, grey (2-dodecyl-THF)) for the hydrodeoxygenation/hydrogenation of 2-dodecanoylfuran at 100 psi H_2

Acylation products of both myristic and stearic acid were also subject to the same set of reaction conditions (100 psi H_2, 220 °C) and similar values of conversions and selectivities were obtained.

The purity of the product 2-dodecylfuran after rotary evaporation and flash chromatography is shown in **Figure 3-13**. After concentration and purification using a rotary evaporator, the product was separated from the rest of the reaction mixture at 87% purity which was further purified to 94.6% via flash chromatography. GC-MS and ^{1}H and ^{13}C NMR (**Figure 3-14** and **Figure 3-15**) analysis results of 2-dodecylfuran post purification confirm the formation of the desired product.

GC-MS (EI) m/z (relative intensity): 236 (17.7), 123 (17.6), 96 (12.1), 95 (58.3), 94 (13.5), 82 (42.6), 81 (99.9), 53 (10.1), 43 (10.2), 41 (12.3)

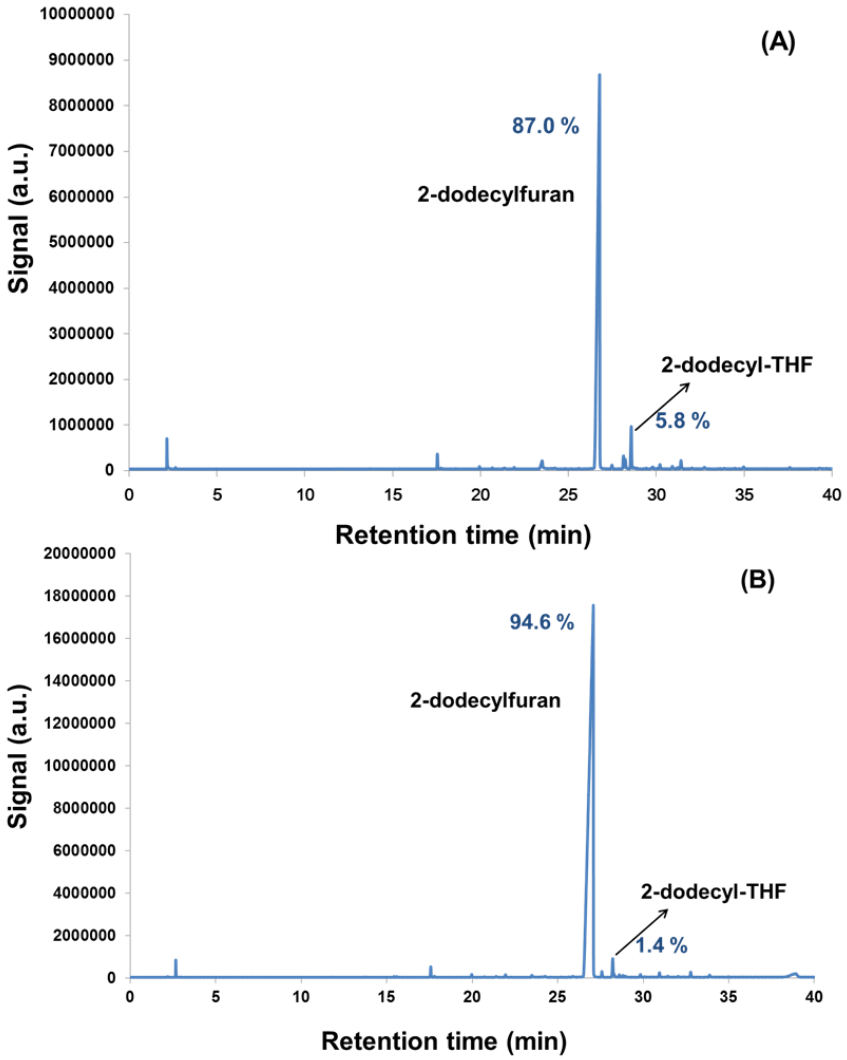

Figure 3-13. Typical GC profiles of product mixtures after hydrodeoxygenation. **A.** Concentrated samples by rotary evaporator and, **B.** Purified by flash chromatography followed by rotary evaporation to remove eluent

^{1}H-NMR (400 MHz, $CDCl_3$) δ 0.87-0.90 (t, 3H), 1.26 (brm, 18H), 1.60-1.67 (m, 2H), 2.59-2.63 (t, 2H), 5.96-5.97 (q, 1H), 6.27-6.28 (q, 1H), 7.29-7.30 (q, 1H) ppm

^{13}C-NMR (100 MHz, $CDCl_3$) δ 14.12, 22.71, 27.99, 28.06, 29.21, 29.37, 29.38, 29.57, 29.65, 29.68, 31.94, 104.50, 110.02, 140.60, 156.66 ppm

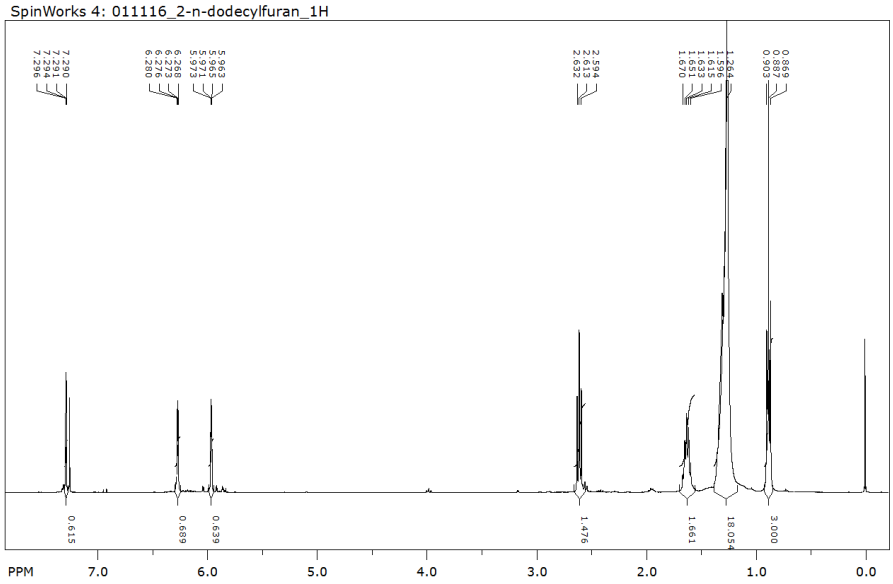

Figure 3-14. ^{1}H NMR of 2-n-dodecylfuran in $CDCl_3$

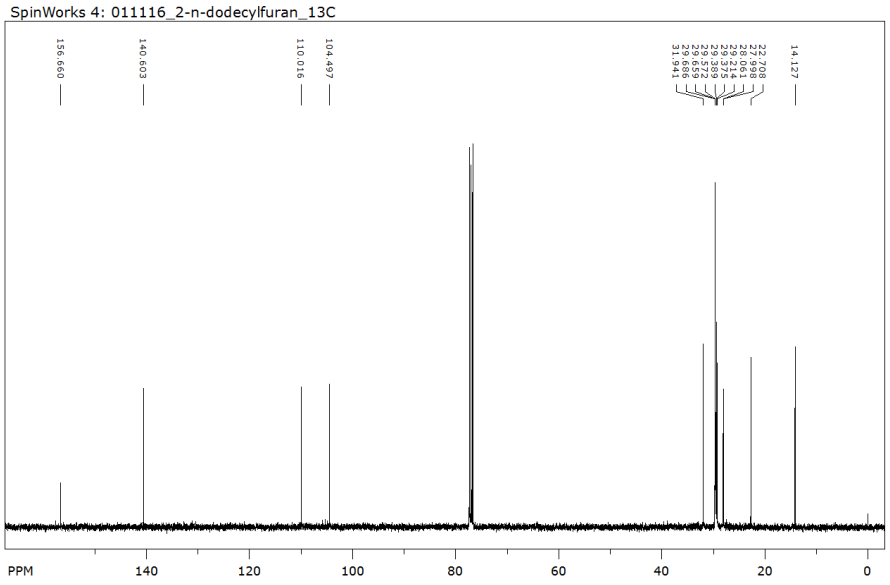

Figure 3-15. ^{13}C NMR of 2-n-dodecylfuran in $CDCl_3$

3.3.3 Aldol Condensation

Aldol condensation is employed within the OFS platform to aid in the incorporation of branching via formation of carbon-carbon bonds within OFS structures for tuning surfactant properties. This reaction is a characteristic reaction of carbonyl compounds i.e. between two aldehydes or between an aldehyde and a ketone. Aldol addition results in the formation of a β-hydroxyketone or a β-hydroxyaldehyde when the reaction is between a ketone and an aldehyde or between two aldehydes respectively and can be catalyzed by both acids and bases.[91–93] The reaction between two ketones is not very successful because of their low reactivity to nucleophilic addition due to electronic and steric effects.[94,95] These aldol products can undergo a facile dehydration to form α,β-unsaturated carbonyl compounds either under acid or base catalysis or even under thermal conditions. This spontaneous dehydration is a result of the driving force to form a conjugated system. Aldol addition combined with dehydration is together called as aldol condensation. As shown in **Scheme 3-4**, 2-dodecanoylfuran (2-DOF) reacts with acetaldehyde (AA) via aldol addition preferentially at the second carbon of the linear chain and subsequently undergoes dehydration to form the unsaturated compound termed 'Al-DOF'. Various solid acid and base catalysts were used for this reaction (**Figure 3-16**). The use of NaOH as the catalyst resulted in 99% conversion of acetaldehyde at 22% 2-DOF conversion giving an Al-DOF yield less than 2%. Solid acid catalysts such as Al-SPP and HY improved yields to approximately under 20% at acetaldehyde conversions almost three times higher than that of 2-DOF. Strangely enough, for the same set of reaction conditions, the seemingly *uncatalyzed* reaction system resulted in the best yield of 23%. Optimization of acetaldehyde to 2-DOF ratio revealed a significantly higher yield of 23% for a 10:1 ratio when compared to a yield less than 5% corresponding to a 1:1 ratio. All the results

summarized in **Figure 3-16** indicate potential side reactions of acetaldehyde competing with the desired reaction to form Al-DOF.

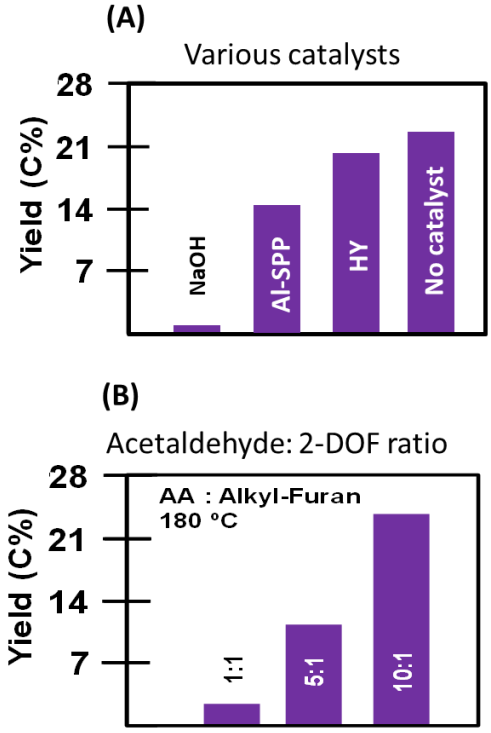

Figure 3-16. Aldol condensation with **A.** various acid and base catalysts at 10:1 molar ratio of acetaldehyde (AA, 0.054 mol) and 2-dodecanoylfuran, and **B.** varying ratios of AA and 2-dodecanoylfuran (alkyl-furan) at 180 °C. after 24 h in 20 ml hexane and 200 psi N_2

To understand the competing side reactions of acetaldehyde, it is imperative to gain a deeper understanding of the mechanism for an aldol condensation reaction. **Scheme 3-7** depicts both acid and base-catalyzed mechanism for the aldol addition-dehydration reaction between 2-DOF and acetaldehyde. The acid catalyzed mechanism proceeds via the formation of an enol species. In the reaction between an aldehyde (acetaldehyde) and a ketone (2-DOF), the carbonyl oxygen is protonated by the acid catalyst resulting in ketone forming the electrophilic enol species. It loses an α-hydrogen followed by carbonyl protonation of the aldehyde and subsequent addition and dehydration to form the Al-DOF product. The base-catalyzed reaction on the other hand proceeds via an enolate formation

mechanism. The α-hydrogen of the ketone is abstracted by the base catalyst resulting in the formation of a nucleophilic enolate species. This carbanion on the α-carbon undergoes an addition with the electrophilic carbonyl carbon of the aldehyde followed by dehydration to form the final product. From both acid and base catalyzed mechanisms, we see that it is imperative for at least one of the reactants to possess an α-hydrogen for the reaction to proceed. What is interesting to note however, is the presence of a similar α-hydrogen in the co-reactant acetaldehyde. This implies that acetaldehyde could undergo a self-aldol condensation reaction i.e. it can react with itself to form various α,β-unsaturated compounds. Furthermore, as stated earlier, aldehydes are generally more reactive than ketones and hence, it wouldn't be surprising to use this phenomenon as an explanation for very high conversions of acetaldehyde at relatively lower conversions of 2-DOF. In fact, upon careful GC-MS analysis of reaction mixtures, several compounds belonging to the self-aldol condensation product profile of acetaldehyde were identified such as 2-butenal and 2,4,6-octatrienal. It can also undergo oligomerization to form ring-like species such as paraldehyde. The overall reaction scheme for the aldol addition and dehydration of acetaldehyde with itself and with 2-DOF is depicted in **Scheme 3-8**.

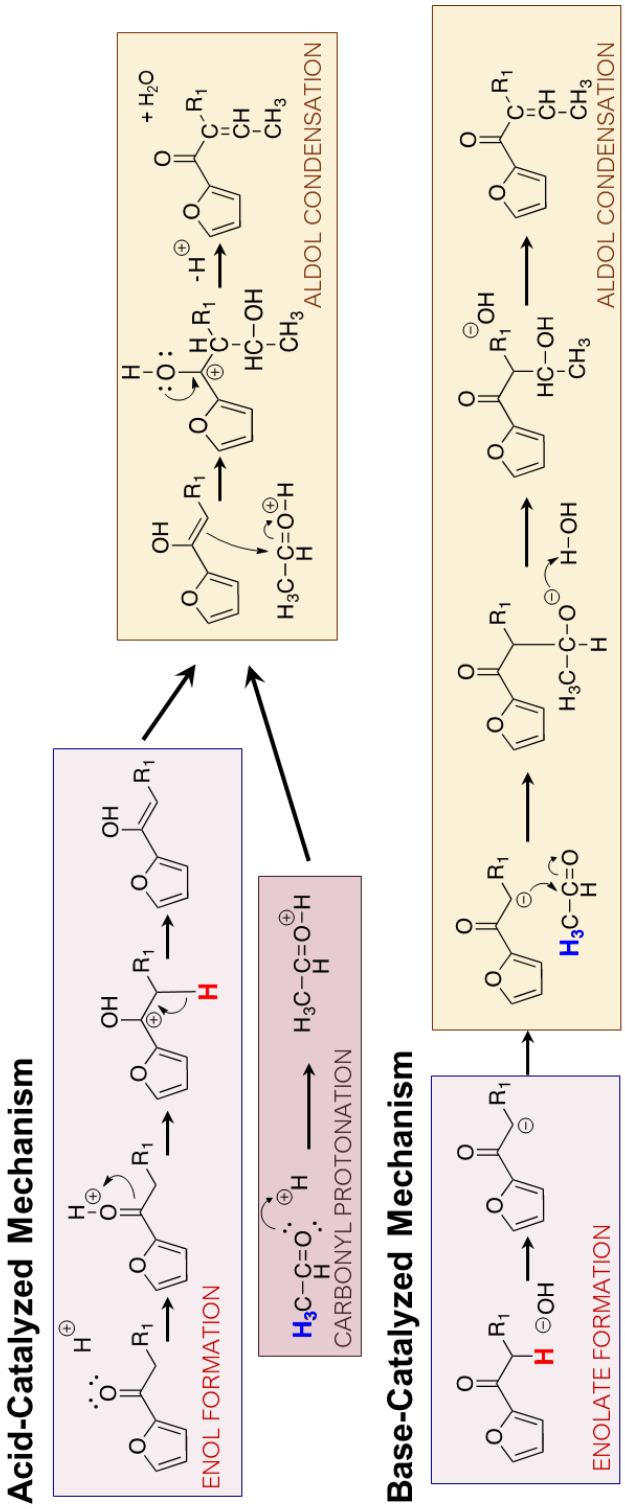

Scheme 3-7. Acid catalyzed and base catalyzed mechanism for sequential aldol addition-dehydration reaction between 2-dodecanoylfuran and acetaldehyde

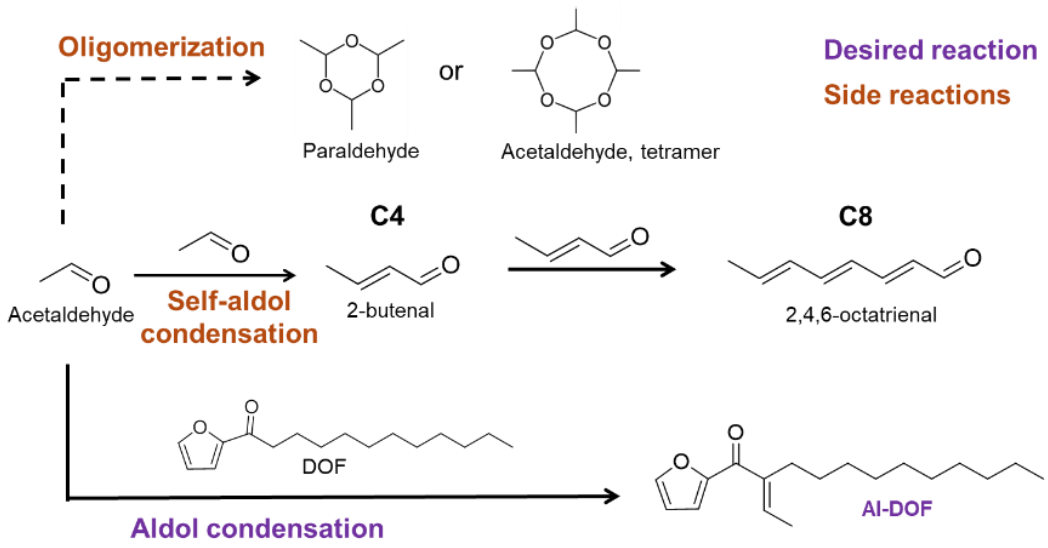

Scheme 3-8. Main and competing side reactions in the aldol condensation reaction system between 2-dodecanoylfuran (2-DOF) and acetaldehyde

Selectivities towards side products of acetaldehyde observed at different temperatures, reaction times, catalysts, and at varying molar ratios of acetaldehyde to 2-DOF are summarized in **Table 3-5**, **Table 3-6** and **Table 3-7**.

Table 3-5. Summarized results for observable side product formation due to self-aldol condensation of acetaldehyde (AA) at 1:10 molar ratio of 2-DOF to AA over various acid and base catalysts.

Conditions	Conversion (%)	Selectivity (%)		
	AA	C_4	C_8	Paraldehyde
Al-BEA (200 ℃, 6 h)	74.7	4.6	1.2	0.05
KBEA (200 ℃, 6 h)	62.3	9.5	1.3	0.03
HY (200 ℃, 6 h)	73.5	10.2	1.4	0.04
Mg-Zr-O (200 ℃, 6 h)	99.5	0.08	0.9	0.01
HY (220 ℃, 6 h)	78.8	8.5	1.4	0.02
HY (180 ℃, 6 h)	73.7	8.3	0.7	0.06
KY (180 ℃, 6 h)	72.1	10.5	0.8	0.03
HY (180 ℃, 24 h)	85.2	7.1	1.7	0.02
HY (180 ℃, 48 h)	93.9	7.7	18.7	0.04
Reaction Conditions: 200 psi (N_2), 0.054 mol of acetaldehyde (AA) and 0.0054 mol of 2-dodecanoylfuran (2-DOF) in hexane (20 ml), 0.2 g catalyst				

Table 3-6. Summarized results for observable side product formation due to self-aldol condensation of acetaldehyde (AA) over various acid and base catalysts.

Conditions	Conversion (%)	Selectivity (%)		
	AA	C_4	C_8	Paraldehyde
HY (1 g, 24 h)	93.0	5.3	1.3	0.02
HY (0.2 g, 24 h)	85.2	7.1	1.7	0.02
HY (0.1 g, 24 h)	74.0	11.3	2.4	0.6
Si-SPP (0.1 g, 24 h)	82.0	8.1	3.5	0.06
Al-SPP (0.1 g, 24 h)	81.5	11.2	9.4	0.06
Al-MWW (0.1 g, 24 h)	90	3.8	3.2	0.05
NaOH (0.1 g, 24 h)	99	0.06	0.2	0.3
No Cat. (24 h)	72.3	7.8	1.1	0.2
No Cat. (48 h)	87.5	7.8	0.9	0.1
No Cat. (72 h)	93.1	4.1	0.6	0.04
Reaction Conditions: 200 psi (N_2), 0.054 mol of acetaldehyde (AA) and 0.0054 mol of 2-dodecanoylfuran (2-DOF) in hexane (20 ml), 0.2 g catalyst, 180 ℃				

Table 3-7. Summarized results for observable side product formation due to self-aldol condensation of acetaldehyde (AA) at different molar ratios over various acid and base catalysts.

Mole ratio AA:2-DOF	Conversion (%)	Selectivity (%)		
	AA	C_4	C_8	Paraldehyde
15:1	60.4	16.2	2.0	0.5
10:1	72.3	7.8	1.1	0.2
5:1	72.8	7.9	0.5	0.2
1:1	70.0	1.4	0	0
1:2	82.7	0.9	0	0
Reaction Conditions: 200 psi (N_2), 0.054 mol of acetaldehyde (AA) and 0.0054 mol of 2-dodecanoylfuran (2-DOF) (10:1 ratio) in hexane (20 ml), uncatalyzed, 180 ℃				

As seen earlier, the best yield obtained from all the experiments performed was 23% and was oddly enough obtained from a non-catalytic reaction system (**Figure 3-16**). This

necessitated further investigation into the purity of all reagents and catalysts used for the reaction. Upon careful analysis, the reactant 2-dodecanoylfuran was found to contain trace amounts of trifluoroacetic acid (TFA, 0.015 M) left behind due to incomplete purification of the reactant. To verify if TFA imparted any catalytic activity via homogenous catalysis, the reactant was further purified by heating it to 100 ℃ and left overnight on the hot plate until GC analysis revealed zero contamination by TFA. This high purity 2-DOF was then subjected to aldol condensation with acetaldehyde in a 10:1 molar ratio of aldehyde to 2-DOF at 180 ℃ for 24 h in the absence of any solid acid/base catalyst. The yield obtained was 1.5% contrary to the 23.4% yield obtained from the sample that contained TFA contamination under the same reaction conditions. To further strengthen the claim of homogenous catalysis by TFA in the aldol condensation reaction between 2-DOF and acetaldehyde, TFA was added to the reaction mixture in varying amounts and the product yields were evaluated the results of which are summarized in **Table 3-8**.

Table 3-8. Summarized results for aldol condensation between 2-dodecanoylfuran (2-DOF) and acetaldehyde in the presence of trifluoroacetic acid (TFA) as an impurity and otherwise

Concentration (M)[a]		**2-DOF Conversion (%)**		**Al-DOF Yield (%)[b]**	
TFA (in 2-DOF)	**TFA (added)**	**6 h**	**24 h**	**6 h**	**24 h**
0.015	-	8.12	25.00	7.72	23.40
-	-	0.27	1.58	0.25	1.50
-	0.007	1.98	-	1.83	-
-	0.104	28.97	-	27.55	-

[a]molarity calculated with respect to total reaction volume
[b]yield calculated with respect to 2-DOF
Reaction conditions: 200 psi (N_2), 0.054 mol of acetaldehyde (AA) and 0.0054 mol of 2-dodecanoylfuran (2-DOF) in hexane (20 ml), uncatalyzed, 180 ℃

It was found that higher concentrations of TFA result in higher yields. At 0.104 M concentration of TFA in 2-DOF, which is approximately ten times greater than the impurity concentration, the yield after 6 h (27.55%) in the former case exceeded the yield obtained after 24 h in the latter case (23.40%). This brings us to the conclusion that the aldol

condensation system was truly homogenously catalyzed rather than uncatalyzed in the experiments conducted previously.

Due to similarities in the functional group structure and molecular weight and because of low conversions of the reactant 2-DOF, post solvent evaporation in high vacuum, a 77:23 mole ratio mixture of 2-DOF:Al-DOF is obtained. The purity of this mixture after rotary evaporation and flash chromatography is shown in **Figure 3-17**. After concentration and purification using a rotary evaporator, the 2-DOF:Al-DOF mixture was separated from the rest of the reaction mixture via flash chromatography at a new molar ratio of 70:30 due to losses in the process of purification with 91% purity.

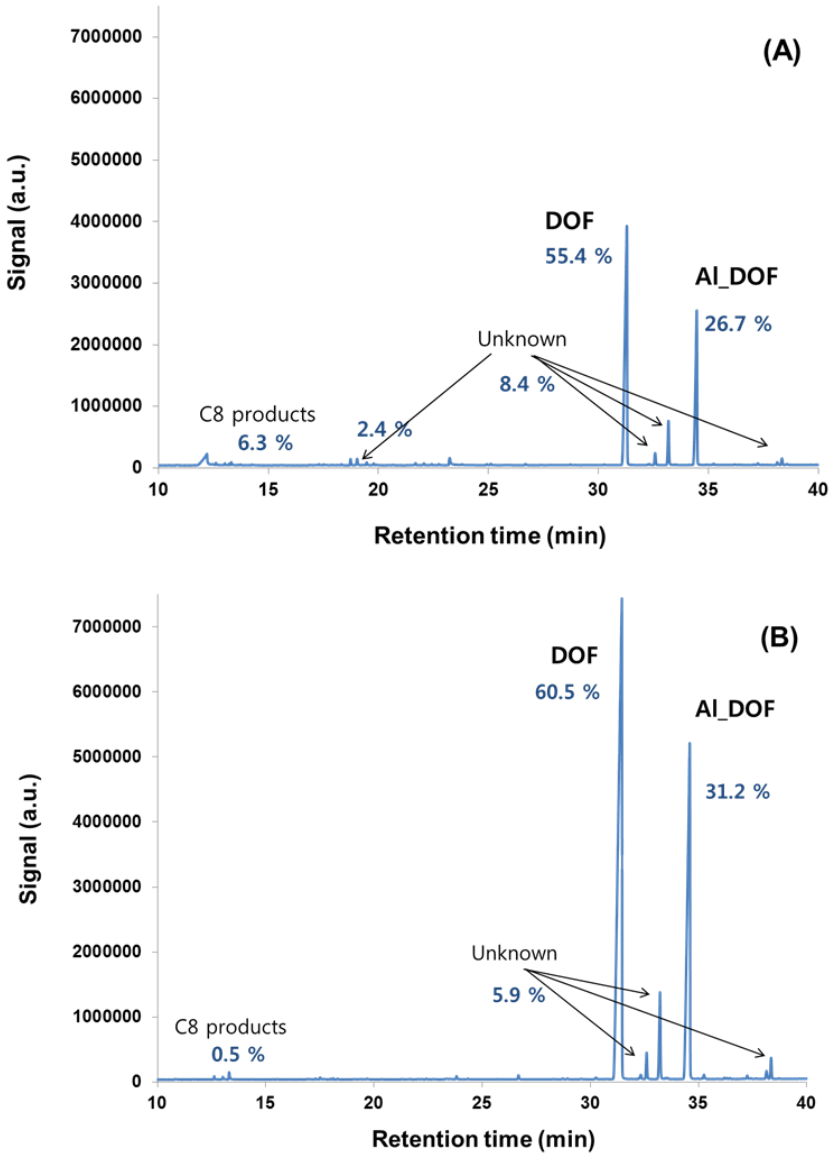

Figure 3-17. Typical GC profiles of product mixtures after aldol condensation. **A.** Concentrated samples by rotary evaporator and, **B.** Purified and separated by flash chromatography.

3.3.4 Hydrogenation/Hydrodeoxygenation

The mixture of Al-DOF and 2-DOF obtained from the sequential aldol addition, dehydration reaction was subjected to hydrogenation using copper chromite. Al-DOF possesses two functional groups that undergo reduction, namely the carbonyl group and the unsaturation in the branching to form branched alkylfuran molecules. While the carbonyl group undergoes hydrodeoxygenation similar to the discussion in **Section 3.3.2**, the double bond undergoes hydrogenation to lose the unsaturation. The reaction could possibly occur via either of the two pathways shown in **Scheme 3-9**.

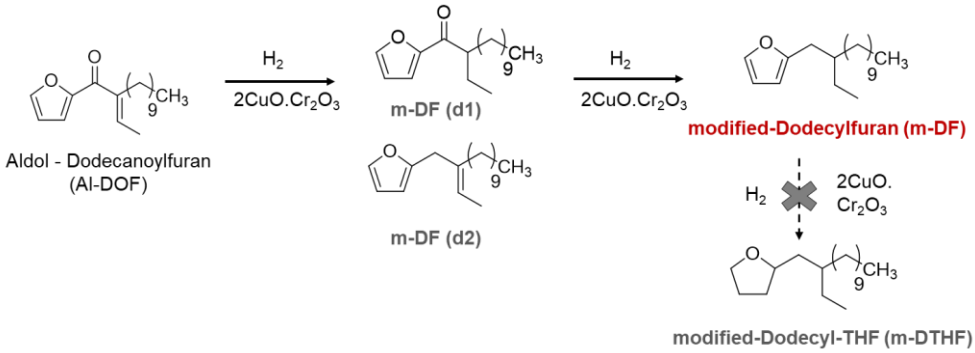

Scheme 3-9. Reaction scheme for the hydrogenation and hydrodeoxygenation of Al-DOF

From the product profile observed, traces of m-DF (d1) was found indicating that Al-DOF first undergoes hydrogenation for removal of unsaturation followed by hydrodeoxygenation to form m-DF. Both reactions were achieved in a single-pot process using copper chromite at 100 psi H_2 pressure, 220 ℃ over a reaction time of 7 h. By controlling reaction conditions, the formation of THF species was minimized. The results obtained are summarized in **Table 3-9** and the time-on stream data for the reactant mixture containing 70:30 molar ratio of 2-DOF to Al-DOF is depicted in **Figure 3-18**.

Table 3-9. Summarized results for combined hydrogenation and hydrodeoxygenation of Al-DOF

	Al-DOF	m-DF	m-DF(d1)	m-DTHF
Conversion (%)	98.3	-	-	-
Selectivity (%)	-	93.9	1.5	4.6

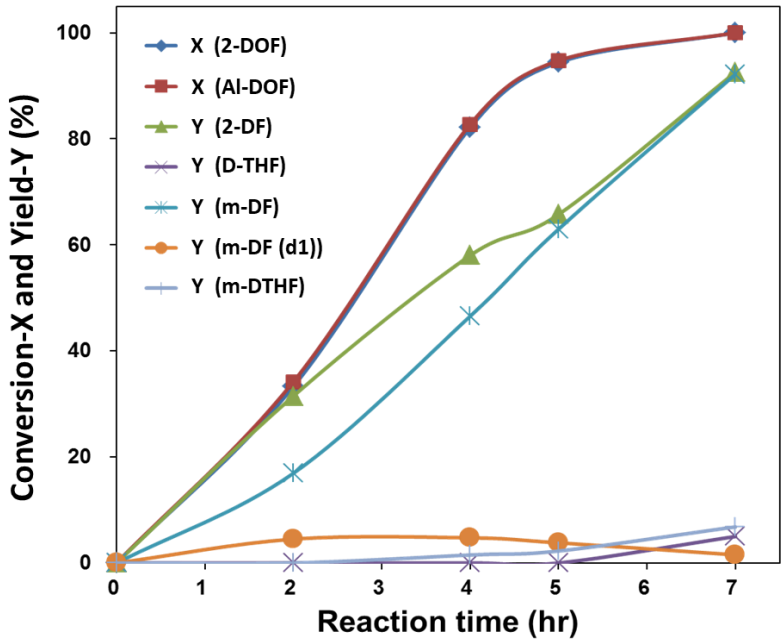

Figure 3-18. Time-on-stream results for the hydrodeoxygenation/hydrogenation of mixture of 2-dodecanoylfuran (2-DOF) and aldol-product (Al-DOF), (220 ℃, 100 psi of H_2, 0.5 g copper chromite, 7 h)

GC profiles of the reactant mixture containing 2-DOF and Al-DOF and product mixture containing 2-DF and m-DF are given in **Figure 3-19**. Post purification via evaporation and flash chromatography, the final ratio of DF to m-DF is 60:40. GC-MS, ^{1}H and ^{13}C NMR analysis of the mixture confirms the structure of the desired product.

GC-MS (EI) m/z (relative intensity): 264 (7.7), 235 (8.0), 123 (25.6), 82 (99.9), 81 (65.8), 71 (36.3), 57 (56.8), 43 (38.7), 41 (23.7), 28 (91.9)

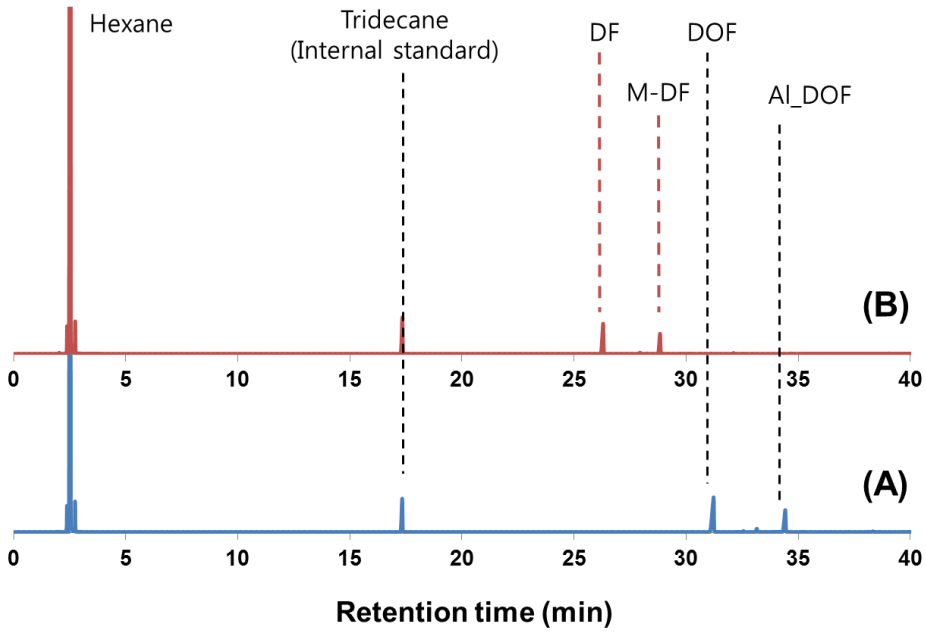

Figure 3-19. Typical GC profiles of **A.** reactant mixture and **B.** products in hydrogenation of 2-DOF and Al-DOF mixture (DOF: 2-dodecanoylfuran, Al-DOF: aldol product, DF: 2-dodecylfuran, M-DF: Mono-ethyl branched dodecylfuran)

^{1}H-NMR (400 MHz, $CDCl_3$) δ 0.86-0.90 (t, 3H), 0.87-0.91 (t,3H), 1.26 (brm, 18H), 1.59-1.67 (q, 2H), 2.55-2.56 (d, 2H), 2.59-2.63 (t, 1H) 5.96-5.97 (t, 1H), 6.27-6.28 (q, 1H), 7.29-7.30 (q, 1H) ppm.

^{13}C-NMR (100 MHz, $CDCl_3$) δ 10.86, 14.13, 22.71, 25.92, 26.66, 28.00, 28.06, 29.21, 29.38, 29.58, 29.67, 29.69, 29.99, 31.94, 32.02, 33.06, 38.75, 105.73, 110.00, 140.64, 155.65 ppm

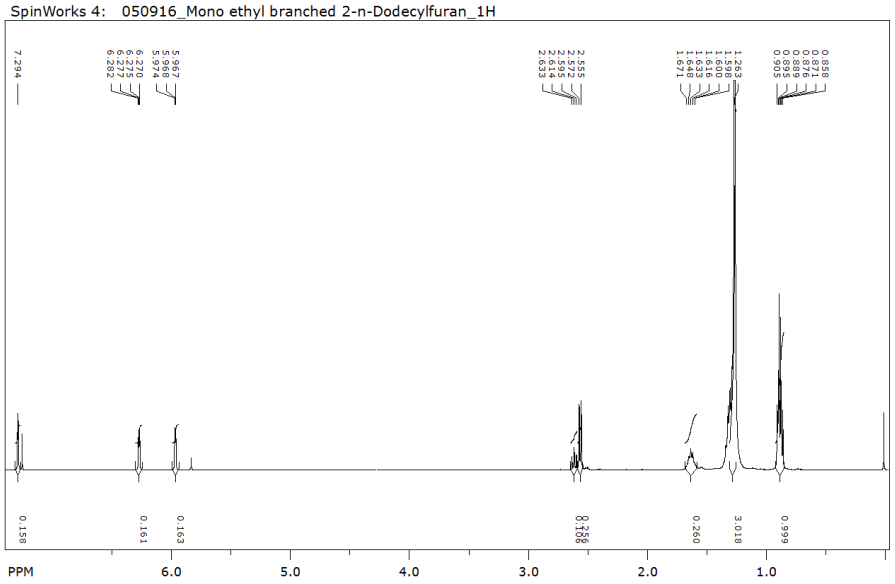

Figure 3-20. ^{1}H NMR of mono ethyl branched 2-n-dodecylfuran, m-DF (Mixture with 60 % of 2-n-dodecylfuran) in $CDCl_3$

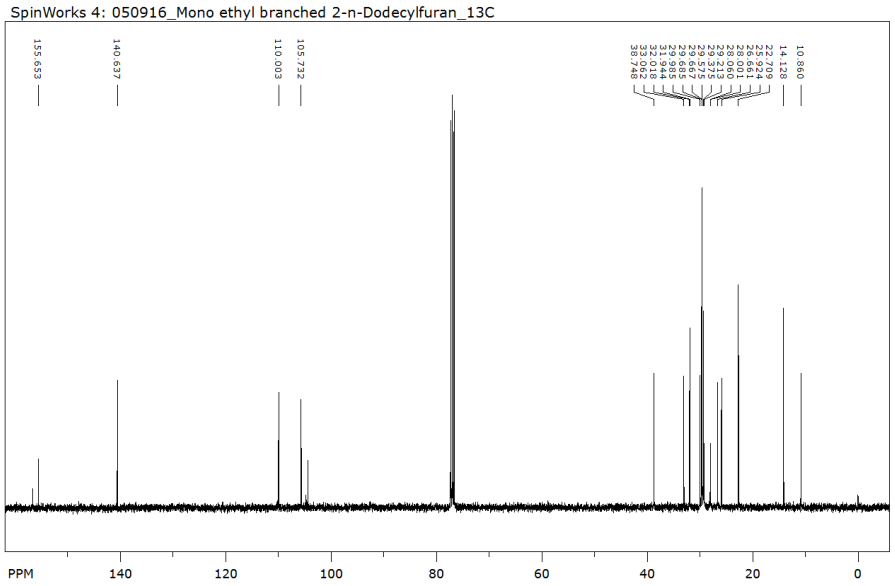

Figure 3-21. ^{13}C NMR of mono ethyl branched 2-n-dodecylfuran, m-DF (Mixture with 60 % of 2-n-dodecylfuran) in $CDCl_3$

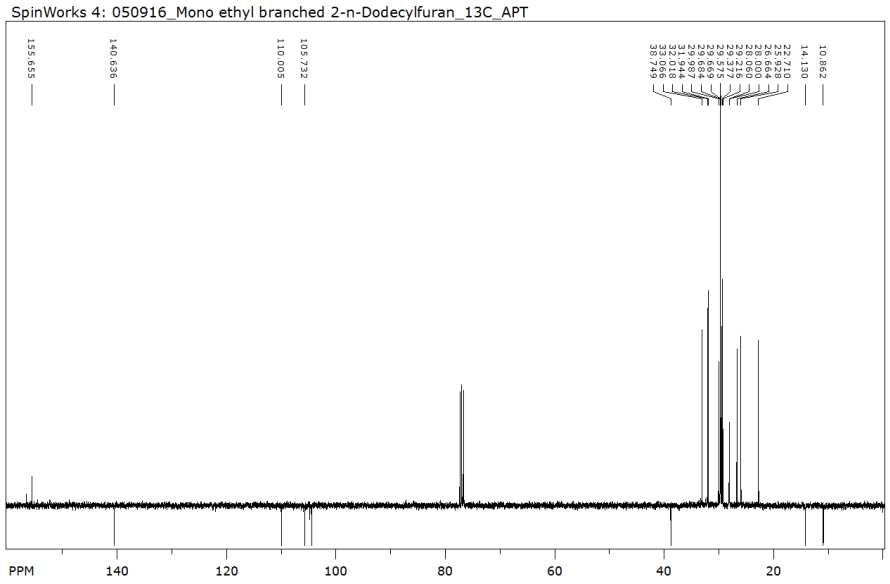

Figure 3-22. ^{13}C-APT NMR of mono ethyl branched 2-n-dodecylfuran, m-DF (Mixture with 60 % of 2-n-dodecylfuran) in $CDCl_3$

3.3.5 Sulfonation

While a single acylation occurred overwhelmingly at one of the furan α carbons, the remaining furan α carbon was sulfonated with a sulfur trioxide−pyridine complex which yielded high purity alkylfuran sulfonate. ^{1}H and ^{13}C NMR revealed structural conformity of the synthesized OFS molecules as shown in **Figure 3-23** and **Figure 3-24**.

^{1}H-NMR (400 MHz, DMSO-d6) δ 0.84-0.87 (t, 3H), 1.24 (brm, 22H), 1.53-1.59 (m, 2H), 2.53-2.57 (t, 2H), 5.96-5.97 (d, 1H), 6.23-6.24 (d, 1H) ppm.

^{13}C-NMR (100 MHz, DMSO-d6) δ 13.95, 22.09, 27.39, 27.54, 28.58, 28.70, 28.74, 28.97, 29.00, 29.03, 31.28, 104.98, 108.09, 154.98, 155.69 ppm.

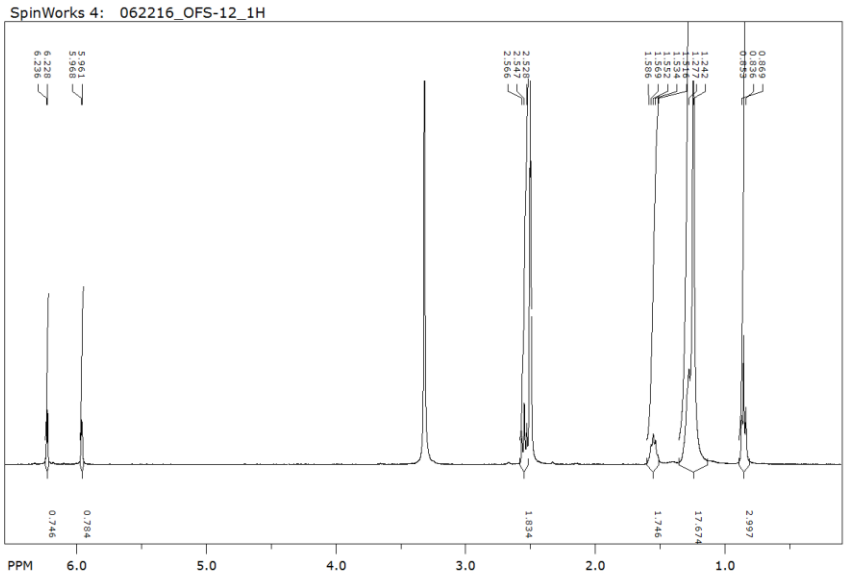

Figure 3-23. ^{1}H NMR of OFS-12 in DMSO-d_6

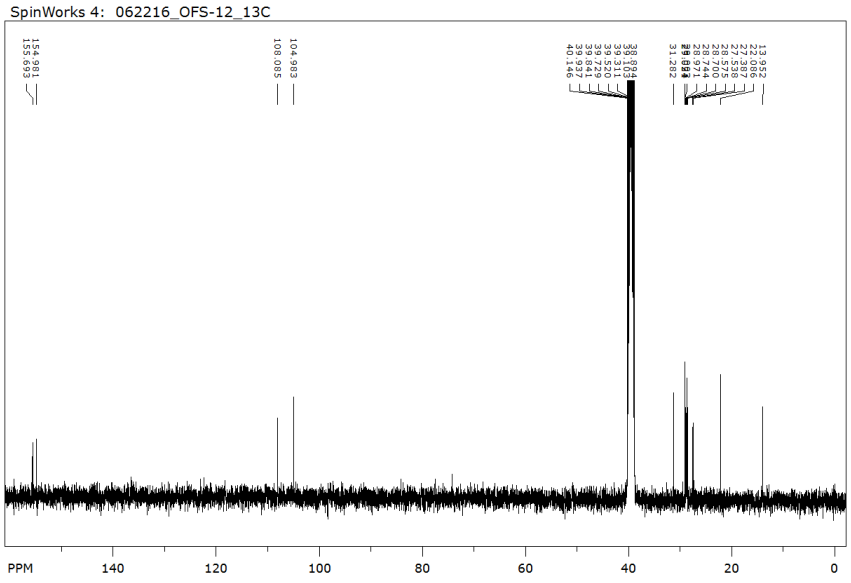

Figure 3-24. ^{13}C NMR of OFS-12 in DMSO-d_6

As listed in **Figure 3-25**, sulfonation of three acylated furans including C_{12}, C_{14}, and C_{18} yielded three oleo-furan sulfonate surfactants identified as OFS-n-1/O to denote the ketone functionality on the alkyl chain at the first carbon position. A fourth ketone surfactant was

prepared from cocinic acid, a mixture of C_8 to C_{18} fatty acids. Linear (OFS-n) surfactants prepared by hydrodeoxygenation and branched (OFS-12-2/C2H5) surfactants prepared by aldol condensation were sulfonated by the same method.

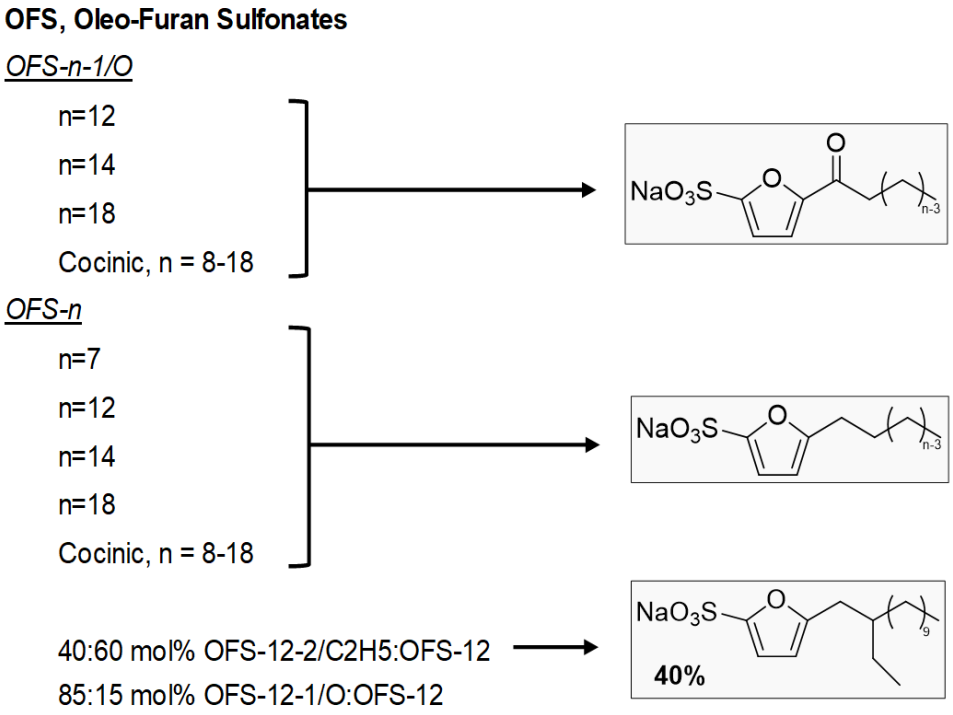

Figure 3-25. Structures of various oleo-furan sulfonate surfactants synthesized from furan and fatty acids

3.4 Conclusions[2]

Facile assembly of xylose-derived furan molecules with triglyceride-derived fatty acids into oleo-furan surfactants demonstrates a highly tunable method for renewable surfactant synthesis. These surfactants utilize straight alkyl chains that are optimal for biodegradation.[25,96,97] The synthesis of OFS molecules is highly tunable. Surfactant properties

[2] (Permissions obtained from ACE Central Science: Park, D. S., et al., ACS Central Science 2: 820–824, 2016, http://pubs.acs.org/doi/pdfplus/10.1021/acscentsci.6b00208)

can be selected by using different sources of triglycerides and by coupling various chemistries to obtain a wide range of surfactants incorporating linear or branched structure or different chemical functionalities. Fatty acids with varying chain lengths, from 7 to 18 carbon atoms, were used to synthesize a wide range of surfactants with different hydrophobic tail lengths. The coupling of chemistries such as acylation, hydrogenation, aldol condensation, and sulfonation aid in the synthesis of linear, branched, and functionalized surfactants exhibiting high control over the tunability of reactions and surfactant structure (**Figure 3-26**). High yield and selectivity (>90%) toward the desired OFS precursor can be achieved in the presence of a zeolite catalyst. The acylation reaction is advantageous over alkylation, because acylated aromatic products do not easily isomerize or continue to acylate (e.g. multiple bonding of alkyl chains to an aromatic ring). Conversely, alkylated benzene molecules tend to isomerize, forming products with alkyl branches with variable length, thereby reducing selectivity toward desired products. Additionally, aromatics with terminal linear alkyl substituents can be made by acylation, a product that cannot be produced via alkylation.[98]

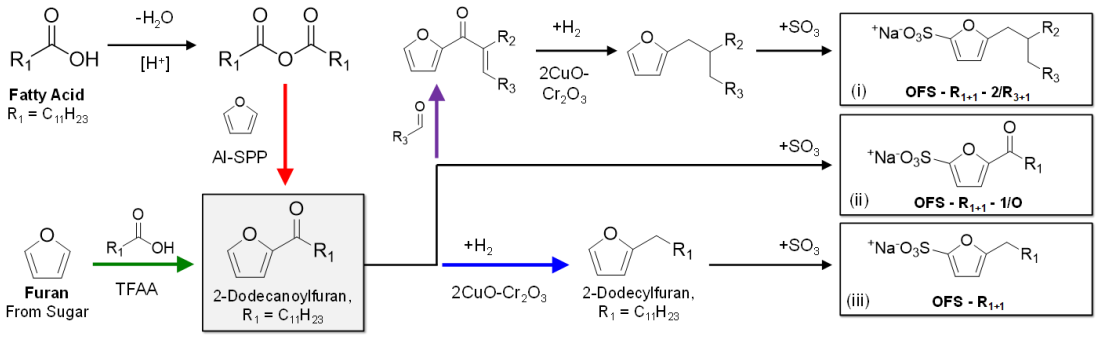

Figure 3-26. Furan acylation to renewable oleo-furan sulfonate (OFS) surfactants

Using the aforementioned chemistries (acylation, hydrodeoxygenation and aldol condensation), 10 different OFS surfactant prototypes were synthesized in high purity with variation in the chain length and functionality of the hydrophobic group (**Figure 3-25**). Improvement in the yield of aldol condensation or assessing alternate chemistries will be

pursued in the future. Similarly, evaluation of toxicity, biodegradability and performance in a conventional detergent formulation also remains to be tested.

The ability to precisely select and assemble with heterogeneous catalysts amenable to chemical processing allows for the chemical targeting of specific surfactant performance.

Chapter 4 Performance Evaluation & Structure-Property Relationship of Oleo-Furan Sulfonate Surfactants

4.1 Introduction

In addition to modifying interfacial surface energy, surfactants are characterized by their ability to make and stabilize foams, to wet porous materials such as fibers and particles, and to operate in aggressive conditions such as high temperature or hard water.[99] The breadth of performance targets is sufficiently large that modern surfactant structures cannot be independently optimized for all properties, requiring the use of substantial additives for effective application.[51,100] Chapter 3 discussed the coupling of several chemistries using heterogenous catalysts for the efficient synthesis of surfactants from renewable furans and fatty acids. Here we report the optimization of these oleo-furan sulfonate surfactant structures to form micelles in hard water (e.g. Ca^{2+}) at low temperatures. The limited opportunity for tuning the LAS class of surfactants to further enhance its properties has necessitated incorporation of chemical agents such as metal chelants as depicted in **Figure 4-1**. For example, LAS surfactants in hard water (with Mg^{2+} and Ca^{2+}) require additives such as ethylenediaminetetraacetic acid (EDTA), which preferentially bind to and suspend hard water ions, preventing the ions from forming inactive precipitates or multilamellar vesicles with surfactants.[31,101] Hard water conditions, which often exceed 200 ppm of Ca^{2+},[102] require coformulation of chelating agents with surfactants in equal parts,[31] increasing cost and complexity. Moreover, incorporation of chelating agents is region and application specific, with many compounds such as EDTA and phosphates banned due to their environmental impact.[31,32,103] Despite development of a large variety of alternative chelating

agents including zeolites,[104] citrates, and polycarboxylates,[32] sodium tripolyphosphate remains the standard by which all other chelants are measured.[101]

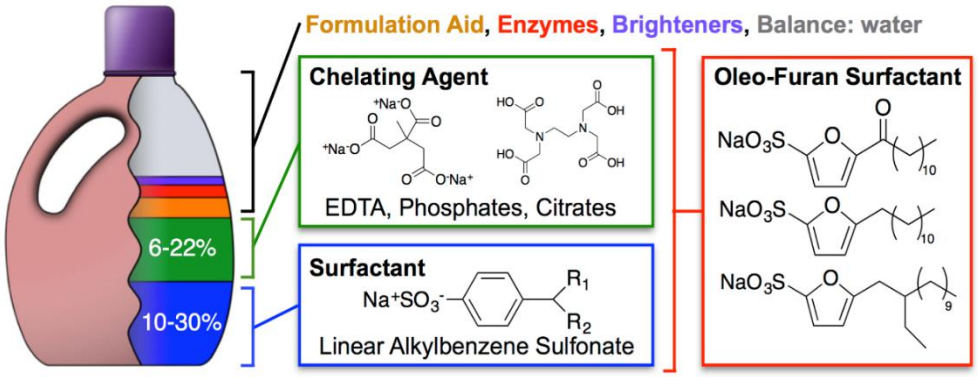

Figure 4-1. Oleo-furan sulfonate surfactant structure and function. Water-based linear alkylbenzene sulfonate (LAS, blue) surfactants require metal chelating agents (green), both of which are replaced by a single oleo-furan sulfonate surfactant (OFS, red)

The oleo-furan sulfonate (OFS) surfactants link polar and hydrophobic alkyl chains from the fatty acids of natural oils[61] such that they retain detergency without the need for additives such as chelants. We hypothesize that substitution of benzene with furan will increase overall solubility in water and alter the balance of polar and nonpolar groups, thereby allowing for OFS surfactants with straight (unbranched) alkyl chains derived from fatty acids. For each variation of molecular design, surfactant performance is characterized to elucidate the structure−property relationships[105,106] accounting for solvation in water, capability for forming micelles, and stability in hard water; this insight is then used to identify an ideal OFS molecule.[8,58,59]

4.2 Materials and Methods

4.2.1 Chemicals

For the purpose of evaluation and comparison of the renewable oleo-furan sulfonate (OFS) surfactant performance, four different anionic commercial surfactants were purchased; linear alkylbenzene sulfonate (sodium dodecylbenzene sulfonate, 79.7%, Sigma-Aldrich),

sodium lauryl sulfate (sodium dodecyl sulfate, 99.1%, Sigma-Aldrich), sodium lauryl ether sulfate (70.4%, BOC Sciences) and methyl ester sulfonate (Alpha-Step MC-48, 38.76%, Stepan)

4.2.2 Micelle Characterization

a. Dynamic Light Scattering

Dynamic Light Scattering (DLS) has been used in the past for studying surfactant aggregates.[107] Micelle size distribution studies of the OFS-12 surfactant was performed using the Microtrac NANO-flex analyzer which employs a 180° scattering angle DLS technique.[107] Two different surfactant concentration samples were prepared (5.0, 10 × CMC and 20.0 × CMC corresponding to 0.35, 0.70 and 1.40 wt.%) by dissolving the required amount of surfactant in deionized water and filtering the solution after surfactant dissolution using a 0.2μ micropore filter to remove any dust particles. Prior to each sample run, a blank solution (DI water) was used to set the baseline to zero. The average values were computed based on five individual trials each lasting 120 s.

b. Small Angle X-Ray Scattering[3]

Small angle X-ray scattering (SAXS) experiments were performed at the beamline 12-IDB of the Advanced Photon Source, Argonne, IL. The data was obtained at 42 ℃ using a quartz capillary flow cell to minimize beam damage to the sample. The flow cell is equipped with a Peltier heating/cooling device to control the temperature of the sample in the capillary. The X-ray energy was 14 keV (corresponding to a wavelength of 0.886 Å). To avoid radiation damage, the exposure time for each image frame was set to no more than one second. 20-40 images were collected for each sample/solvent

[3] Performed by Meera Shete, Dr. Xiaobing Zuo and Dr. Byeongdu Lee

to obtain good signal-to-noise ratio. The 2D isotropic scattering images were azimuthally averaged to 1D data sets using the computer program provided at the beamline, followed by averaging of the 1D data sets.

4.2.3 Critical Micelle Concentration (CMC)

The value of CMC of the surfactant was measured by recording the decrease in surface tension with increasing surfactant concentration. Six to eight samples with increasing surfactant concentration were prepared by dissolving the required amount of surfactant in deionized water. The solution temperature was kept high enough to ensure that all the surfactant is in solution i.e. the solution temperature was kept above the Krafft point of the surfactant. Surface tension measurements were made using the Krüss digital tensiometer K10ST via the Wilhelmy plate method. The temperature of the solution was monitored during measurement. The surface tension at each concentration was measured three times.

4.2.4 Krafft Point/Temperature

A 1.0 wt.% solution of surfactant in deionized water was prepared for all surfactants except in the case of OFS-12-1/O where a 2.0 wt% solution was used instead. 50 ml of the prepared solution was poured into a beaker surrounded by a freezing mixture of ice and salt (sodium chloride) mounted on a laboratory hot plate with magnetic stirring. The Krafft point (T_K) of the surfactants was measured by estimating the degree of counterion dissociation using a conductivity meter (COND 6+, Oakton/Eutech Instruments) immersed in the surfactant solution capable of measuring both, conductivity, and temperature. The magnetic stirring speed was set to 650 rpm and the solution was first allowed to cool to 0 °C. Upon attainment of this temperature, the solution was slowly heated, and the conductivity was measured in every 0.5 °C increments until it reached a steady value.[108,109]

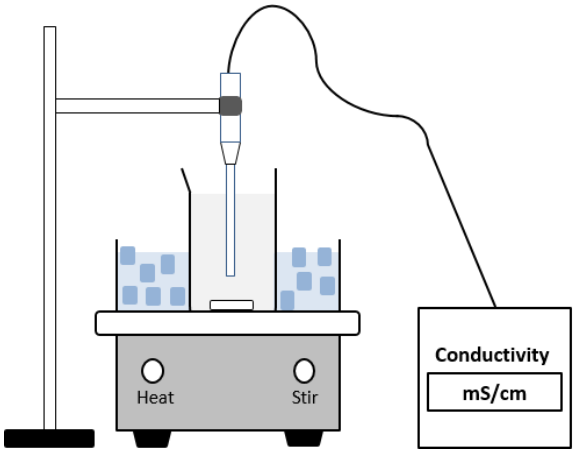

Figure 4-2. Schematic of apparatus used for measurement of Krafft point

4.2.5 Surfactant Foaming

The foaming properties of the surfactants were studied by bubbling air through a 0.5 wt.% surfactant solution in 100 ml of deionized water. The surfactant solution was poured into a 500 mL glass graduated cylinder carefully to avoid any foam formation. Air was bubbled through a 1/8-inch diameter and 16-inch length SS 316 tubing, which was immersed in the solution. A clearance of 1 inch was maintained between the end of the tubing and the bottom of the cylinder. The air flow rate was maintained at 30 sccm using a Brooks 5850E mass flow controller. The cylinder was mounted on a laboratory hot plate with magnetic stirring. A magnetic stirrer rotating at 380 rpm was also used to ensure uniform distribution of bubbles. All measurements were done above the Krafft point of the surfactant solutions. For those surfactants with a Krafft point above room temperature (OFS-12, OFS-14), the graduated cylinder was surrounded by a heated sand bath mounted on the hot plate. The temperature of the sand bath was set such that the solution temperature is just above its Krafft point. Air was bubbled through the solution until the foam height reached a steady value and the height was recorded every thirty seconds by means of a camera.

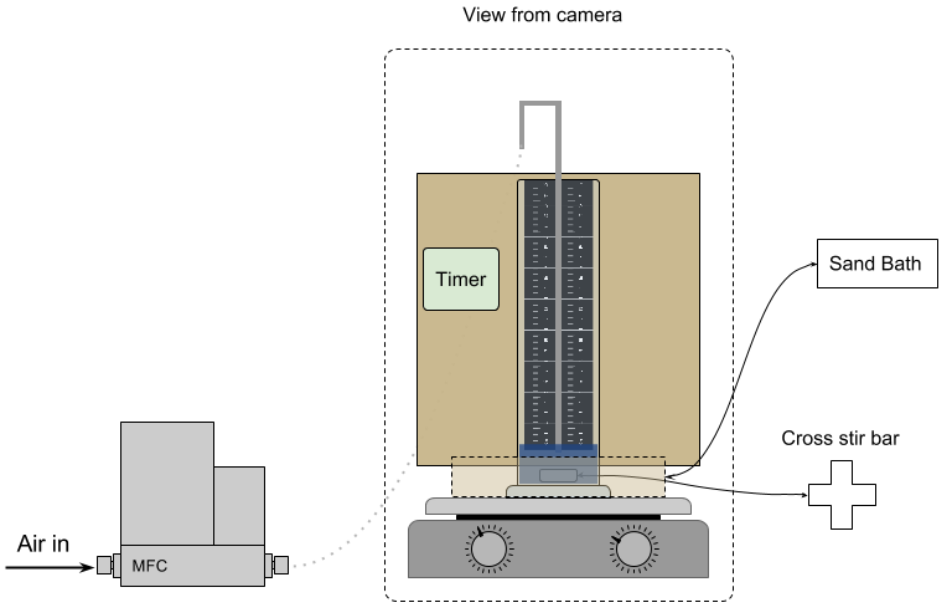

Figure 4-3. Schematic of foaming apparatus set up

4.2.6 Draves Wetting Index

The wettability or the wetting properties of the surfactant were measured according to the ASTM D2281 standard.[110,111] 500 ml of 0.25 wt.% surfactant solution was poured slowly into a 500 ml graduated cylinder to ensure that no foam was created while pouring. Any foam that was created was removed using a bulb-pipet. The temperature of the surfactant solution was maintained around its Krafft point by employing a heated sand bath throughout the course of the experiment. A cotton skein (Test Fabrics, Item# 1203007), weighing approximately 5 g, was folded, and fastened to an S-shaped 3 g copper hook tied to a 40 g lead anchor (lead slug) using a fine linen thread ¾ inch long (Test Fabrics, Item# WEIGHT & HOOK). The ends of the skein were cut at the opposite end and the skein was made compact by drawing the cut skein through fingers before testing the surfactant. It was then dropped into the graduated cylinder containing the solution and the time taken for the

thread to relax and the skein to sink to bottom was recorded as the wetting time (T_D) for 0.25 wt% solution.

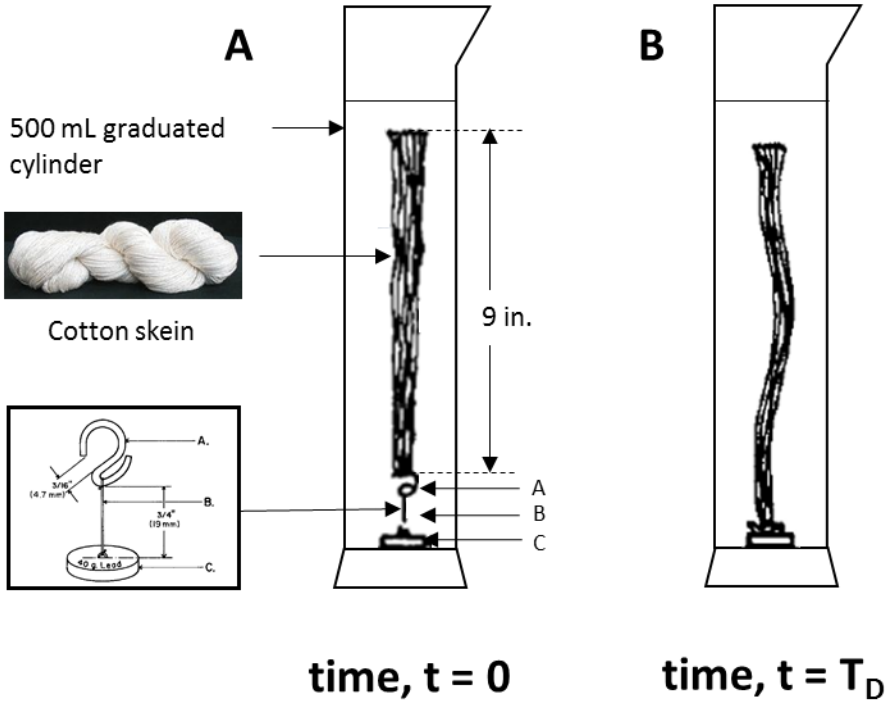

Figure 4-4. Schematic of the apparatus used for the Draves test[111] **A.** The skein is just immersed into the solution at t = 0 s. **B.** The skein sinks after wetting time T_D

4.2.7 Hard water Tolerance

Calcium chloride was used as a divalent counterion, and surface tension of the surfactant solution was measured with increasing concentration of $CaCl_2$ from 1 mM to 450 mM.[112–114] Surface tension measurements were made using the Krüss digital tensiometer K10ST via the Wilhelmy plate method. The temperature of the solution was monitored during measurement. The surface tension at each concentration was measured three times. All experiments were carried out at a concentration equal to twice CMC of each surfactant, and the point of transition from a clear solution to a turbid one was also monitored.[115]

4.3 Results and Discussion

Preparation of precise oleo-furan surfactant molecules permitted evaluation of colloidal properties relative to surfactant structure. Assessment of performance was undertaken by comparing its properties to its structural analog, LAS, and other commercial surfactants such as sodium lauryl ether sulfate (SLES), methyl ester sulfonate (MES) and sodium lauryl sulfate (SLS). Understanding structure property relationships requires a basic understanding of the principles of interfacial science.[116] When a surfactant is added to water, the initial molecules reorient and adsorb on the air-water interface to reduce free energy of the system and this results in a decrease in the surface tension of the solution (**Figure 4-5 A**).[117] Upon surface saturation, additional molecules added to water enter the bulk of the solution to form aggregates known as micelles and further addition of surfactant molecules results in the formation of multiple micellar aggregates (**Figure 4-5 B-C**). The surfactant concentration which marks the onset of micelle formation is defined as the critical micelle concentration (CMC) and is an important property for all surfactants. A micelle in water consists of a definite number of surfactant monomers packed with their hydrophobic tails forming the core and the hydrophilic head oriented outside towards the aqueous phase.[118] Micelles are capable of dissolving compounds that are normally insoluble thereby acting as emulsifiers. Detergents are an example of this phenomenon where micelles can be used to trap oil-like or lipophilic dirt that is normally insoluble in water. Micelle characterization is, thus, an important field to understand their size, shape, and structure in order to determine suitability for various applications. In this study, micelles were characterized via dynamic light scattering and small angle X-ray scattering.

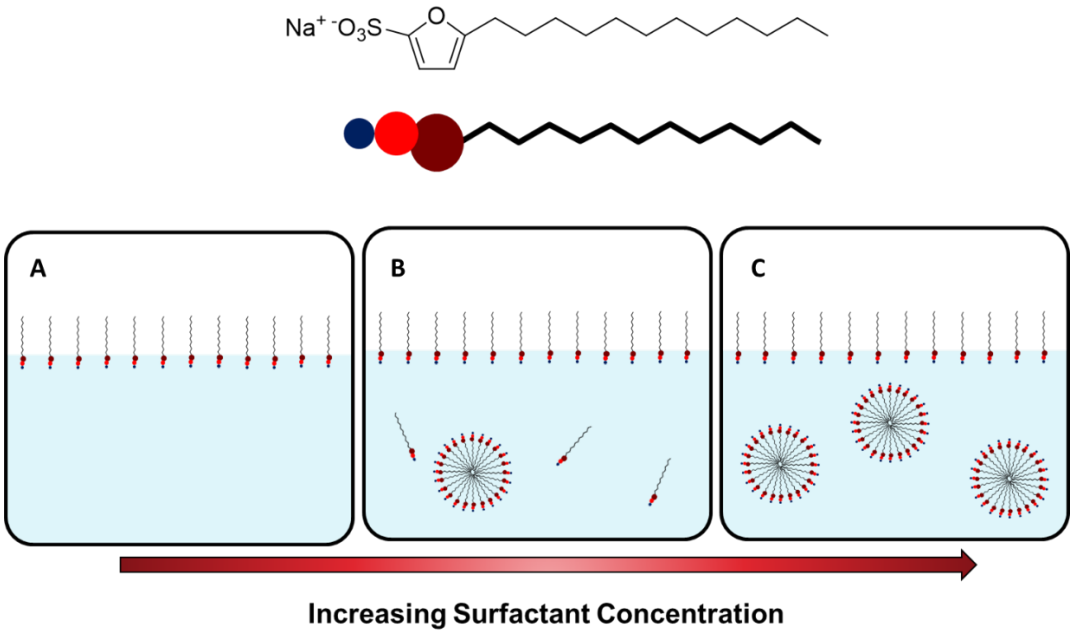

Figure 4-5. Schematic of surfactant adsorption and micelle formation in water

4.3.1 Dynamic Light Scattering

Figure 4-6 shows the average particle size distribution plots for the surfactant solutions at concentrations of 5.0 × CMC, 10.0 × CMC and 20.0 × CMC. From the results we see that all three solutions report an average micelle size between 5-8 nm.

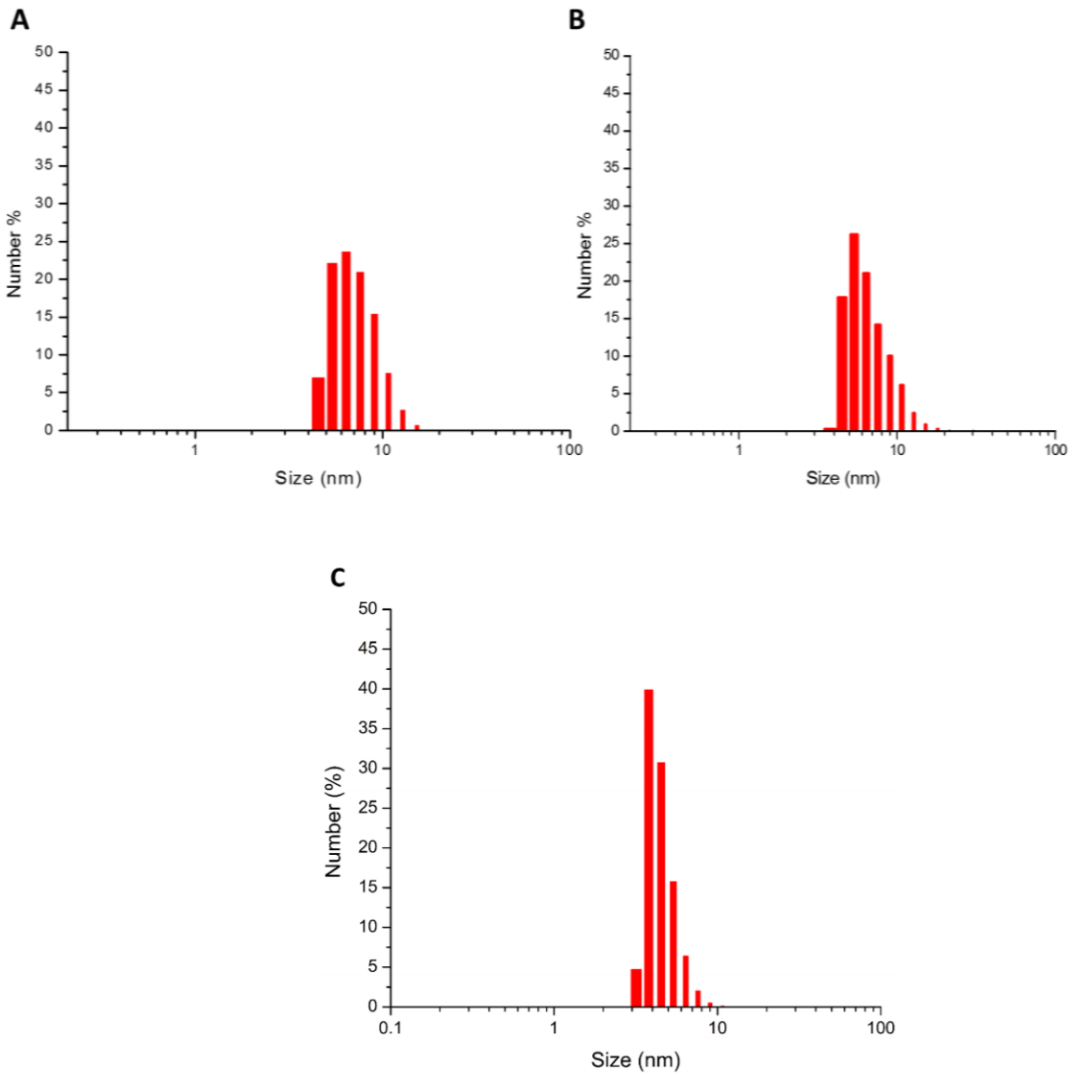

Figure 4-6. Particle size (number) distribution for micelles in OFS-12 surfactant solution with concentration **A.** 5.0 × CMC (average size, 7.41 nm), **B.** 10.0 × CMC (average size, 6.29 nm) and, **C.** 20.0 × CMC (average size, 5 nm)

4.3.2 Small Angle X-Ray Scattering

Figure 4-7A shows the SAXS scattering plots obtained for different concentrations of the OFS-12 surfactant in water while **Figure 4-7B** depicts the background subtracted data. From **Figure 4-7**, we see that, at a surfactant concentration corresponding to 0.5 times the critical micelle concentration (0.5 × CMC, 0.035 wt.%), the sample scattering profile

resembles that of water and there is no scattering feature in the background subtracted SAXS profile (black curve in **Figure 4-7B**). This conforms to the fact that no micelles are formed in solution below its CMC. As we increase the concentration above CMC (10 × CMC and 20 × CMC corresponding to 0.7 and 1.4 wt.%), the appearance of a form factor oscillation at $q > 0.1$ Å $^{-1}$ is indicative of the formation and presence of micelles within the aqueous system. Similar profiles are also reported in literature, where SAXS experiments have been conducted for a commercial sodium lauryl/dodecyl sulfate (SLS/SDS) sample.[119]

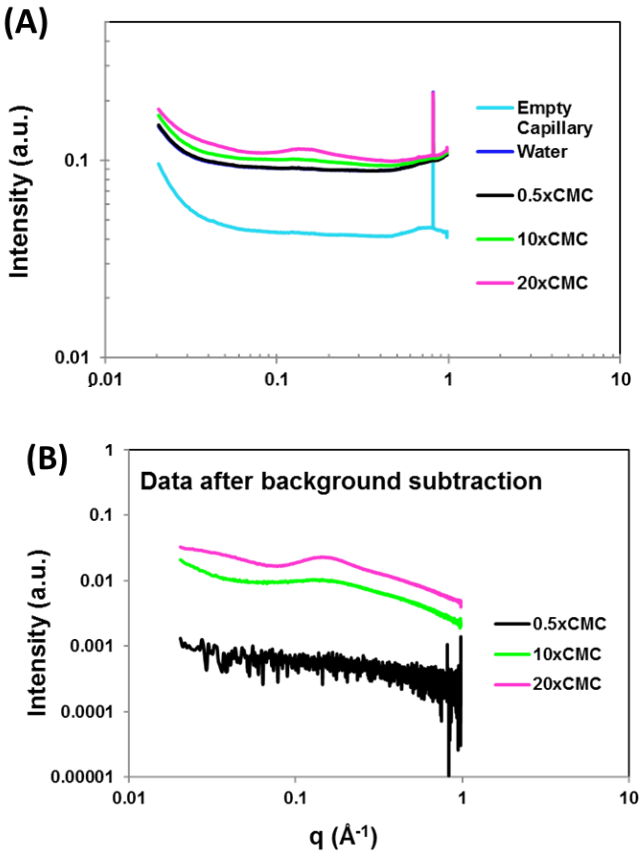

Figure 4-7. Small Angle X-Ray Scattering. **A.** Experimental SAXS profiles for varying concentrations of OFS-12 surfactant below and above CMC and for the solvent (water) **B.** Scattering profiles obtained after subtracting the background (capillary with water).

Pair Distance Distribution Function

SAXS data of surfactant micelles have been analyzed using pair distance distribution function (PDDF), which is defined as

$$P(x) = x^2 \langle \int \eta(\vec{u})\eta(\vec{x}+\vec{u})d\vec{u} \rangle$$

Where $\eta(\vec{u}) = \rho(\vec{u}) - \rho_{solvent}$ and $\rho(\vec{u})$ and $\rho_{solvent}$ are the electron density at position $\vec{u}$ and solvent, respectively (**Figure 4-8**). Thus $\eta_{\text{solvent}} = 0$. The bracket depicts the orientational average.

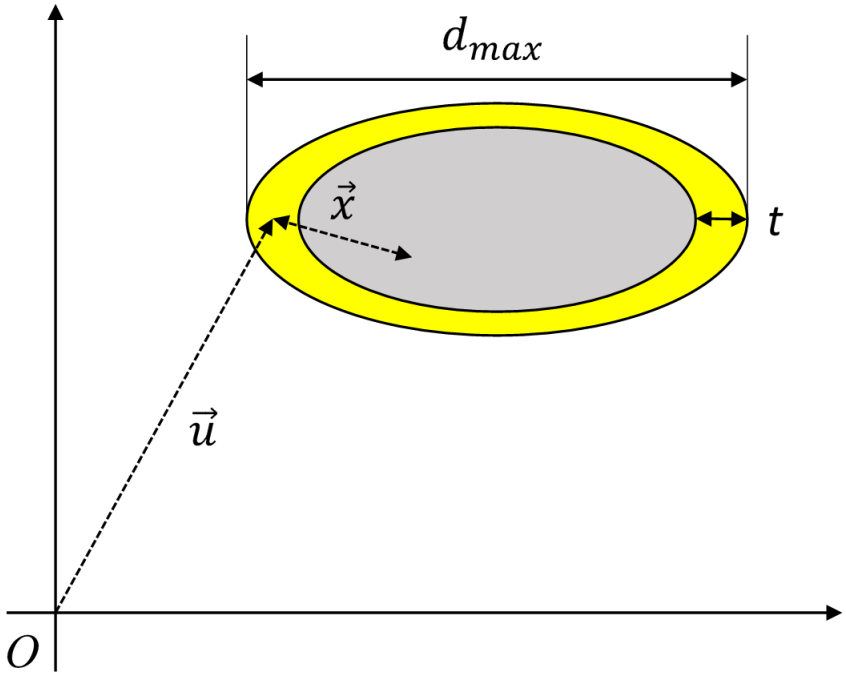

Figure 4-8. Vector representation of a micelle

In a micelle, $\eta_{shell} > 0$ and $\eta_{core} < 0$. When both ends of the vector $\vec{x}$ ($\vec{u}$ or $\vec{x}+\vec{u}$) is either in the shell or core, $\eta(\vec{u})\eta(\vec{x}+\vec{u})$ is positive. When one of its end is on solvent phase, $\eta(\vec{u})\eta(\vec{x}+\vec{u})$=0. When one end is on the shell and the other is on the core, $\eta(\vec{u})\eta(\vec{x}+\vec{u})$ becomes negative. Therefore, it is possible to approximately picture the shape of the PDDF function of a core-shell structure. When x is shorter than the shell

thickness $P(x)$ is likely positive. When x is longer than the shell thickness, it may become negative. When x is larger than maximum size of the core, it can be positive again. Finally, when x is larger than d_{max}, $P(x) = 0$. If an object is made of only single phase without a shell, $P(x)$ will be positive at any x smaller than d_{max} and will be $P(x) = 0$ for x larger than d_{max}. The PDDF can be calculated from an experimental data using software program such as GNOM.[120] The PDDF plot shown in **Figure 4-9B** obtained via the fit in **Figure 4-9A** of the SAXS data (20 × CMC, OFS-12) shows a typical PDDF expected from the core-shell structure.[119] The largest dimension obtained from the PDDF was about 7~8 nm determined from **Figure 4-9B**. This agrees with the DLS data of **Figure 4-6C** (which is the same sample at 20 × CMC) with particle sizes of 4-8 nm.

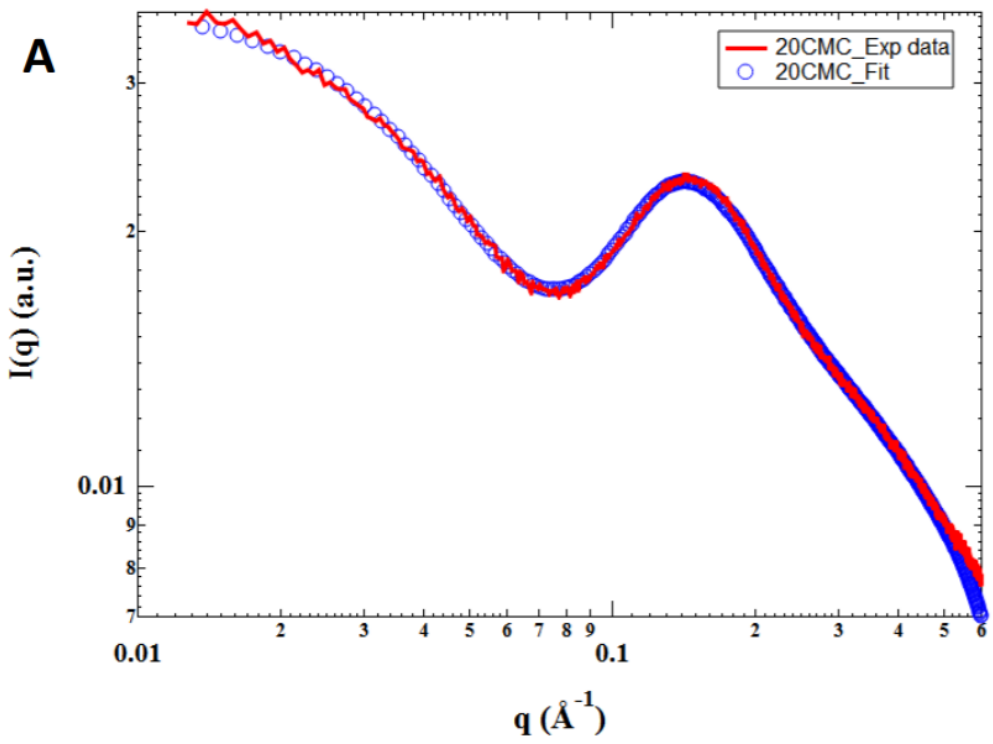

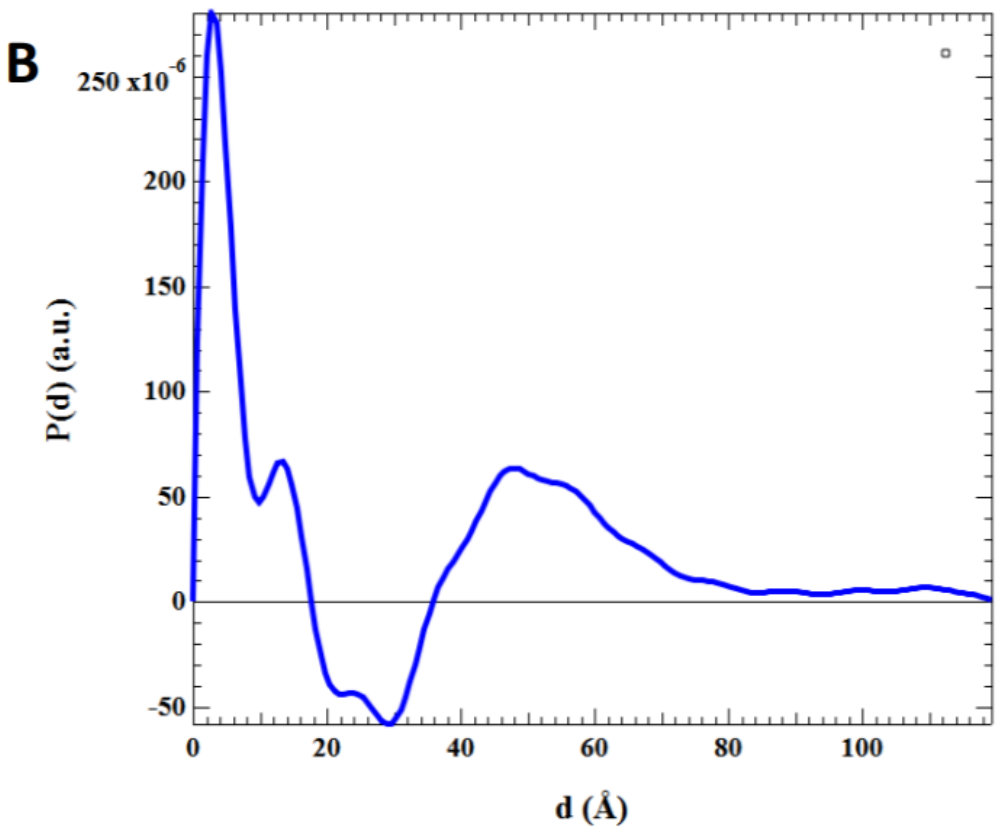

Figure 4-9. PDDF of OFS-12 SAXS Data. **A.** The SAXS data (red) and fit (blue). **B.** Intraparticle Pair Distance

4.3.3 Critical Micelle Concentration

Surfactant performance was evaluated by measuring the critical micelle concentration (CMC), defined as the minimum concentration for which dissolved surfactants spontaneously self-assemble to micelles. The value of CMC of the surfactant was measured by recording the decrease in surface tension with increasing surfactant concentration. CMC was reported as the value of concentration corresponding to the point of intersection of two straight lines drawn to fit the plot of surface tension vs. ln (surfactant concentration). The CMC plots for commercial surfactants (LAS, SLES, SLS and MES) and oleo-furan

sulfonate surfactants (OFS-n-1/O, OFS-n, OFS-12-2/C2H5 and OFS-Cocinic) are shown in **Figure 4-10**, **Figure 4-11**and **Figure 4-12**.

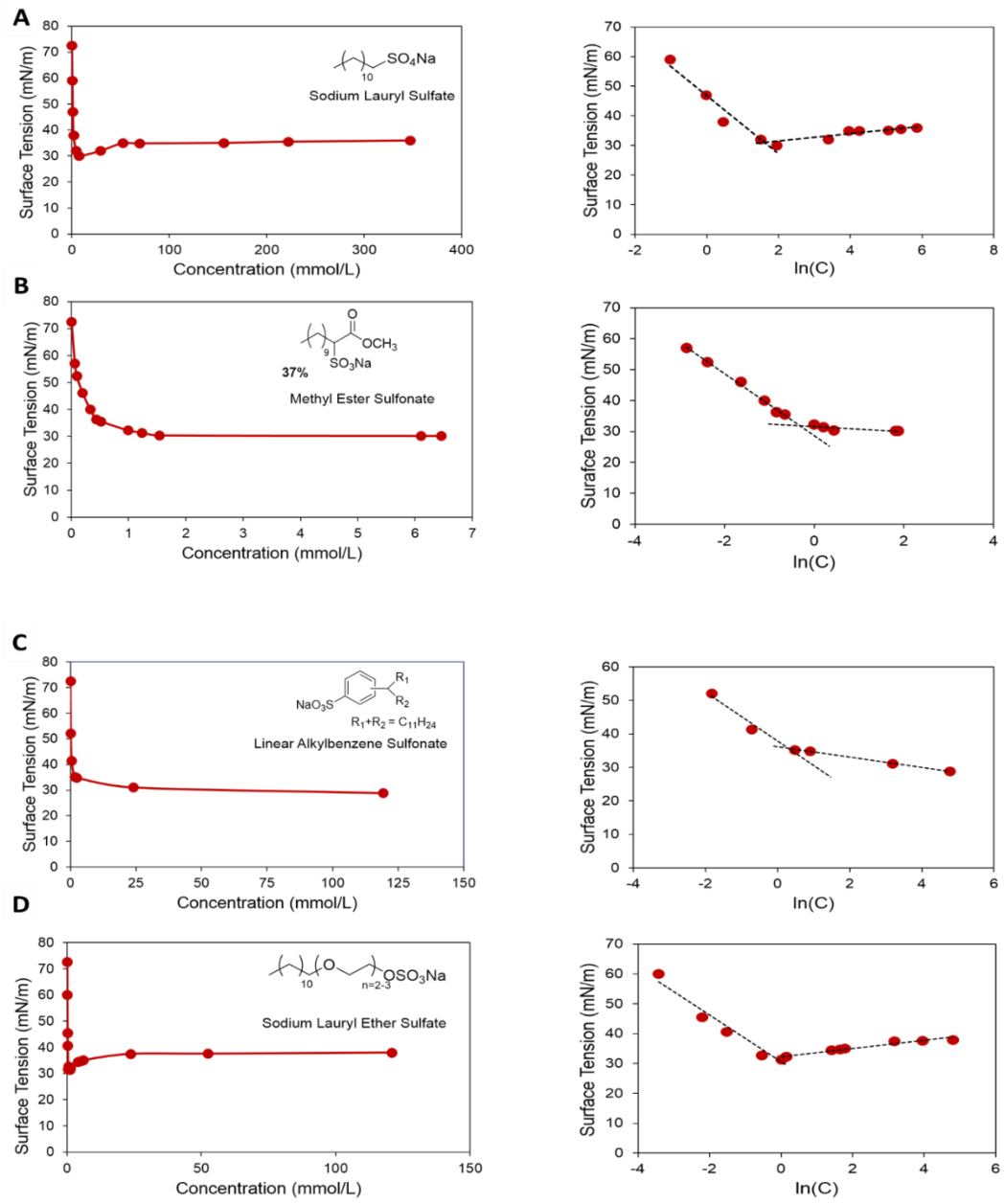

Figure 4-10. Surface tension versus surfactant concentration of commercial surfactants: **A.** Sodium Lauryl Sulfate (SLS), **B.** Methyl Ester Sulfonate (MES), **C.** Linear Alkylbenzene Sulfonate (LAS) and, **D.** Sodium Lauryl Ether Sulfate (SLES).

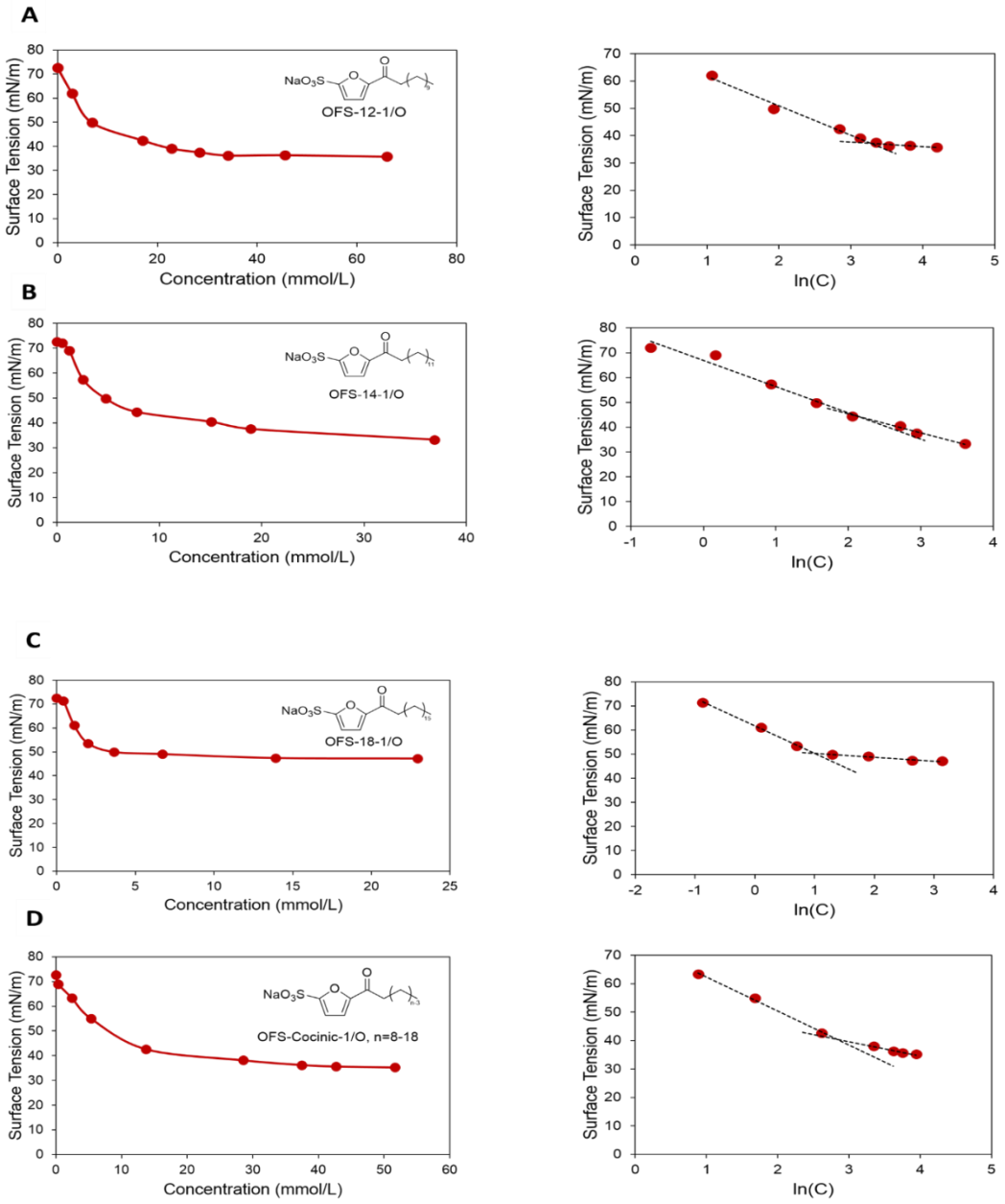

Figure 4-11. Surface tension versus surfactant concentration of renewable OFS-n-1/O surfactants: **A.** OFS-12-1/O, **B.** OFS-14-1/O, **C.** OFS-18-1/O and, **D.** OFS-Cocinic-1/O, n = 8-18

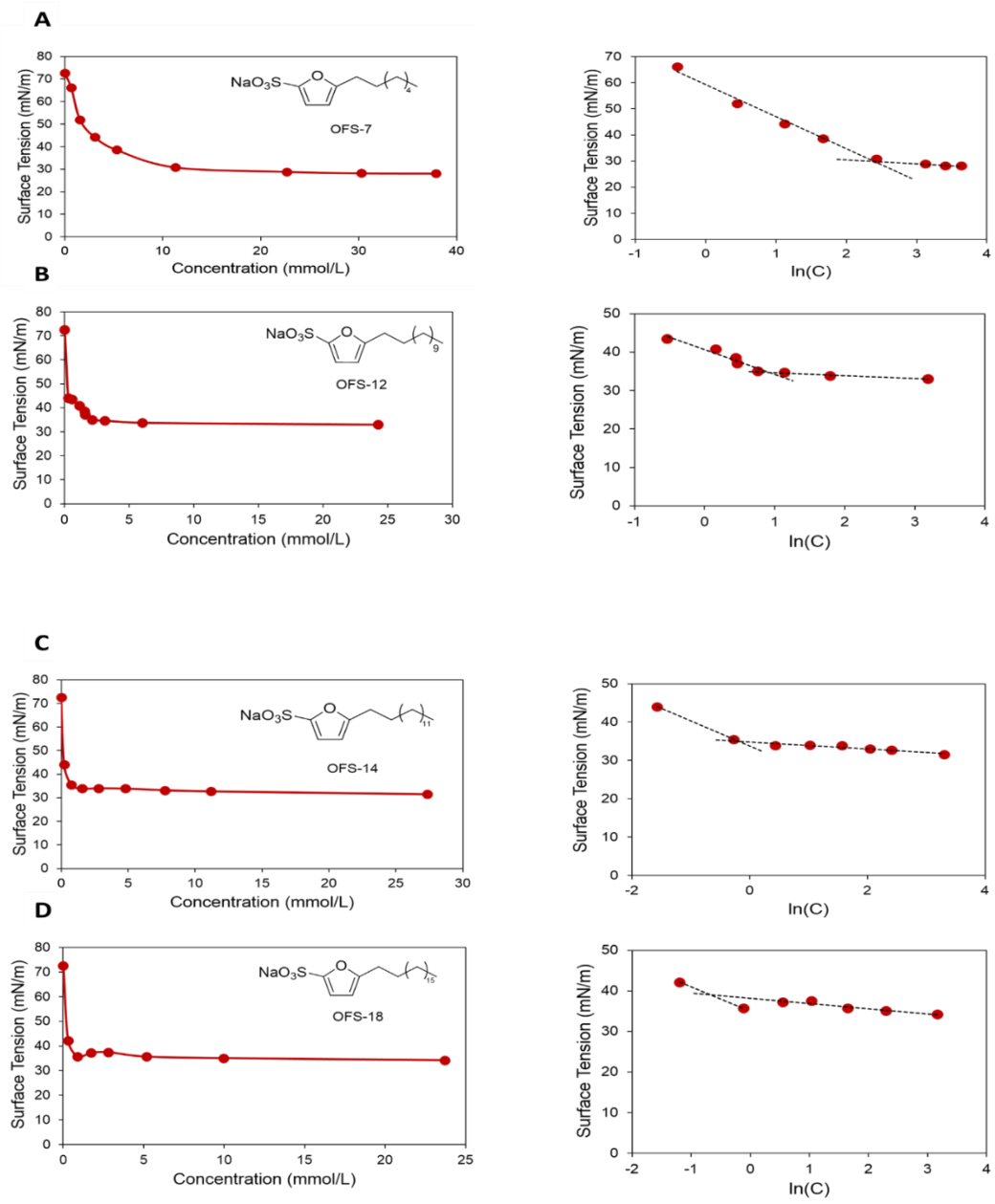
A
Surface Tension (mN/m)
Concentration (mmol/L)
NaO3S
OFS-7
ln(C)
B
OFS-12
C
OFS-14
D
OFS-18

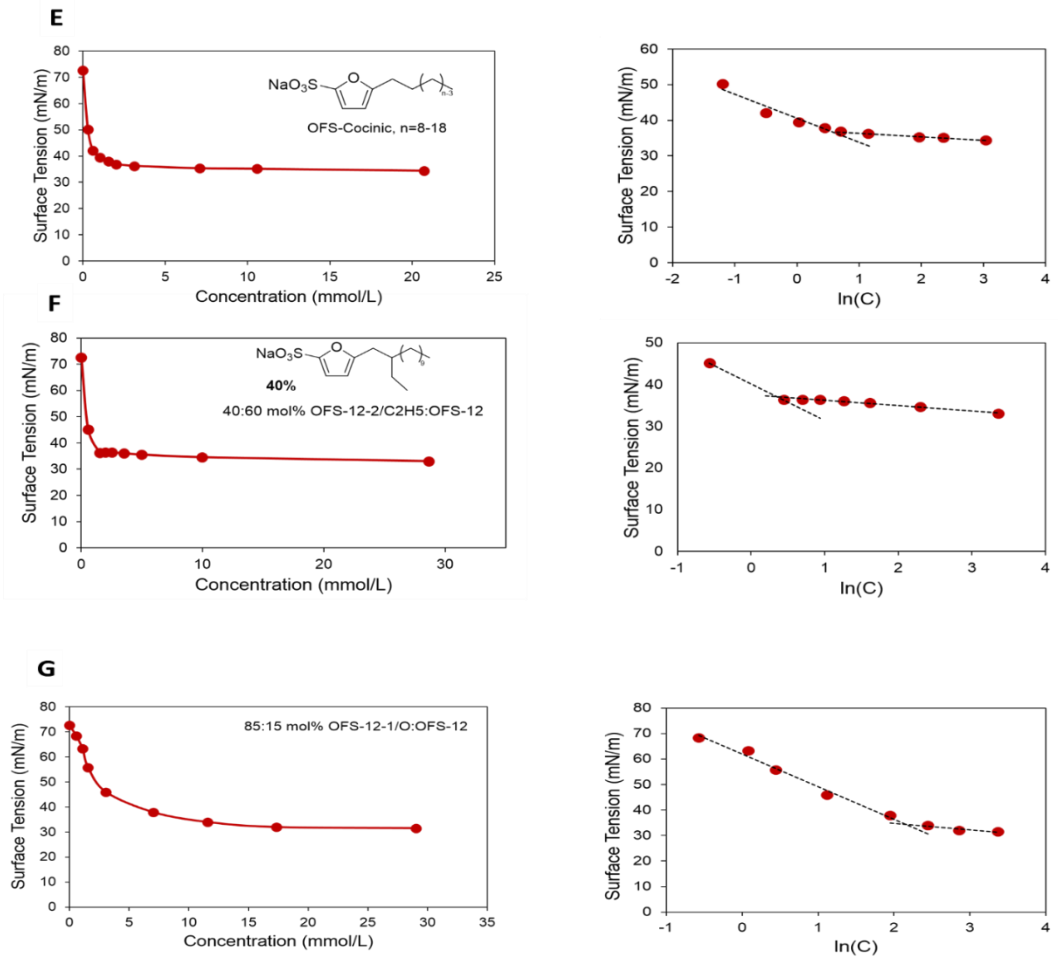

Figure 4-12. Surface tension versus surfactant concentration of renewable OFS-n surfactants: **A.** OFS-7, **B.** OFS-12, **C.** OFS-14, **D.** OFS-18, **E.** OFS-Cocinic, n = 8-18, **F.** 40:60 mol% OFS-12-2/C2H5:OFS-12 and, **G.** 85:15 mol% OFS-12-1/O:OFS-12

The values obtained for the CMC of commercial and OFS surfactants are summarized in **Table 4-1**.

Table 4-1. Summary of CMC values for all surfactants in ppm and mmol/L (mM)

		CMC*	
Surfactant		[ppm]	mmol/L
Commercial			
	SLS, Sodium Lauryl Sulfate	2010	6.97
	MES, Methyl Ester Sulfonate	130	0.41
	LAS, Linear Alkylbenzene Sulfonate	460	1.33
	SLES, Sodium Lauryl Ether Sulfate	380	1.01
OFS, Oleo-Furan Sulfonates			
	OFS-12-1/O	11520	33.11
	OFS-14-1/O	3127	8.26
	OFS-18-1/O	1156	2.65
	OFS-Cocinic-1/O	4890	14.01
	OFS-7	2669	9.99
	OFS-12	720	2.13
	OFS-14	267	0.72
	OFS-18	316	0.75
	OFS-Cocinic	512	1.51
	40:60 mol% OFS-12-2/C2H5:OFS-12	496	1.43
	85:15 mol% OFS-12-1/O:OFS-12	2445	7.01
*Critical Micelle Concentration, measured above Krafft point			

We observe the trend of decreasing CMCs with increasing carbon number in the chain. This is because increasing the carbon number increases hydrophobicity of the molecule and hence promotes micelle formation at lower surfactant concentrations. The ketonic OFS-n-1/O species were found to have poorer CMC values when compared to the straight chain OFS-n analogs. One hypothesis for this observation is that the presence of the carbonyl group increases the overall hydrophilic nature of the molecule due to extended conjugation. As the carbon number in the ketone series increases, we see an order of magnitude decrease in the CMC value from 11,520 to 1156 ppm for OFS-12-1/O and OFS-18-1/O respectively. Another interesting comparison is between the CMC of the commercial surfactant LAS and OFS-Cocinic which are both mixtures. It is observed that the furan mixture performs better and has a lower CMC than the LAS mixture.

4.3.4 Krafft Point/Temperature

Surfactants were also characterized by their Krafft temperature or Krafft point (T_K), defined as the temperature below which surfactants form solid crystals i.e. it is the minimum temperature at which surfactants form micelles. Below Krafft point, the surfactants precipitate out of solution and remain in the crystalline phase.[110] A 1.0 wt.% solution of surfactant in deionized water was prepared for all surfactants except in the case of OFS-12-1/O where a 2.0 wt% solution was used instead, since its CMC is roughly about 1.1 wt%. The Krafft point was taken as the temperature where the conductivity vs. temperature plot exhibited a sharp change in slope. Visually, this corresponded to the surfactant solution transitioning from a turbid system due to the precipitated surfactant crystals below the Krafft point to a clear solution indicating the dissolution of surfactants and the formation of micelles in water. The Krafft point data plots for commercial surfactants (SLS and LAS) and oleo-furan sulfonate surfactants (OFS-n, OFS-12-2/C2H5 and OFS-Cocinic) are shown in **Figure 4-13**and **Figure 4-14**.

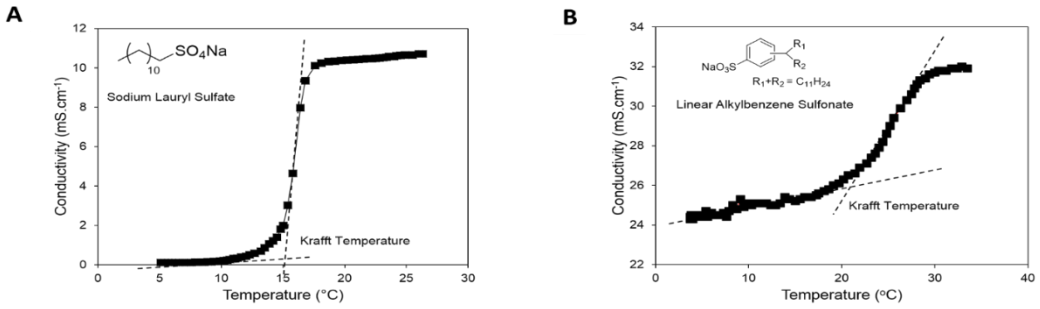

Figure 4-13. Conductivity versus temperature of 1.0 wt% commercial surfactant solutions for determination of Krafft point: **A.** Sodium Lauryl Sulfate (SLS) and, **B.** Linear Alkylbenzene Sulfonate (LAS)

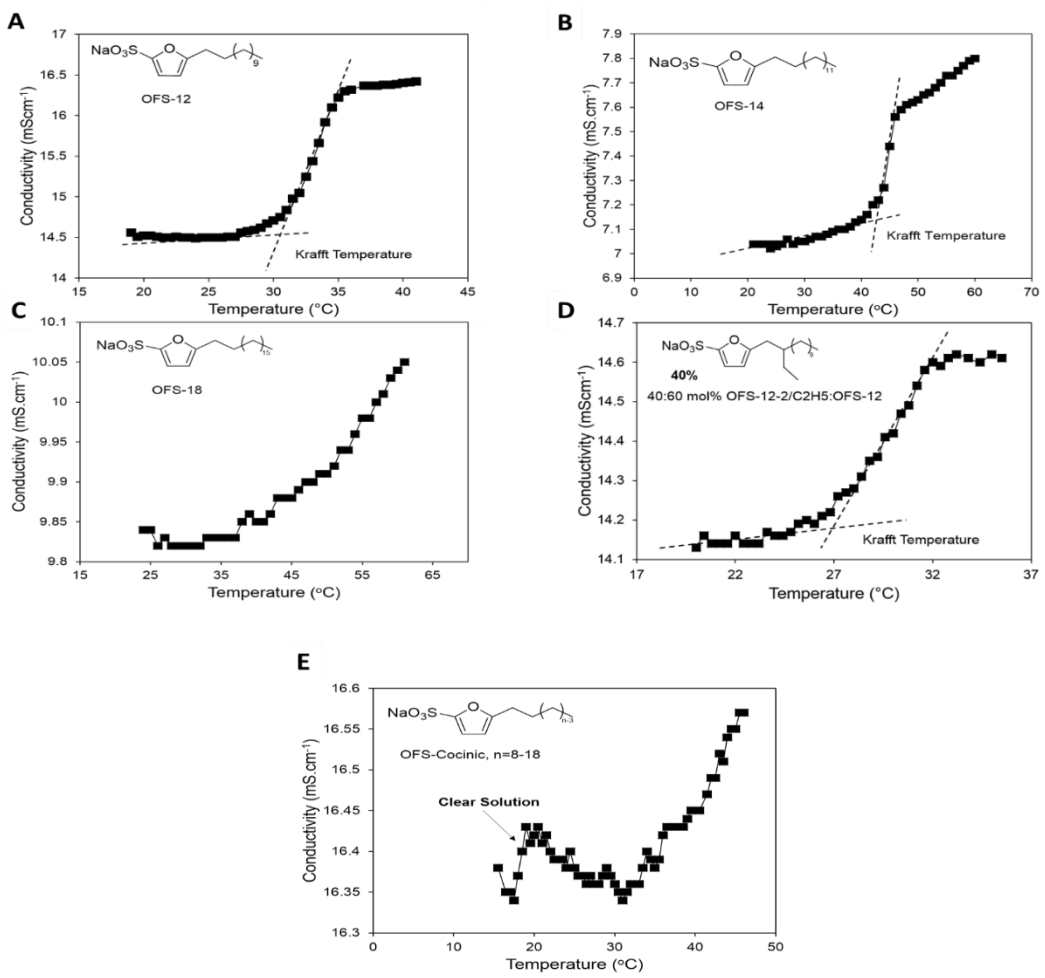

Figure 4-14. Conductivity vs temperature of 1.0 wt.% renewable OFS-n surfactant solutions for determination of Krafft point: **A.** OFS-12, **B.** OFS-14, **C.** OFS-18, **D.** 40:60 mol% OFS-12-2/C2H5:OFS-12 and, **E.** OFS-Cocinic, n = 8-18

The values obtained for the Krafft point of commercial and OFS surfactants are summarized in **Table 4-2**.

Table 4-2. Summary of Krafft points for all surfactants

Surfactant		Krafft Point* [ºC]
Commercial		
	SLS, Sodium Lauryl Sulfate	15.0 ± 1.2
	MES, Methyl Ester Sulfonate	< 0
	LAS, Linear Alkylbenzene Sulfonate	20.0 ± 2.5
	SLES, Sodium Lauryl Ether Sulfate	< 0
OFS, Oleo-Furan Sulfonates		
	OFS-12-1/O	< 0
	OFS-14-1/O	< 0
	OFS-18-1/O	< 0
	OFS-Cocinic-1/O	< 0
	OFS-7	< 0
	OFS-12	30.0 ± 1.0
	OFS-14	41.5 ± 0.9
	OFS-18	> 50
	OFS-Cocinic	18.5 ± 0.5
	40:60 mol% OFS-12-2/C2H5:OFS-12	25.7 ± 0.5
	85:15 mol% OFS-12-1/O:OFS-12	< 0
*Measured at 1.0 wt% surfactant in water except for OFS-12-1/O		

In the case of OFS-18, maximum temperature operation limits of the conductivity probe did not allow the estimation of Krafft point, and thus the value is reported as >50 ºC. For the OFS-Cocinic, n = 8-18 surfactant, the conductivity vs temperature plot was erratic, which is attributed to the presence of 6 different surfactants in the mixture. The solution changed from turbid to clear at approximately 18.5 ºC which was, therefore, reported as the Krafft point. Methyl Ester Sulfonate (MES), Sodium Lauryl Ether Sulfate (SLES), OFS-7 and all OFS-n-1/O surfactant solutions remained clear even at 0 ºC; the Krafft point was thus reported as <0 ºC. It was observed that an increase in the Krafft point is promoted by the increase in number of carbon atoms in the chain. Factors that contribute towards increased water solubility help lower the Krafft point. Increasing the number of carbon

atoms increases the hydrophobicity of the molecule thereby leading to an increase in Krafft point. A similar reasoning can be used to elucidate very low values of Krafft point for the ketonic OFS-n-1/O species when compared to their linear OFS-n counterparts. Another interesting observation is the lowering in Krafft point upon introduction of branching in the structure. The temperature drops by almost 15 ℃ upon the addition of a single branching for a fourteen-carbon alkyl chain as seen for OFS-14 and OFS-12-2/C2H5.

Figure 4-15 compares the performance of commercial and OFS surfactants based on their CMC and Krafft point values. Dashed lines denoting the requirements of common aqueous application concentration (2000 ppm, red) and cold-water detergency (30 °C, blue) form the bounds of the lower left region of **Figure 4-15**, at which the surfactant has desirable properties in cold water and dilute conditions. Direct comparison of OFS and LAS reveals that the oleo-furan structure exhibits superior detergency. OFS-12 with a linear alkyl chain achieves feasible performance (CMC of 720 ppm, T_K of 30 °C) while the analogous LAS-12 linear alkyl chain has a higher Krafft temperature of 58 °C;[27] the furan linker moiety can therefore be interpreted as improving surfactant solubility relative to benzene. Introduction of moderate two-carbon branching in a 40:60 ratio of OFS-12-2/C2H5:OFS-12 also lowers the CMC and Krafft temperature, further improving surfactancy. However, the most dramatic performance enhancement was derived from the mixture of linear alkyl chains found in OFS-cocinic (CMC of 512 ppm, T_K of 18 ℃): the variation of linear alkyl chain lengths in OFS-cocinic with a furan linker is comparable to that of branched LAS (CMC of 460 ppm, T_K = 20 °C).

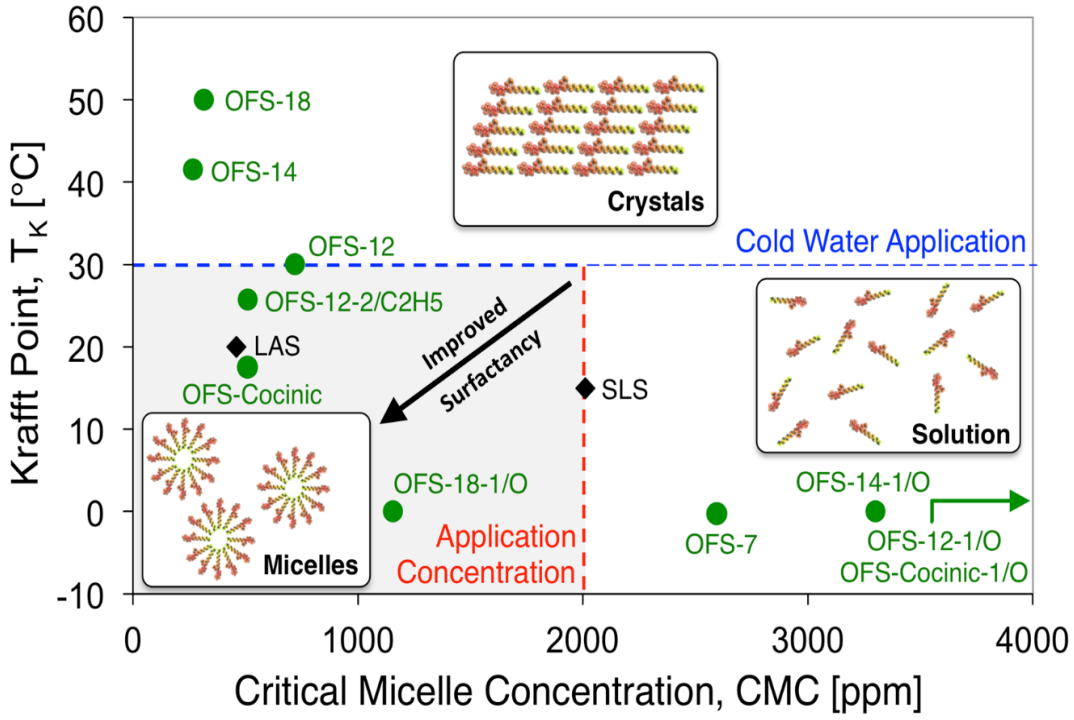

Figure 4-15. Oleo-furan surfactant performance. Comparison of the surfactant critical micelle concentration (CMC) above which micelles form and the Krafft temperature (T_K) below which surfactants crystallize as a separate solid phase. Optimal conditions for aqueous applications (gray box) require a Krafft point below 30 °C and a critical micelle concentration below about 2000 ppm. Linear chain oleo-furan sulfonate surfactants (OFS-12 and OFS-cocinic) and branched OFS-12-2/C2H5 exhibit comparable or better properties when compared with linear alkylbenzene sulfonates (LAS)

4.3.5 Surfactant Foaming

Aqueous surfactant solutions were characterized for their ability to grow foams and stabilize a height of foam at steady state. The initial rate of foam growth was measured by calculating the slope of the linear region of the height vs. time plot before it attained equilibrium. The height of the foam column is indicative of the foaming capacity of the surfactant; the foam height after 60 min of air bubbling was, thus, used as a parameter to report foaming capacity. All surfactant foam heights reached an equilibrium value within 60 min with sodium lauryl ether sulfate (SLES) being an exception. For the purpose of

comparison, Sodium Lauryl Sulfate (SLS) was chosen as a 'reference' surfactant and the initial foam growth rates and 60 min foam heights of all other surfactants were normalized with respect to SLS i.e. foam growth rate metric is reported as ratio of slope of linear region of surfactant *i* to that of SLS (r_i/r_{SLS}) and the foam height metric is reported as the ratio of foam height of surfactant *i* after 60 min (3600 s) to that of SLS ($h_{i\text{-}60}/h_{i\text{-}SLS}$) as shown in **Table 4-3**. **Figure 4-16** shows the evolution of foam and the attainment of foam height equilibrium with time while the foaming data for commercial surfactants (SLS, MES, LAS, and SLES) and oleo-furan sulfonate surfactants (OFS-n, OFS-12-2/C2H5 and OFS-Cocinic) are shown in **Figure 4-13** and **Figure 4-14**. The slope of the linear region (dashed line) represents the initial foam growth rate (r) while the height of the foam column (h60), after 60 min (3600s), is used as a foaming capacity indicator.

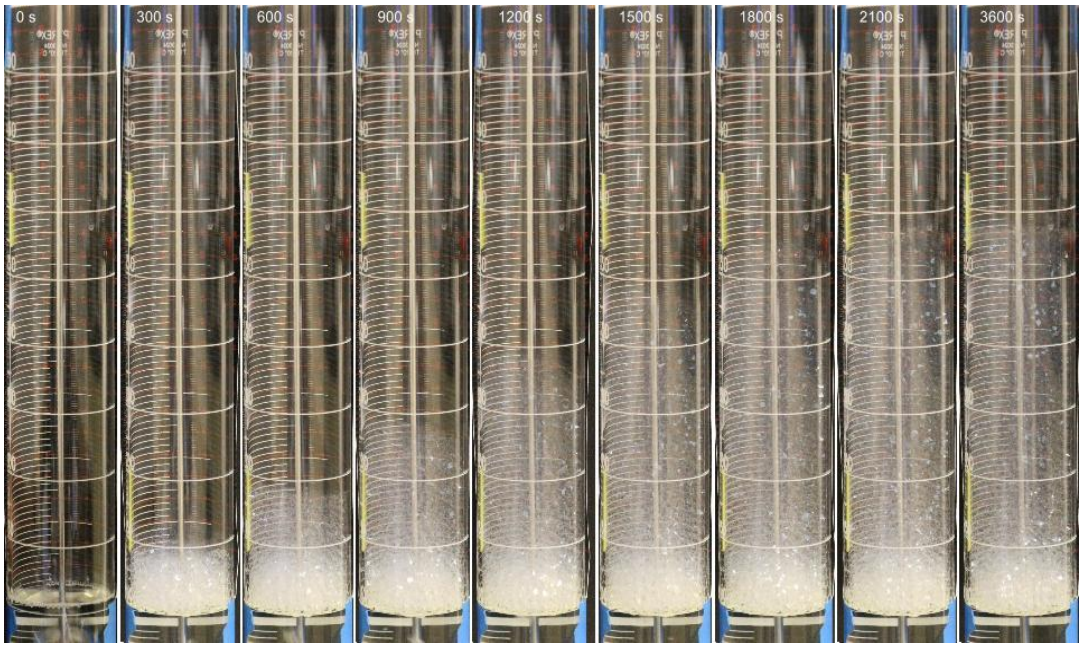

Figure 4-16. Foam growth of 0.5 wt% solution of OFS-12 for increasing times (left to right) up to 1 h (times in seconds are indicated on upper left insets)

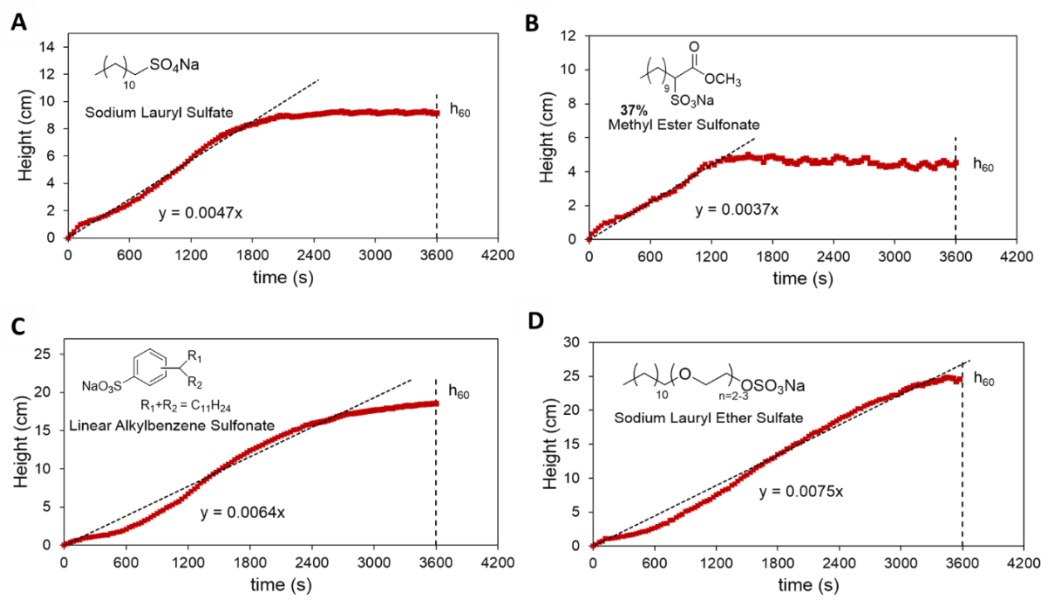

Figure 4-17. Foam height vs. time of 0.5 wt% commercial surfactant solutions: **A.** Sodium Lauryl Sulfate (SLS), **B.** Methyl Ester Sulfonate (MES), **C.** Linear Alkylbenzene Sulfonate (LAS) and, **D.** Sodium Lauryl Ether Sulfate (SLES)

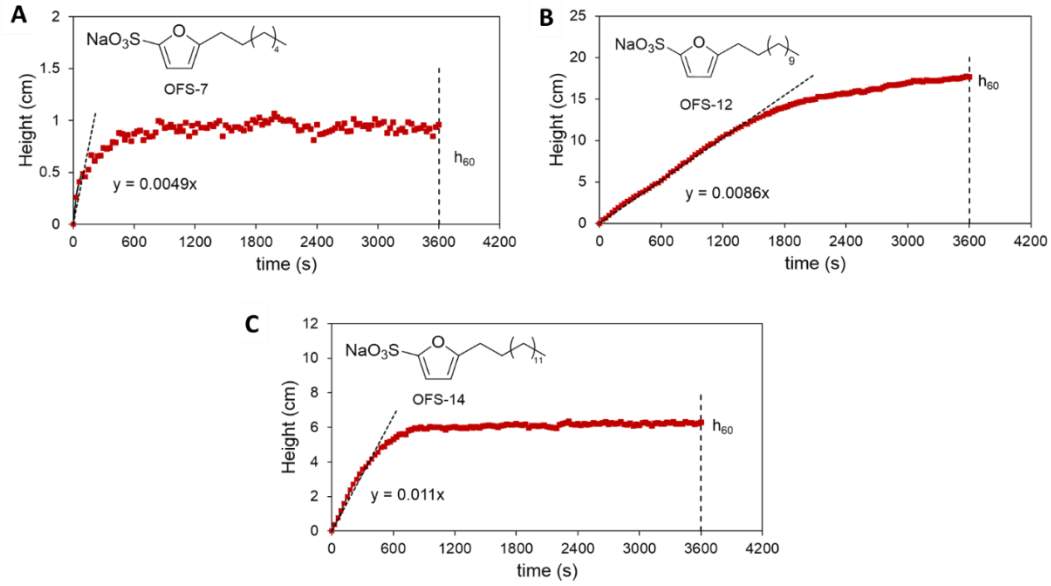

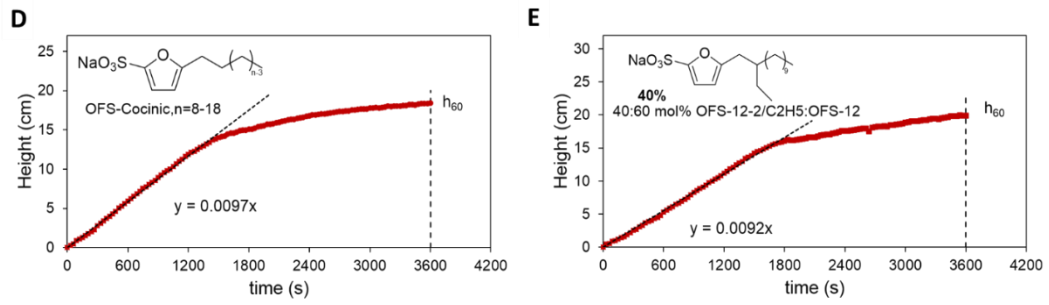

Figure 4-18. Foam height versus time of 0.5 wt% renewable OFS-n surfactant solutions: **A.** OFS-7, **B.** OFS-12, C. OFS-14, **D.** OFS-Cocinic, n = 8-18 and, **E.** 40:60 mol% OFS-12-2/C2H5:OFS-12.

Table 4-3 summarizes the normalized values of foam growth rate and foam height with respect to SLS.

Table 4-3. Summary of foaming parameters of all surfactants; normalized initial growth rates and foam heights after 60 min with respect to SLS

Surfactant	**Foam Growth Rate[a]** r_i / r_{SLS} [-]	**Foam Height$_{60}$[a,b]** $h_{i\text{-}60} / h_{i\text{-}SLS}$ [-]
Commercial		
SLS, Sodium Lauryl Sulfate	1.00	1.00
MES, Methyl Ester Sulfonate	0.79	0.54
LAS, Linear Alkylbenzene Sulfonate	1.36	2.20
SLES, Sodium Lauryl Ether Sulfate	1.60	2.94
OFS, Oleo-Furan Sulfonates		
OFS-12-1/O	0	0
OFS-14-1/O	0	0
OFS-18-1/O	0	0
OFS-Cocinic-1/O	0	0
OFS-7	1.04	0.12
OFS-12	1.83	2.11
OFS-14	2.34	0.75
OFS-18	-	-
OFS-Cocinic	2.06	2.19
40:60 mol% OFS-12-2/C2H5:OFS-12	1.96	2.37
85:15 mol% OFS-12-1/O:OFS-12	-	-

[a]Measured at 0.5 wt.% in water [b]After 60 min (3600 s)

Comparison of foaming metrics of LAS with the furan linear analog OFS-12 reveals similar performance characteristics with OFS-12 possessing a slightly faster foam growth rate. The mixture analog, OFS-Cocinic possesses an even faster growth rate; however, all three surfactants, LAS, OFS-12 and OFS-Cocinic had similar final foam height values. Interestingly, we observe that the addition of two more carbons to the linear chain lowers the foaming capacity by almost one-third as seen in the case of OFS-14. This tunability in size offers great variability in foaming characteristics which is of importance due to varying requirements for different applications (e.g. laundry detergent vs handwashing soap) and hence aids in precise control over properties.

4.3.6 Draves Wetting Index

The results obtained for the wetting time for all the surfactants evaluated in this study are summarized in **Table 4-4**.

Table 4-4. Summary of Draves wetting time for all surfactants

Surfactant		Draves Wetting* [s]
Commercial		
	SLS, Sodium Lauryl Sulfate	6.3 ± 2.7
	MES, Methyl Ester Sulfonate	15.1 ± 3.8
	LAS, Linear Alkylbenzene Sulfonate	4.9 ± 3.2
	SLES, Sodium Lauryl Ether Sulfate	15.4 ± 4.0
OFS, Oleo-Furan Sulfonates		
	OFS-12-1/O	> 3600
	OFS-14-1/O	> 3600
	OFS-18-1/O	> 3600
	OFS-Cocinic-1/O	> 3600
	OFS-7	> 3600
	OFS-12	48.9 ± 13.3
	OFS-14	39.4 ± 7.0
	OFS-18	-
	OFS-Cocinic	58.0 ± 9.4
	40:60 mol% OFS-12-2/C2H5:OFS-12	18.5 ± 1.9
	85:15 mol% OFS-12-1/O:OFS-12	-
*Measured at 0.25 wt% surfactant in water		

Surfactant wetting kinetics, as measured by the Draves test, determines the rate at which an aqueous surfactant solution wets hydrophobic surfaces. The time (T_D) required for surfactant wetting of a cotton skein (i.e., Draves wetting test) in **Table 4-4** indicates desirable wetting characteristics for all OFS-n structures (T_D less than 1 min), suitable for applications requiring fast-acting surfactants.[31]

Branching was found to help reduce the wetting time by almost half as seen in the case of OFS-14 (39.4 min) and OFS-12-2/C2H5 (18.5 min). Molecules with large diffusion coefficients, small molecular weights and large surface area per molecule at the air-water interface have been reported to possess short wetting times.[110] Branching results in larger surface area per molecule at the air-water interface and promotes faster diffusion to the

surface of the yarn. A faster diffusion time warrants a quicker adsorption of the surfactant on the surface of the wetted material and hence quicker wetting times.

4.3.7 Hard water Tolerance

Performance of OFS in hard water conditions indicates dramatically enhanced surfactant stability of furan-based OFS molecules compared with conventional benzene-based and linear surfactants. As increasing amounts of calcium are added to the surfactant solution, the value of calcium concentration above which the surface tension of the surfactant solution increased was recorded as the tolerance value of the surfactant towards calcium as indicated by the dashed red line in **Figure 4-19** - **Figure 4-22**. At the tolerance value, the Ca^{2+} ions disrupt the micelle structure and this value of calcium concentration is referred to as micelle stability.

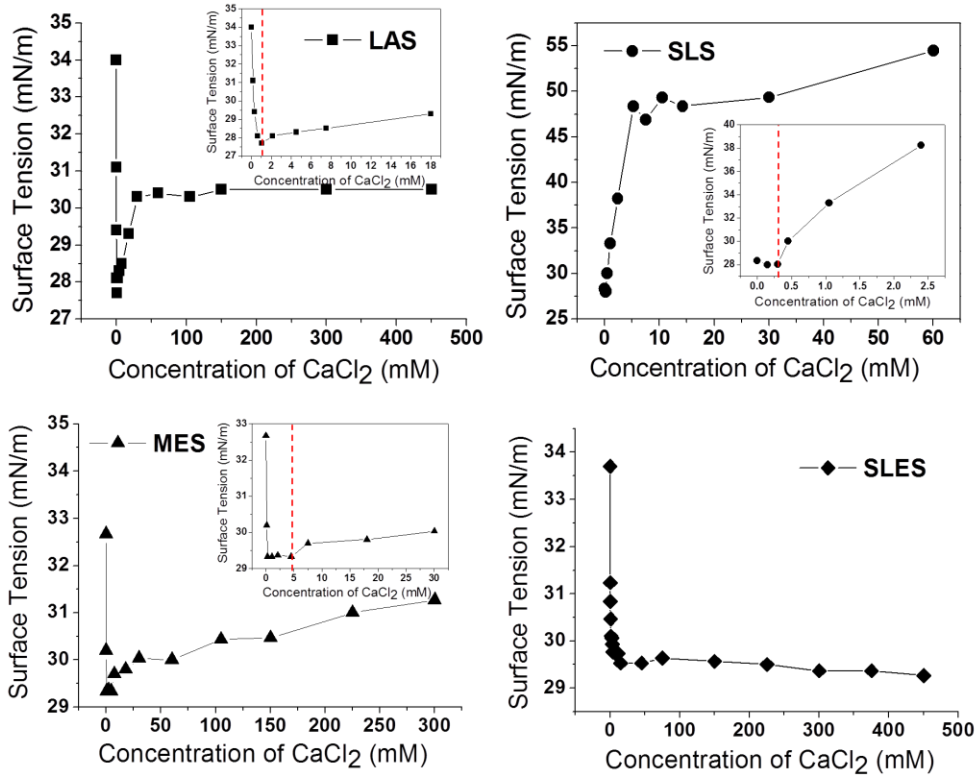

Figure 4-19. Surface tension versus $CaCl_2$ concentration of the standard commercial surfactants, LAS, SLS, MES, and SLES (Concentration of the surfactant: 2.0 × CMC)

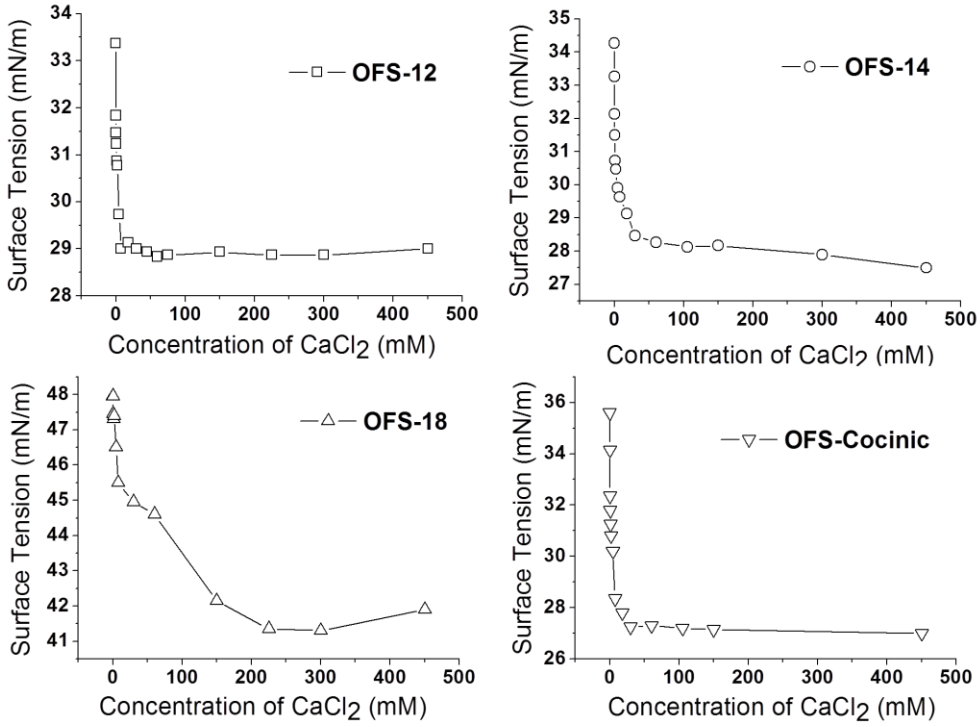

Figure 4-20. Surface tension vs. $CaCl_2$ concentration of the linear OFS-n surfactants (Concentration of the surfactant: 2.0 × CMC)

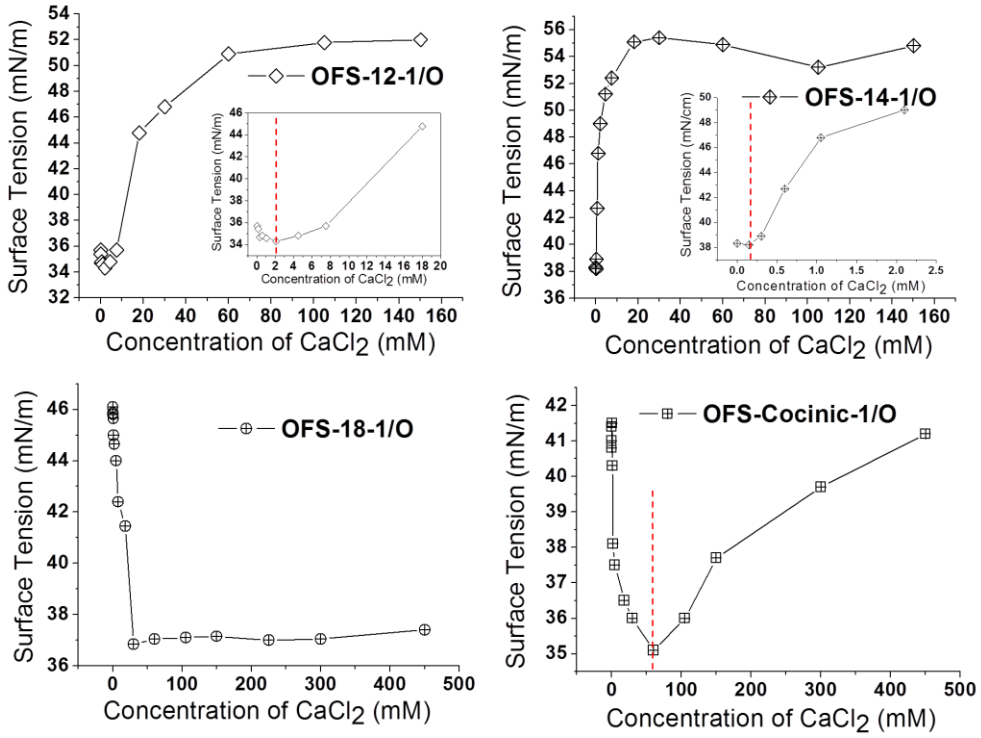

Figure 4-21. Surface tension vs. CaCl2 concentration of the linear OFS-n-1/O surfactants (Concentration of the surfactant: 2.0 × CMC)

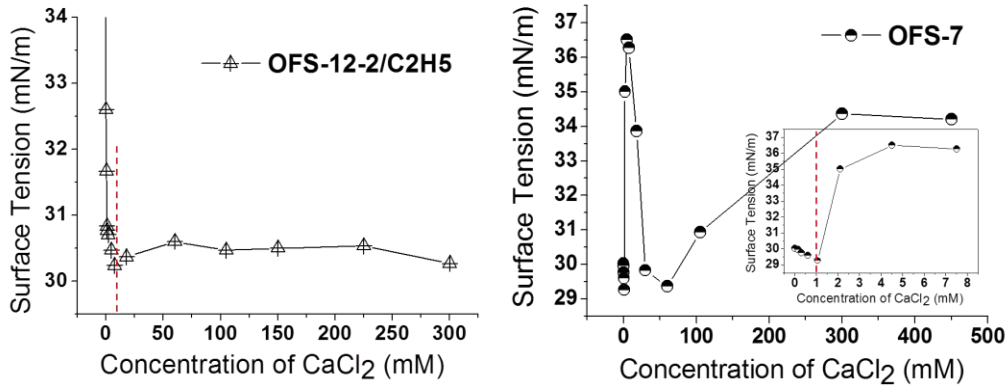

Figure 4-22. Surface tension versus CaCl2 concentration of OFS-12-2/C2H5 and OFS-7 (Concentration of the surfactant: 2.0 × CMC)

Figure 4-23 illustrates this effect for a linear alkylbenzene sulfonate (LAS) solution. Below the turbid point, the surfactant solution was clear as shown by insets A and B in **Figure**

4-23 which changed to a cloudy solution at calcium concentrations equal to and greater than the turbid point (inset C and D). The point of micelle stability was marked by an increase in the surface tension of the surfactant solution with an increase in calcium concentration. In **Figure 4-23**, inset B corresponds to the micelle stability concentration and inset C corresponds to the turbid concentration.

A. Clear solution at low calcium concentration (33 ppm, corresponding to soft water conditions)

B. LAS solution at 100 ppm of Ca^{2+} corresponding to the tolerance value (micelle stability)

C. Cloudy solution at the turbid concentration (230 ppm, corresponding to hard water conditions)

D. Cloudy solution with the formation of calcium precipitates (3300 ppm, corresponding to extreme hard water conditions)

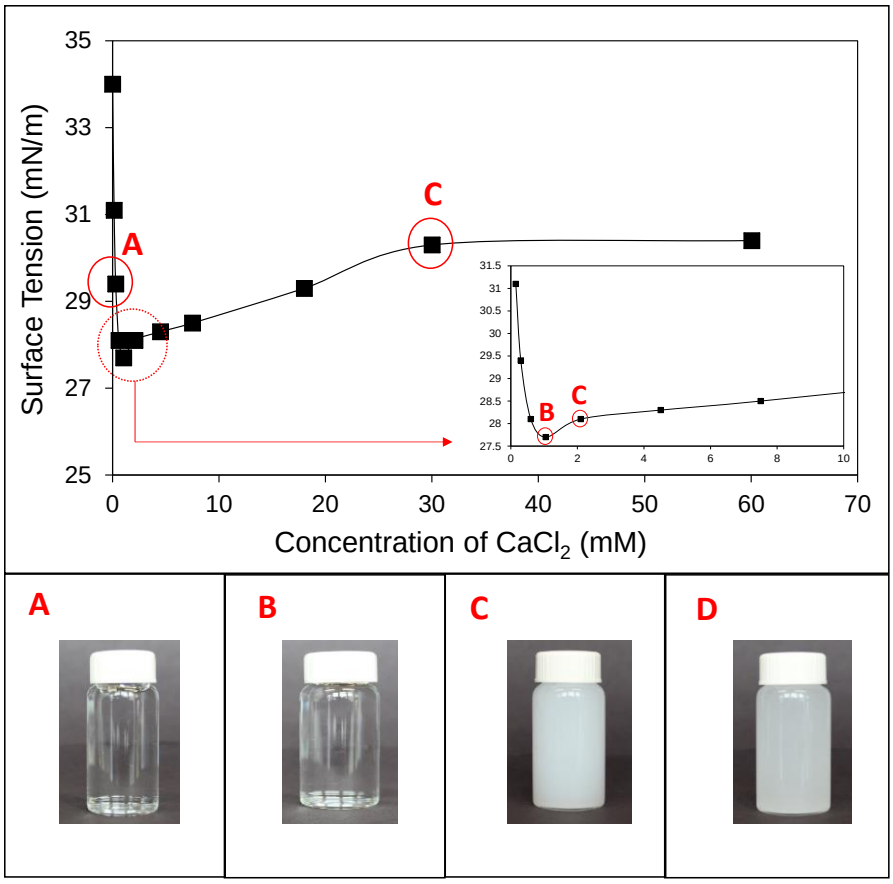

Figure 4-23. Surface tension versus $CaCl_2$ concentration for LAS solution demonstrating the effect of increasing calcium concentration. (Concentration of the surfactant: 2.0 × CMC)

Figure 4-24 depicts the concentration [ppm] of hard water ions, Ca^{2+}, with the two surfactant performance descriptors. As described earlier, solution turbidity [ppm] was defined as the Ca^{2+} concentration for which the aqueous surfactant solution visually lost its clarity due to formation of crystals. Micelle stability was identified as the Ca^{2+} concentration [ppm] at which the solution surface tension began increasing associated with loss in surfactant performance. Comparison of OFS stability overlaid with Ca^{2+} concentrations common to soft and hard water applications[101] demonstrates a two-order-of-magnitude increase in stability of OFS molecules when compared with conventional surfactants. OFS-n surfactants exhibit Ca^{2+} turbidity and stability concentrations in the range of 10,000 ppm, while conventional LAS and SLS surfactants are in the 10−100 ppm

range. For a range of soft to moderately hard (0−120 ppm), hard (121−150 ppm), and very hard (>251 ppm) water, it is revealed that most oleo-furan surfactants remain clear and functional in hard water conditions when viewed through a cuvette (**Figure 4-24 B**), while conventional surfactants such as LAS become cloudy (230 ppm) and precipitate (10,000 ppm).

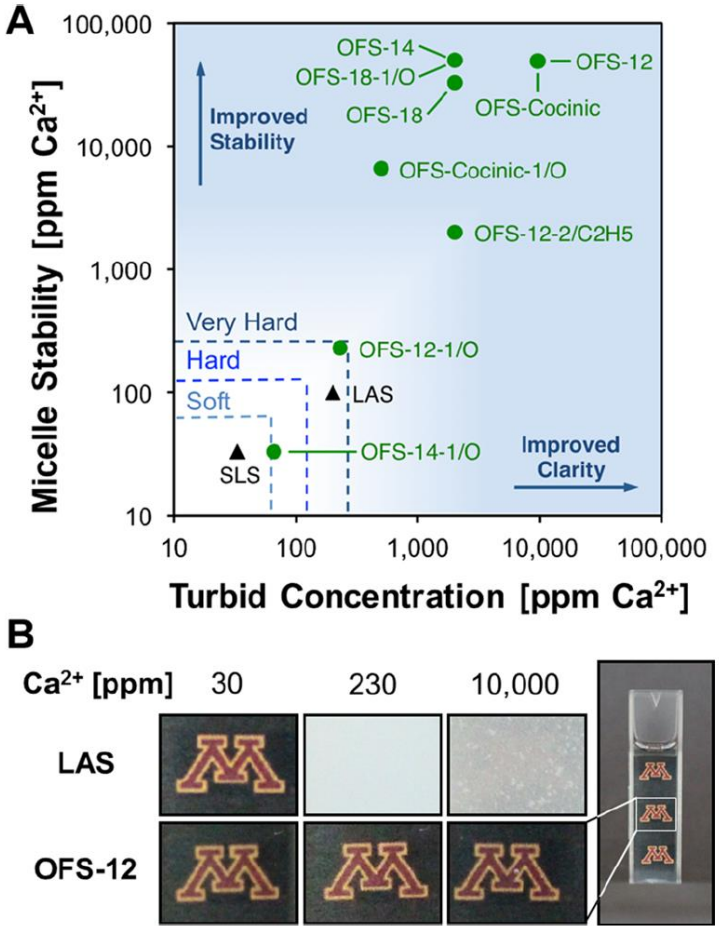

Figure 4-24. Hard water performance of oleo-furan sulfonate surfactants **A.** Comparison of sulfonated surfactants for micelle stability and solution turbidity, **B.** when viewed through a cuvette

The superior performance of OFS-n is depicted visually in **Figure 4-25** which compares the appearance of commercial surfactants (SLS and LAS) with other OFS surfactants.

Thus, OFS surfactants retain surfactancy in extreme hard water conditions without the need for coformulation of chelating agents.

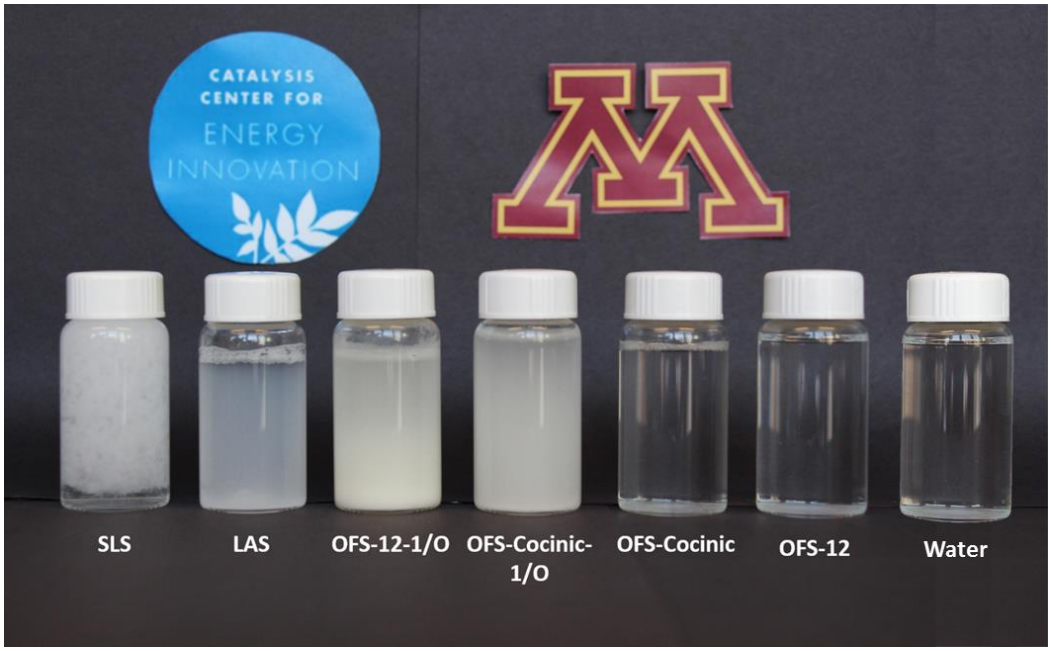

Figure 4-25. Surfactant solutions after addition of $CaCl_2$ (Surfactant concentration: 2 × CMC, Concentration of $CaCl_2$: 50,000 ppm) *Note: Image taken after two weeks of making the solution*

For the OFS-n surfactants, a momentary turbidity was observed in the surfactant solution upon addition of $CaCl_2$ due to localized concentration gradients which disappeared upon stirring unlike the OFS-n-1/O, LAS and SLS surfactants where the turbidity/precipitation continued to persist even upon vigorous stirring. **Table 4-3** summarizes the results obtained for micelle stability and turbid concentration for the commercial and OFS surfactants.

Table 4-5. Summary of hard water stability tests for all surfactants

Surfactant		Micelle Stability [ppm of $CaCl_2$][a]	Turbid Conc. [ppm of $CaCl_2$][b]
Commercial			
	SLS, Sodium Lauryl Sulfate	33	33
	MES, Methyl Ester Sulfonate	500	>50,000
	LAS, Linear Alkylbenzene Sulfonate	100	230
	SLES, Sodium Lauryl Ether Sulfate	>50,000	>50,000
OFS, Oleo-Furan Sulfonates			
	OFS-12-1/O	230	230
	OFS-14-1/O	33	10,000
	OFS-18-1/O	>50,000	2,000
	OFS-Cocinic-1/O	6,600	500
	OFS-7	110	230
	OFS-12	>50,000	10,000
	OFS-14	>50,000	2,000
	OFS-18	33,000	2,000
	OFS-Cocinic	50,000	10,000
	40:60 mol% OFS-12-2/C2H5:OFS-12	2000	2,000
	85:15 mol% OFS-12-1/O:OFS-12	-	-

4.4 Conclusions[4]

The natural oil and sugar-derived structures of oleo-furan surfactants harness their inherent function for improved detergency, solubility, and exceptional stability in hard water conditions. The ability to precisely select and assemble with heterogeneous catalysts amenable to chemical processing allows for the chemical targeting of specific surfactant performance. By this approach, the optimal OFS molecules such as OFS-12 or OFS-cocinic demonstrate strong surfactant performance in minimal concentration and low temperatures compared with current large volume surfactants. Surfactant performance was evaluated by testing standard properties, such as critical micelle concentration (CMC), Krafft point, foaming, wetting, and stability in

[4] (Permissions obtained from ACE Central Science: Park, D. S., et al., ACS Central Science 2: 820–824, 2016, http://pubs.acs.org/doi/pdfplus/10.1021/acscentsci.6b00208)

hard water. **Table 4-6** summarizes the results obtained from surfactant performance evaluation. Ideally, surfactants should possess low CMC and Krafft points to ensure a wide range of operating conditions, especially in detergency applications. In comparison with LAS, OFS surfactants were found to have similar values of CMC and lower Krafft points, enabling application in dilute conditions and cold water. More importantly, OFS (predominantly, OFS-12 and OFS-Cocinic) were found to possess superior detergency in hard water conditions. While LAS precipitates at low ion concentrations (230 ppm) and forms a cloudy solution rendering it unusable, OFS remains stable in solution even at hundredfold ion concentration. They eliminate the use of a chelants, significantly simplifying the ingredient list of a formulation and reduce toxicity and cost.

OFS surfactants have the added benefit of superior performance when compared with synthetic surfactants like LAS. Apart from being bio-renewable, OFS molecules have revealed high tunability during synthesis, good surfactant properties, and superior stability in hard water—all of which are expected to be of high importance for detergents and other applications, where the water used for formulations or cleaning do not necessarily undergo pretreatment.

Surfactant	Structure	CMC[a] [ppm]	Krafft Point[b] [°C]	Draves Wetting[c] [s]	Foam Growth Rate[d] r_i / r_{SLS} [-]	Foam Height$_{60}$[e] $h_{i\text{-}60}$ / $h_{SLS\text{-}60}$ [-]	Micelle Stability[f] [ppm Ca^{2+}]
Commercial							
SLS, Sodium Lauryl Sulfate	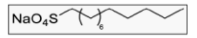	2010	15	6.3	1.00	1.00	33
MES, Methyl Ester Sulfonate		130	< 0	15.1	0.79	0.54	500
LAS, Linear Alkylbenzene Sulfonate	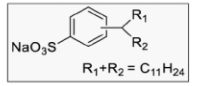	460	20	4.9	1.36	2.20	100
SLES, Sodium Lauryl Ether Sulfate		380	< 0	15.4	1.60	2.94	> 50,000
OFS, Oleo-Furan Sulfonates							
OFS-n-1/O							
n=12	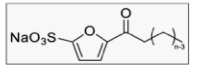	11520	< 0	> 3600	0	0	230
n=14		3127	< 0	> 3600	0	0	33
n=18		1156	< 0	> 3600	0	0	> 50,000
Cocinic, n = 8-18		4890	< 0	> 3600	0	0	6600
OFS-n							
n=7	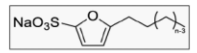	2669	< 0	> 3600	1.04	0.12	120
n=12		720	30	48.9	1.83	2.11	> 50,000
n=14		267	41.5	39.4	2.34	0.75	> 50,000
n=18		316	> 50	-	-	-	33,000
Cocinic, n = 8-18		512	18.5	58.0	2.06	2.19	> 50,000
40:60 mol% OFS-12-2/C2H5:OFS-12	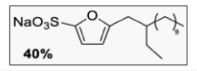	510	25.7	18.5	1.96	2.37	2000
85:15 mol% OFS-12-1/O:OFS-12		2445	< 0	-	-	-	-

[a]Critical micelle concentration, measured above Krafft point. [b]Measured at 1.0 wt % surfactant in water. [c]Measured at 0.25 wt % in water. [d]Measured at 0.5 wt % in water. [e]At 60 min. [f]Measured at twice CMC.

Chapter 5 Broadening the Scope of Surfactant Chemistries for New OFS molecules

5.1 Introduction

In the previous chapters we discussed the development and characterization of a new class of renewable surfactants called “Oleo-Furan Sulfonate” (OFS) that provide advanced properties made possible through the molecular structure of biomass-derived chemicals. OFS were developed to replace conventional detergent molecules referred to as LAS (linear alkylbenzene sulfonate), which combine hydrophilic sulfonate functionality with a hydrophobic alkyl chain using a benzene linker. Alternatively, the OFS structure utilizes a furan linker, which changes the characteristics of the sulfonate and stabilizes the formation of micelles relative to conventional LAS. OFS surfactants allow for selective preparation of surfactants with targeted properties specific to each application. While conventional LAS exhibits a distribution of aliphatic branching and broad range of properties, OFS surfactants are prepared using acylation chemistry that specifically defines the aliphatic chain. This unique synthesis approach also allows for controlled branching via side-chain aldol condensation and permits tunable surfactant properties necessary for applications in agriculture, cleaning, food preparation, and oil recovery. Importantly, our strategy has also enabled us to tune the hydrophobic tail of OFS, creating unique, emergent properties. Large hydrophobic tails ($\geq C_{12}$) can be built using either long acylating agents, e.g., fatty acids (straight OFS) or a few shorter molecules, derived from sustainable and inexpensive feedstocks, e.g., sugars or shale gas, via cascade of acylation and aldol condensation (branched OFS).

Assembly of the general surfactant structure can be achieved in numerous permutations of several reaction chemistries to synthesize structures with desirable properties. The key technology consists of the acylation reaction forming an acylated molecule which acts as a backbone for several

surfactant structures. The presence of the carbonyl group imparts chemical reactivity and functionality that allows the extension of possible reactions beyond the scope of hydrogenation, hydrodeoxygenation and aldol condensation discussed in earlier chapters. In this chapter[58,59] we look at two chemistries namely unimolecular and bimolecular dehydration reactions that allow imparting additional functionalities to form surfactant precursors which could potentially aid the coupling of different hydrophobic tail groups to form a class of surfactants called gemini surfactants.[121]

5.2 Materials and Methods

5.2.1 Chemicals

Hexane (95 %), Furan (99 %), and Trifluoroacetic anhydride (99 %) were purchased from Sigma-Aldrich. The saturated fatty acid, lauric acid (C_{12}, 99 %, Acros), was used in furan acylation for the first step in overall reaction pathway. H-BEA (CP814E, SiO_2/Al_2O_3 = 25), H-Y (CBV720, SiO_2/Al_2O_3 = 30), and copper chromite catalyst ($2CuO.Cr_2O_3$) were obtained from Zeolyst and Sigma-Aldrich, respectively. The H-BEA was calcined at 550 ℃ for 12 h at the rate of 1 ℃ min^{-1} in a tube furnace under air flow. The reduction of copper chromite was carried out at 300 ℃ for 3 h under 10 % H_2/Argon flow. Both H-Y and H-BEA were stored in a muffle furnace at 200 ℃ before use to remove any adsorbed moisture.

5.2.2 Chemical Synthesis

a. Acylation

Acylation was conducted at room temperature (25℃, 298K) and atmospheric pressure in a 20 ml glass scintillation vial containing furan, fatty acid and TFAA in 6 ml n-

hexane similar to the method described in **Section 3.2.3 a.** The molar ratio of furan to lauric acid to TFAA was affixed at 1:0.8:1.3.

b. Hydrogenation

1-(Furan-2-yl)dodecan-1-ol (2-DOF Alcohol) was synthesized from 1-(furan-2-yl)dodecan-1-one (2-DOF) via hydrogenation in a 100 ml Parr reactor charged with 2-DOF (reactant, 2 ml), n-tridecane (internal standard, 0.5 ml), ethanol/n-hexane (solvent, 30 ml), and 0.5 g of $2CuO.Cr_2O_3$ (copper chromite) catalyst (**Scheme 5-1**). The reactor was sealed and purged twice using nitrogen to remove any residual air followed by a hydrogen purge. The reactor was then pressurized using 100 psi hydrogen pressure at the desired reaction temperature (120 – 180 °C) under vigorous stirring of 1000 rpm. At the end of the reaction time (5 h), the reactor was finally cooled and vented before taking the final time sample. The selectivity of the 2-DOF Alcohol was calculated by dividing the moles of 2-DOF Alcohol formed by the moles of all products formed.

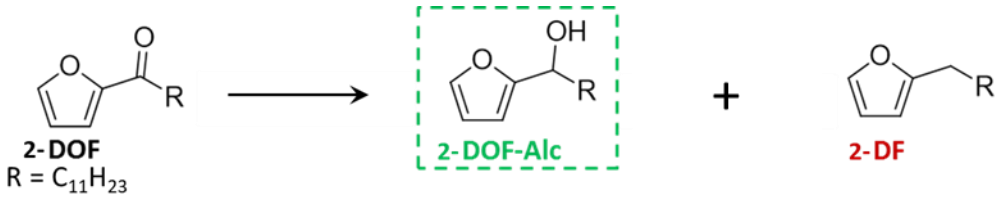

Scheme 5-1. Hydrogenation of 1-(furan-2-yl)dodecan-1-one (2-DOF) to form 1-(furan-2-yl)dodecan-1-ol (2-DOF Alcohol, green)

c. Dehydration

A 100 ml Parr reactor was charged with 2-DOF Alcohol (reactant, 2 ml), ethanol/n-propanol/n-butanol (solvent/ reactant, 30 ml) and 0.1 g of solid acid catalysts (Sn-BEA, H-BEA, and H-Y). For the purposes of quantification, tridecane (0.5 ml) was used as an internal standard. The reactor was sealed and purged with nitrogen to remove any

residual air and pressurized to 200 psi to minimize vaporization of volatile compounds and then heated to temperatures between 50 – 120 ℃ under vigorous stirring (1000 rpm). At the end of the reaction time (3 h), the reactor was finally cooled and vented before taking the final time sample. The selectivity of the product was calculated by dividing the moles of product formed by the moles of all products formed.

5.3 Results and Discussion

From the surfactant performance results obtained in Chapter 3, branched surfactants were found to possess good performance characteristics when compared to other iterations of OFS and LAS surfactants with competitive properties for utilization in detergent formulations (**Table 5-1**). To enable applications in dilute conditions, hard, and cold water we consider a desirable CMC to be <1,000 ppm with a Krafft point lower than 30 ℃ and a hard water stability value greater than 500 ppm since calcium levels in very hard water correspond to concentrations greater than 250 ppm.

Table 5-1. Comparison of CMC, Krafft point and hard water stability between LAS and various OFS surfactants

Surfactant	CMC (ppm)[a]	Krafft Point (℃)[b]	Hard water Stability (Ca^{2+} ppm)[c]
LAS	460	20	100
OFS-12-2/C2H5	510	25	2,000
OFS-n n=12	720	30	>50,000
n=14	267	41.5	>50,000
n=18	316	>50	33,000
OFS-n-1/O	>1000	<0	<300

[a]Desired ppm <1,000 ppm
[b]Desired Krafft Point <30 ℃
[c]Desired hard water stability >500 ppm

Even though the stability of the branched OFS-12-2/C2H5 in hard water is significantly lower than that of the straight chain OFS-n surfactants, it still offers twenty times higher stability when compared to the commercial LAS surfactant. Additional performance metrics indicate that branched OFS surfactants exhibit sufficiently fast wetting kinetics and foaming behavior compared

to other OFS iterations (**Table 4-3** and **Table 4-4**). Branched surfactants however possess lower biodegradability in comparison to their linear counterparts.[122] This design constraint opens the possibility of synthesizing branched surfactants with functional groups contained at the point of branching that render it biodegradable.[96,123,124] We propose here, the incorporation of ether groups in the branching to achieve the design according to **Scheme 5-2**.

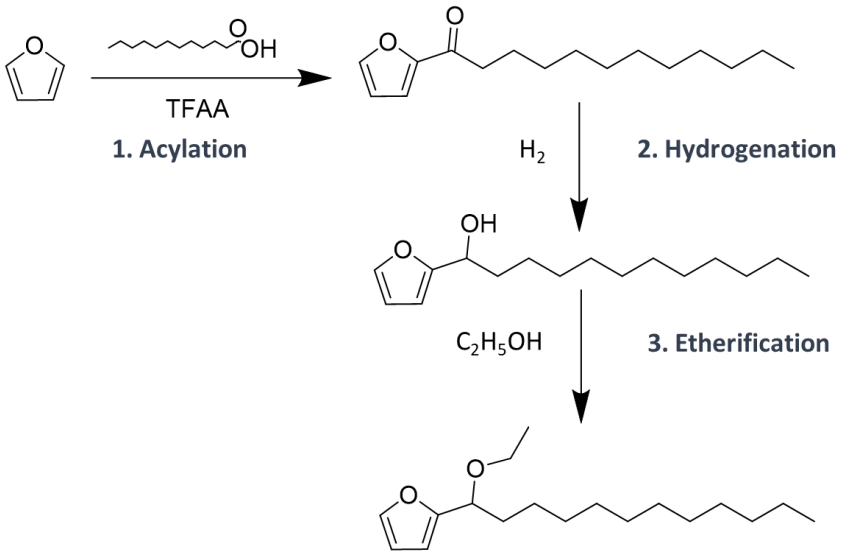

Scheme 5-2. Reaction scheme for incorporation of ether linkage in OFS branching via sequential acylation-hydrogenation-etherification

Another design variability is the incorporation of functional groups in the branching to form gemini surfactants. Gemini surfactants contain two hydrophilic head groups connected to two hydrophobic tails with a spacer in between.[125,126] These molecules are at least an order of magnitude more surface active than conventional surfactants and hence possess extremely low CMC values.[127] They find applications in various fields especially in personal care products.[128] By using the acylated alkylfuran backbone, it is possible to incorporate functional groups that permit linkage of another alkyl furan via a spacer. Two potential reaction schemes that permit synthesis of potential gemini surfactants are shown in **Scheme 5-3**.[129–131]

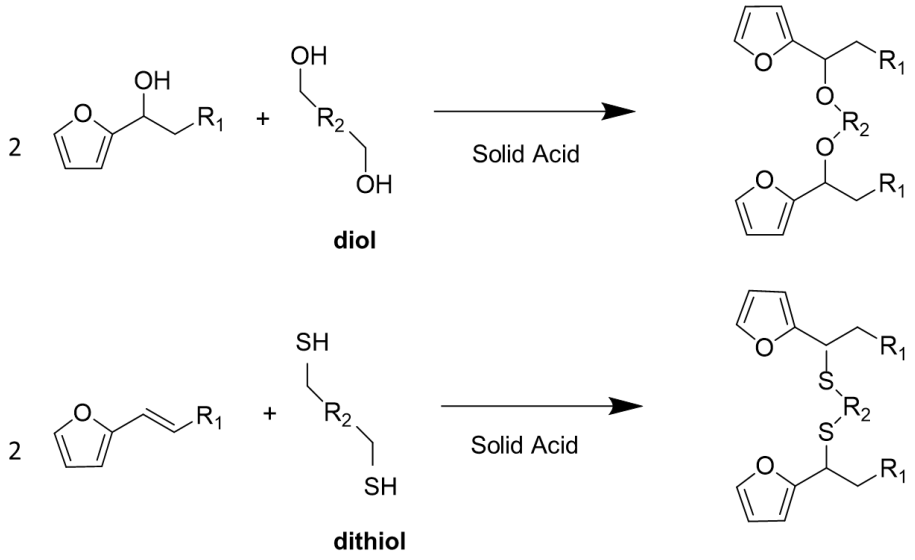

Scheme 5-3. Potential reaction schemes for synthesis of gemini surfactants via di-etherification and di-thiol-ene reactions

While the synthesis of the specific di-ether and di-thioether based gemini surfactants is outside the scope of this thesis and reserved for future work, this chapter deals with the optimization of the reaction pathways to form the ether and alkene precursors required.

5.3.1 Acylation

Acylation was conducted using the method described in **Section 5.2.2 a** and purified as per **Section 3.2.4.** The as-synthesized 2-DOF was then subject to hydrogenation.

5.3.2 Hydrogenation

In contrast to hydrogenations/hydrodeoxygenations carried out earlier in **Chapter 3**, the molecule of interest is the alcohol and not the alkylfuran which is a product of hydrodeoxygenation of 2-DOF. The effect of temperature on this reaction is depicted in **Figure 5-1**.

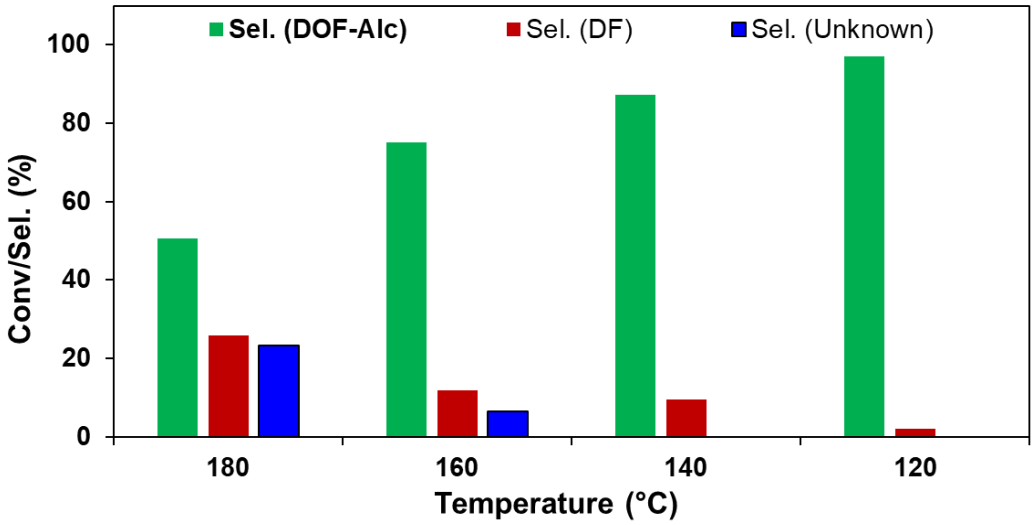

Figure 5-1. Hydrogenation of 2-DOF for the formation of 2-DOF Alcohol (DOF-Alc). Reaction Conditions: 2 ml DOF, 30 ml ethanol, 0.5 g 2CuO-Cr_2O_3, 100 psi H_2, 5 h

While the most dominant product observed at higher temperatures around 180 ℃ is 2-DOF Alcohol, the side product 2-DF is formed at a reasonably high selectivity of ~25%. Lowering the temperatures was found to improve the selectivity towards the desired alcohol product. At 120 ℃, 2-DOF Alcohol is formed at 97% selectivity and 94% yield. Hydrodeoxygenation of aromatic ketones to form alkyl substituents has been reported to occur via two pathways; hydrogenation of the carbonyl to form alcohol followed by hydrogenolysis or via direct hydrogenolysis of the carbonyl.[132,133] While the former mechanism seems to be the likely pathway for the formation of 2-DF in this case, further experiments currently outside the scope of this thesis would be required to establish the true mechanism for formation of the alcohol and alkylfuran with temperature variation. **Figure 5-2** shows the effect of solvent polarity on the hydrogenation reaction. Both hexane and ethanol exhibit favorability towards the alcohol product with ethanol having marginally higher selectivities and conversions. At 120 ℃, ethanol was found to be slightly

more favorable to the polar alcohol than the alkylfuran whereas hexane offered higher selectivities to the non-polar alkylfuran.

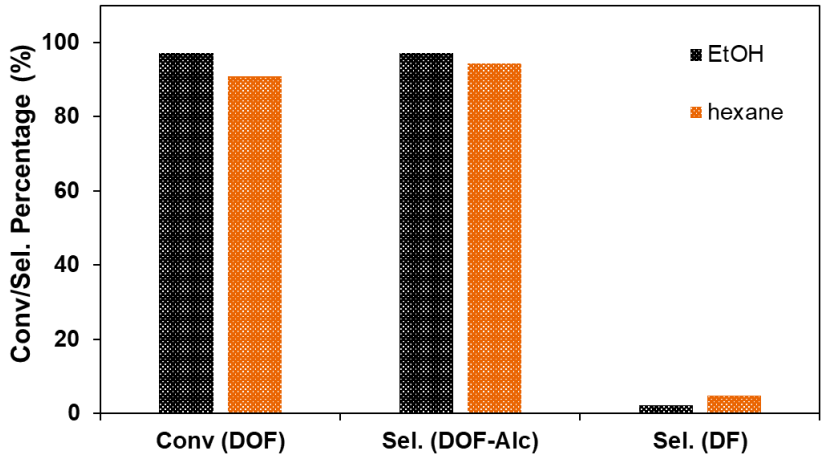

Figure 5-2. Hydrogenation of 2-DOF for the formation of 2-DOF Alcohol (DOF-Alc). Reaction Conditions: 2 ml DOF in 30 ml ethanol(EtOH)/hexane, 0.5 g 2CuO-Cr2O3, 100 psi H_2, 5 h, 120 ℃

The product was purified and concentrated via evaporation and the structure was verified via ^{1}H and ^{13}C-APT (Attached Proton Test) NMR analysis (**Figure 5-3** and **Figure 5-4**).

^{1}H-NMR (400 MHz, CDCl3) δ 0.852-0.896 (t, 3H), 1.296-1.427 (brm, 18H), 1.830-1.854 (q, 2H), 4.642-4.675 (t, 1H), 6.214-6.22 (d, 1H), 6.313-6.325 (q, 1H), 7.362 (d, 1H), ppm.

^{13}C-NMR (100 MHz, $CDCl_3$) δ 14.12, 22.70, 25.55, 29.38, 29.42, 29.54, 29.59, 29.64, 29.66, 29.68, 29.72, 31.93, 31.94, 35.58, 67.86, 105.77, 110.30, 141.61, 157.05 ppm

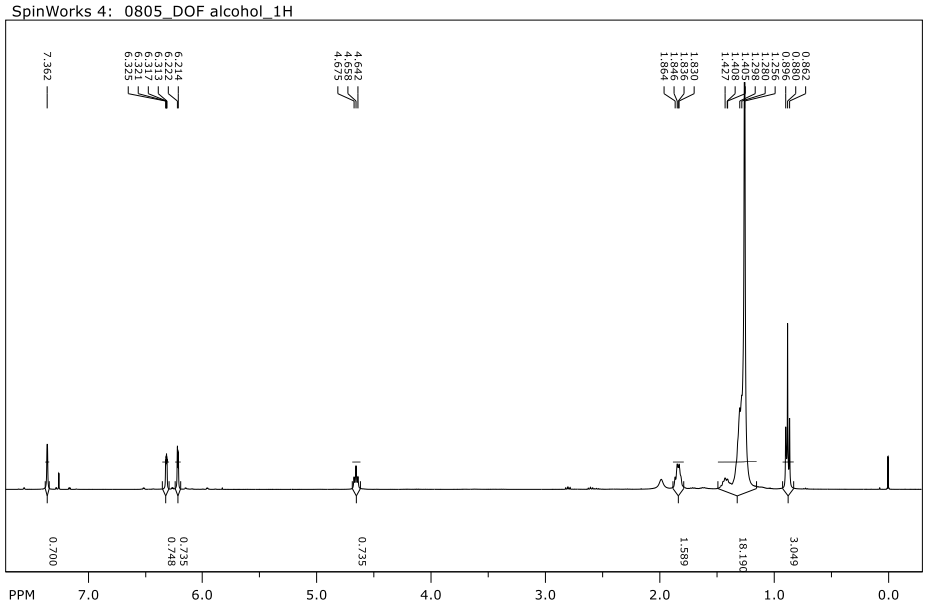

Figure 5-3. ^{1}H NMR of 2-DOF Alcohol in $CDCl_3$

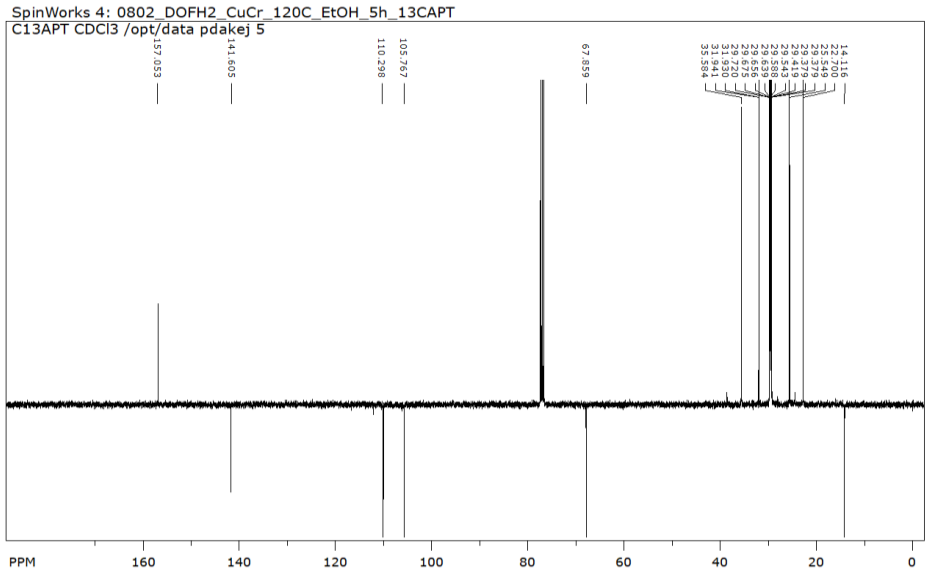

Figure 5-4. ^{13}C -APT NMR of 2-DOF Alcohol in $CDCl_3$

5.3.3 Dehydration

Dehydration is a generic term for a reaction that involves a loss of water molecule and could either be as a result of a unimolecular or a bimolecular reaction. A unimolecular

dehydration of an alcohol occurs when there is an intramolecular loss of water resulting in the formation of an alkene. Alcohols in the presence of an acid catalyst and heat can undergo an E1 mechanism wherein the hydroxyl group gets protonated by the acid making it a good leaving group and resulting in the formation of a carbocation. The carbocation is then deprotonated by water which acts as a base ultimately leading to the formation of an alkene. Reactivity of alcohols decreases in the order tertiary (3^o) > secondary (2^o) > primary (1^o) since the carbocation is most easily stabilized on a tertiary group. On the other hand, a bimolecular dehydration, or an alcohol condensation reaction as it is aptly termed, involves two alcohols reacting with each other to form water and an ether via an S_N2 nucleophilic substitution reaction. The first step in a bimolecular dehydration also involves protonation of the hydroxyl group. However, in the second step, the nucleophilic oxygen on the hydroxyl of the second alcohol molecule attacks the electrophilic carbon of the first alcohol resulting in a C-O cleavage and thereby resulting in water loss. Both reactions differ in the second step, where, in the case of unimolecular dehydration, water acts as a nucleophile to form an alkene while an alcohol acts as the nucleophile in bimolecular dehydration reactions resulting in the formation of an ether. Bimolecular dehydration however competes with unimolecular dehydration and produces useful yields mainly with primary alcohol to form symmetrical ethers (e.g. diethyl ether). 2-DOF Alcohol being a secondary alcohol also undergoes competing dehydration reactions to form an ether (A) or an unsaturated alkylfuran (B) as shown in **Scheme 5-4**.

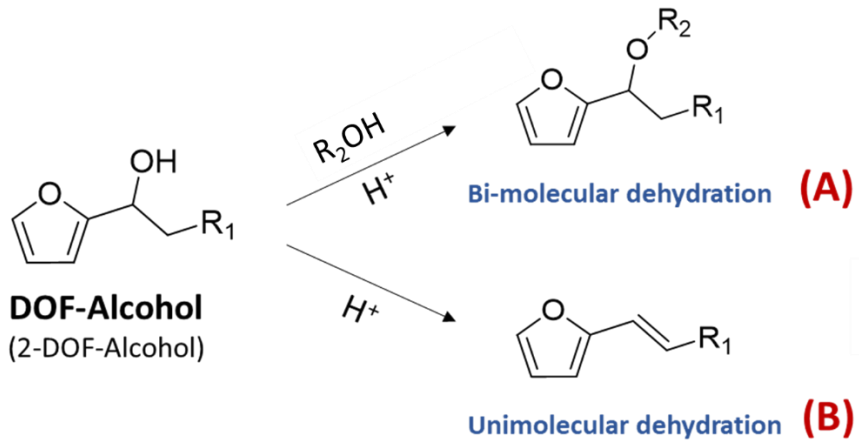

Scheme 5-4. Reaction scheme for competing unimolecular and bimolecular dehydration reactions of 2-DOF Alcohol

Both compounds (ether (A) and alkene (B)) can act as interesting surfactant precursors for different structures potentially possessing different properties as discussed earlier and hence, we discuss in detail, the optimization of both chemistries. Unimolecular dehydration competes with bimolecular dehydration at higher temperatures and hence the effect of temperature and catalyst was investigated.

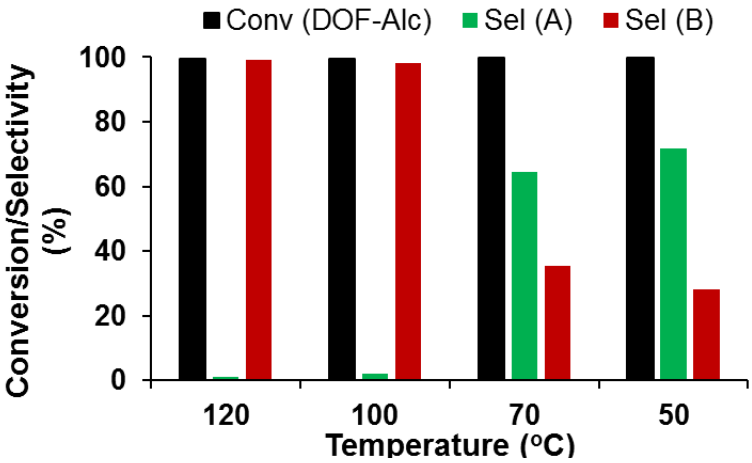

Figure 5-5. Effect of temperature on dehydration of 2-DOF Alcohol. Reaction Conditions: 2 ml DOF-Alcohol, 30 ml ethanol, 0.1 g HBEA, 200 psi N_2, 3 h

Higher temperatures using H-BEA catalyst and ethanol as a co-reactant and solvent favor the formation of the unsaturated alkylfuran as shown in **Figure 5-5**. At 120 ℃, the yield towards the unsaturated alkylfuran (red, B) is greater than 99% with less than 1% yield towards the ether (green, A). From this reaction mixture, we isolate the unsaturated compound in high purity via evaporation and confirmed the structure via ^{1}H and ^{13}C-APT NMR (**Figure 5-6** and **Figure 5-7**).

^{1}H-NMR (400 MHz, $CDCl_3$) δ 0.866-0.900 (t, 3H), 1.267 (brm, 16H), 2.146-2.196 (q, 2H), 6.115-6.123 (d, 1H), 6.165-6.187 (brm, 2H), 6.330-6.342 (q, 1H), 7.297-7.301 (d, 1H) ppm.

^{13}C-APT-NMR (100 MHz, $CDCl_3$) δ 14.115, 22.692, 29.208, 29.260, 29.348, 29.524, 29.630, 29.919, 32.811, 105.798, 109.999, 118.454, 130.328, 141.132, 153.403 ppm.

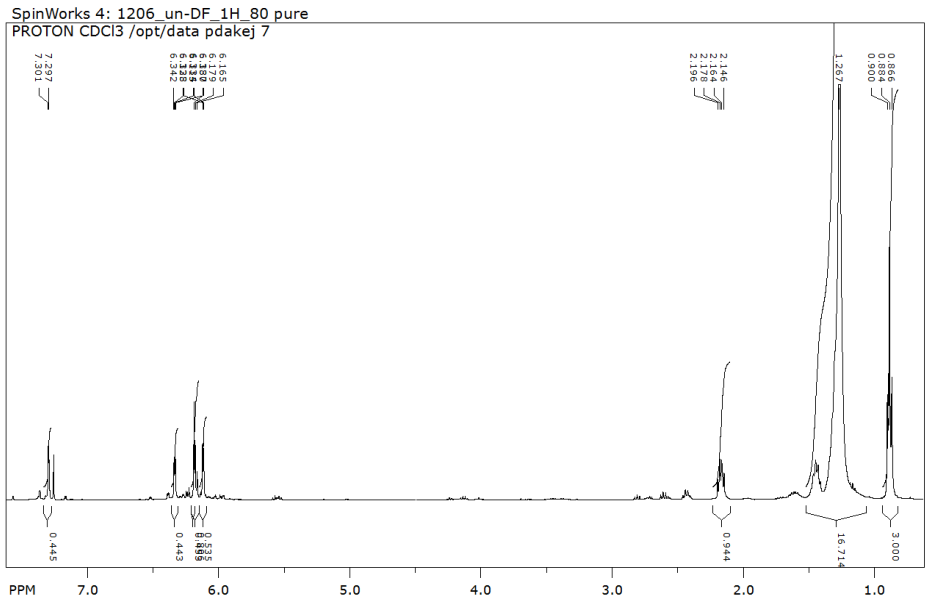

Figure 5-6. ^{1}H NMR of unsaturated dodecylfuran in $CDCl_3$

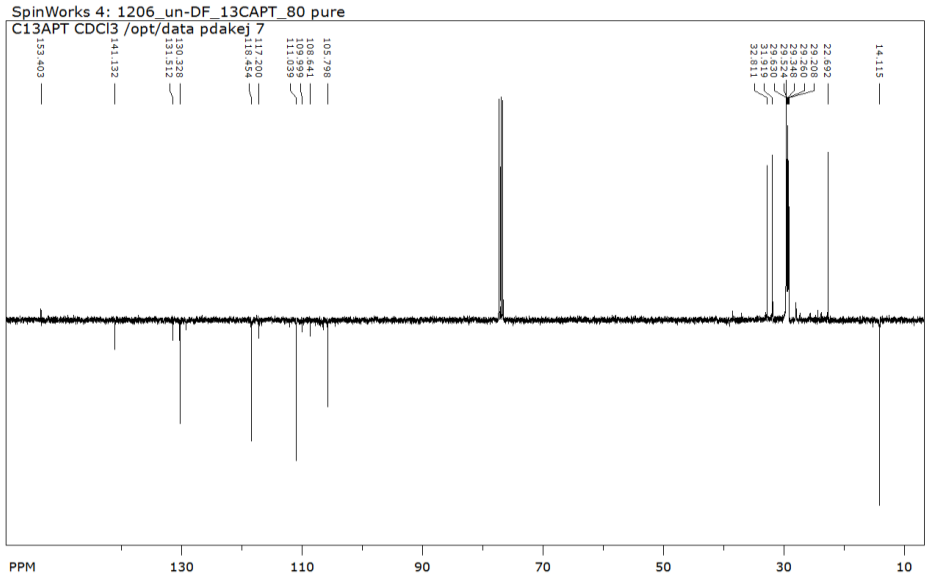

Figure 5-7. ^{13}C-APT NMR of unsaturated dodecylfuran in $CDCl_3$

Lowering the temperature promotes bimolecular dehydration; however, at 50 °C, the best yield is limited to 72%. Different catalysts possessing varying acidity and zeolitic structural framework reveal varying catalytic activity towards dehydration (**Figure 5-8**). Sn-BEA, which is a Lewis acid catalyst, was found to have low activity towards both dehydration routes with higher selectivity towards the ether product (green, A). The most interesting observation was with HY where, at similar reaction conditions, HY produced the ether product with 98.5% selectivity at 99.7% conversion while minimizing the unimolecular reaction. It is important to note here that this bimolecular dehydration reaction was achieved in high yield despite the reaction involving the formation of an unsymmetrical ether using a secondary alcohol both of which are less conducive towards the reaction. This difference in selectivity between H-BEA and H-Y could possibly be attributed to the difference in zeolitic framework where H-Y encompasses a supercage within when compared to H-BEA.[134] Since bimolecular dehydration involves two molecules via an S_N2 mechanism, it is likely that steric hindrance is an important factor when it comes to the

narrower and smaller H-BEA thereby permitting a greater extent of unimolecular dehydration. H-Y on the other hand could allow for spatial orientation of the two alcohol molecules (ethanol and 2-DOF Alcohol) for the S_N2 mechanism.

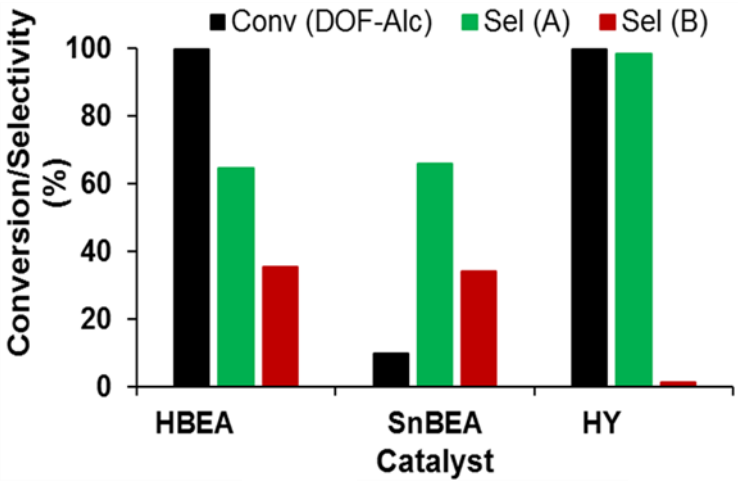

Figure 5-8. Effect of catalyst on dehydration of 2-DOF Alcohol. Reaction Conditions: 2 ml DOF-Alcohol, 30 ml ethanol, 0.1 g catalyst, 200 psi N_2, 3 h

The results obtained by using different chain length alcohols (ethanol, n-propanol, n-butanol) allowed for an increased confidence in this hypothesis (**Figure 5-9**). In both cases (H-BEA and H-Y), we see a drop in the selectivity towards the ether product with increasing chain length. However, this effect is more pronounced in the case of H-BEA where the selectivity towards the ether product (green) drops from 64.5% down to 53.7% and 49.7% on increasing the chain length from two carbons to three and four carbons. In comparison, the selectivity in H-Y drops by 1.2% in going from ethanol to n-propanol implying that steric hindrance is dominant in H-BEA and possibly affects product composition.

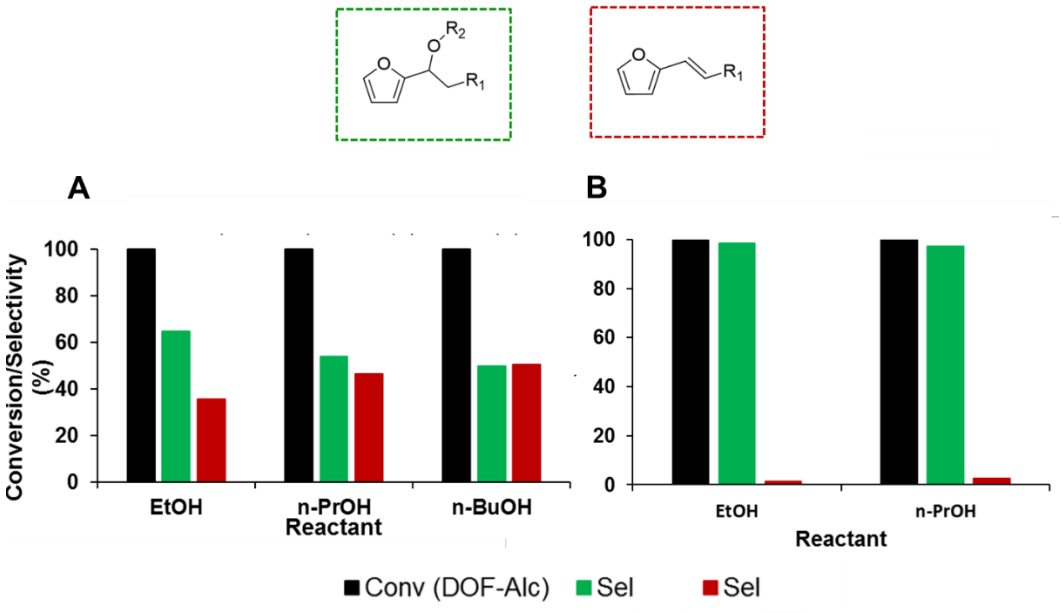

Figure 5-9. Effect of alcohol chain length on bimolecular dehydration of 2-DOF Alcohol. Dehydration of 2-DOF Alcohol in different solvents at 200 psi N_2 for 3h using **A.** H-BEA and **B.** H-Y

Via the two-step sequential hydrogenation-dehydration process, the ether product was made with an overall yield of 92%. A one-pot process was attempted wherein 2 ml of 2-DOF in 30 ml ethanol was charged into a Parr reactor along with a catalyst mixture containing 0.5 g $2CuO.Cr_2O_3$ and 0.1 g H-Y pressurized with 100 psi H_2 at 120 °C which resulted in an ether yield of 80% with a 2-DOF conversion of 98%. The ether product was collected via the two-step process by running repeated dehydration reactions of 2-DOF Alcohol using H-Y as the catalyst and ethanol as the solvent. The product was isolated at ~93% purity via evaporation and the structure was confirmed via ^{1}H and ^{13}C NMR (**Figure 5-10** and **Figure 5-11**).

^{1}H-NMR (400 MHz, $CDCl_3$) δ 0.858-0.892 (t, 3H), 1.142-1.177 (t, 3H), 1.245 (brm, 18H), 1.772-1.915 (brm, 2H), 3.327-3.485 (brm, 2H), 4.219-4.254 (t, 1H), 6.218-6.226 (q, 1H), 6.311-6.323 (q, 1H), 7.372-7.369 (q, 1H) ppm.

^{13}C-APT-NMR (100 MHz, $CDCl_3$) δ 14.107, 15.135, 22.961, 25.433, 29.140, 31.612, 34.289, 64.047, 74.659, 107.407, 109.879, 141.58, 155.393 ppm.

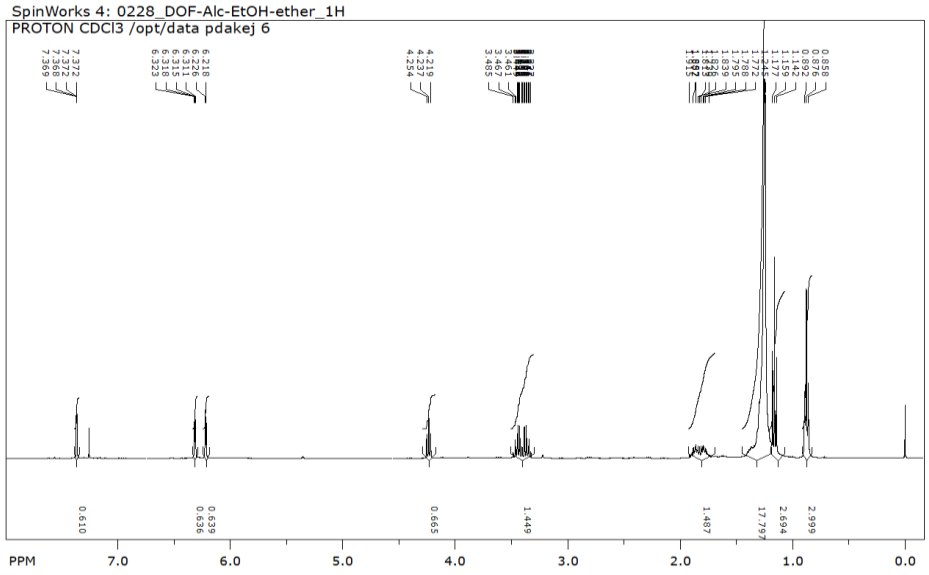

Figure 5-10. ^{1}H NMR of ether product of 2-DOF Alcohol and ethanol in $CDCl_3$

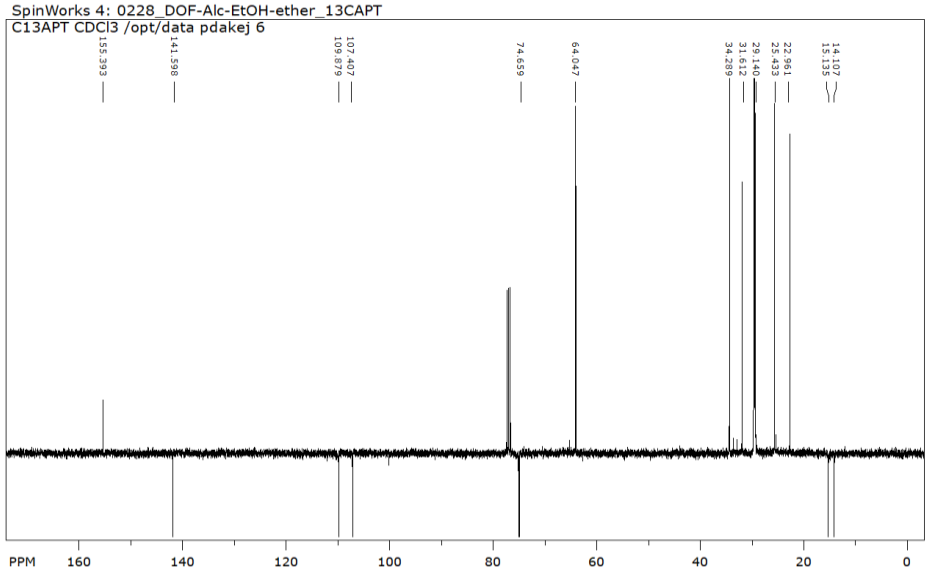

Figure 5-11. ^{13}C-APT NMR of ether product of 2-DOF Alcohol and ethanol in $CDCl_3$

5.4 Future Work and Conclusions

Tunability of OFS surfactants allow for coupling of various catalytic chemistries that result in incorporation of various functional groups permitting selective tuning of surfactant properties. In this chapter, we discussed a dehydration chemistry to form two surfactant precursors that could be potentially used to form gemini surfactants with improved surface wetting properties. Variation in the zeolitic framework results in significant variation in selectivity towards products. While H-BEA favors unimolecular dehydration products (alkenes), H-Y yields higher amounts of the ether product formed as a result of bimolecular dehydration. It is our hypothesis that the supercage-like structure of H-Y permits the desired spatial orientation of two alcohol molecules thereby yielding an unsymmetrical ether. At 120 ℃ while H-BEA formed the unsaturated alkyl furan with greater than 99% yield, H-Y formed the ether product with ethanol at 98% yield at 70 ℃. As the chain length of the solvent alcohol increases, the selectivity towards the ether product decreases with the effect being more pronounced for H-BEA than H-Y. The structures of both, unsaturated and ether products was confirmed via NMR.

The efficacy of the ether and unsaturated alkyl furan molecules as surfactant precursors need to be evaluated in the future. The ether product can be sulfonated to form an OFS molecule with a potentially biodegradable branching.[96,123,124] Susceptibility of this branching to the acidic sulfonation process would have to be tested during synthesis and potentially, alternate sulfonation methods would need to be tried. Etherification of 2-DOF Alcohol using diols could potentially form gemini surfactants with an ether spacer. Thiol-ene coupling chemistry of unsaturated alkylfuran and dithiols could enable formation of gemini molecules with thioether bonds. Identification of the optimum reaction conditions to form these molecules, synthesis followed by surfactant performance evaluation will be pursued in future work.

Acylation chemistry provides a backbone to oleo-furan sulfonate surfactant structures. Expansion of the OFS technology is not limited to just dehydration reactions but allows for coupling of several

catalytic chemistries. The ability to tailor furans with desired functionality in the final surfactant molecule enables the expansion of the acylation chemistry to make a wide variety of OFS and opens the doors to explore the potential of furan-based surfactants for other applications.

Chapter 6 Kinetics of Indirect Fatty Acid Anhydride Acylation of 2-Methylfuran

6.1 Introduction

Friedel-Crafts acylation involves an electrophilic substitution reaction of an acyl group on to an aromatic substrate such as benzene or furan[98] resulting in the formation of a mono acylated product. The carbonyl substituent deactivates the aromatic substrate for any further reaction. Friedel-Crafts alkylation reaction on the other hand result in multiple alkylations on the aromatic ring.[135,136] Linear alkylbenzene sulfonate (LAS) is commercially synthesized via the alkylation reaction resulting in a wide product distribution. Since the structure of a surfactant dictates its performance and efficacy, a poor product selectivity translates to poor control over surfactant properties. Ultra-selective acylation reactions enable precise tuning of surfactant structure and properties. Acylation is, in fact, the key chemistry which enables the oleo-furan surfactant platform via C-C coupling. The stereo-specificity of the acylation chemistry enables tailoring the aliphatic chain to deliver superb properties that can significantly impact industry and environment.

Fundamentally, unraveling the mechanism of acylation and the interactions of amphiphilic molecules with confined spaces can significantly advance the catalysis science of C-C coupling with impact beyond biomass. Acylation using fatty acid anhydrides and solid acid catalysts result in high yield of 2-alkanoylfuran. However, the role of acid site and the catalytic mechanism still needs to be understood. Acylation activity using anhydrides was found to be dependent on zeolitic framework as was seen in **Section 3.3.** A larger pore hierarchical zeolite such as SPP was found to be ~20% more active than a small pore zeolite like MWW and BEA for a twenty-four-carbon anhydride acylation. Elucidation of zeolitic framework and carbon chain length effects allow for precise structure tuning. It also activates a catalyst design strategy via tuning the active site(s) and

pore/pocket size and via solvent selection to stabilize acyl species which are potential intermediates. The main hypothesis is that enhancing the relative rate of the pathway to surface acyl species (and high surface coverage) will maximize activity and selectivity to 1-(furan-2-yl)alkan-1-one by inhibiting potential side reactions. Gathering a kinetic knowledge of the acylation reaction will enable reaction tuning and process scale-up. While the earlier chapters (3, 4, and 5) dealt with reaction yield maximization and product characterization, this chapter deals with preliminary reaction kinetics with the target of obtaining a more fundamental understanding of anhydride acylation.

6.2 Materials and Methods

6.2.1 Chemicals

Hexane (95 %), lauric acid (C_{12}, 99% Acros) and tridecane (> 99.8%) were purchased from Sigma-Aldrich. Reactants lauric anhydride (98%) and 2-methylfuran (99%) were purchased from TCI chemicals. Trifluoroacetic anhydride (99%) used for direct acylation was purchased from Sigma Aldrich. The catalyst used for the reaction was mesoporous aluminosilicate, specifically aluminated MCM-41 (Al-MCM-41) which was purchased from Sigma Aldrich. All chemicals and catalysts were used directly without any prior treatment.

6.2.2 Batch Reaction Rates and Reaction Orders

The activity of Al-MCM-41 was investigated by loading 0.014 mol of 2-methylfuran (reactant), 0.014 mol of lauric anhydride (reactant, acylating agent), 30 ml hexane (solvent), 0.5 ml tridecane (internal standard) and 0.2 g Al-MCM-41 (catalyst) into a 100 ml, high pressure, high temperature Parr benchtop reactor (model 4598HTHP with a 4848-temperature controller) at 150 °C, 200 psi N_2 at 25 ^{o}C for 5 h. Once the reactor was charged

with the reactant mixture and catalyst, it was sealed and purged with nitrogen twice to remove traces of air in the reactor head space after which it was pressurized to 200 psi before heating. The reaction was also carried out at 100 ℃ using a 1.25:1 molar ratio of lauric anhydride to 2-methylfuran. Three different control experiments were run to assess side reactions of reactants in the presence of a catalyst as well as reaction activity in the absence of a catalyst. The presence of side reactions of reactants was probed by running experiments at the similar reaction conditions at 100 ℃ in the absence of the other reactant using 0.1 g solid acid catalyst. The uncatalyzed reaction was run using a mixture of 1.15:1 molar ratio of lauric anhydride to 2-methylfuran (0.014 mol) and 0.5 ml tridecane in 30 ml hexane which was charged into a 100 ml Parr reactor and operated at 100 ℃ and 200 psi N_2. Reaction order experiments were performed by running the reaction using 0.1 g Al-MCM-41at 100 ℃ and 200 psi N_2 under the following reaction conditions for 1 h while sampling every 15 min. Product inhibition and reaction orders were determined by co-feeding the two products in separate experiments. The total reaction volume was maintained at 40 ml by diluting it with n-hexane and 0.5 ml n-tridecane was used as an internal standard for quantification purposes.

- Lauric Anhydride: Lauric anhydride concentrations were varied from 0.209-0.906 M at a constant concentration of 2-methylfuran at 0.52 M.
- 2-Methylfuran: 2-Methylfuran concentrations were varied from 0.094-0.769 M at a constant concentration of lauric anhydride at 0.304 M.
- Lauric acid: Lauric acid concentrations were varied from 0.014-0.190 M at constant concentrations of 2-methylfuran and lauric anhydride (0.467 M and 0.311 M respectively).

- 2-Dodecanoyl-5-methylfuran: 2-Dodecanoyl-5-methylfuran concentrations were varied from 0.003-0.206 M at constant concentrations of 2-methylfuran and lauric anhydride (0.555 M and 0.361 M respectively).

2-Dodecanoyl-5-methylfuran was synthesized using the trifluoroacetic anhydride method discussed in **Section 3.2.3.** For every experiment, time zero was recorded as the time when the reaction mixture reaches reaction temperature, while carbon balance calculations were done with respect to the original reactant mixture before heating.

6.3 Results and Discussion

The reaction scheme for the acylation of 2-methylfuran using lauric anhydride is shown in **Scheme 6-1**.

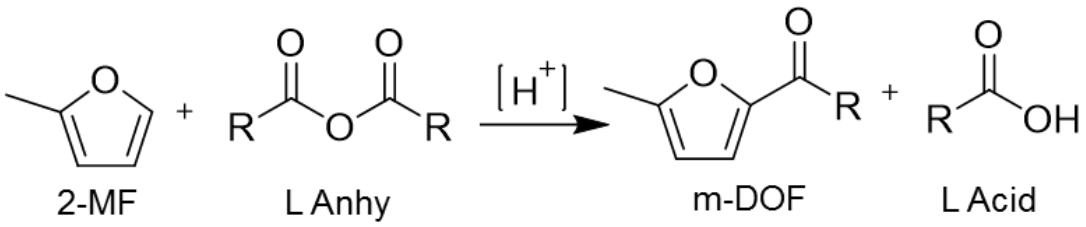

Scheme 6-1. Acylation of 2-methylfuran (2-MF) with lauric anhydride (L Anhy) to form 2-dodecanoyl-5-methylfuran (m-DOF) and lauric acid (L Acid) where R = $C_{11}H_{23}$

2-Methylfuran was used instead of furan as the acylating substrate to enable ease of quantification due to the high vapor pressure of furan under reaction conditions (furan boiling point 31.3 ℃ at 1 atm). **Figure 6-1** (**A** and **B**) shows the change in concentration profiles of the reactants (2-methylfuran and lauric anhydride) and the two products (m-DOF and lauric acid) along with reactant conversion (**C** and **D**) at 150 and 100 ℃ in a span of 5 h. Higher temperatures promote higher conversions as expected and for the purposes of evaluating kinetics under differential conditions (less than 10% conversion), 100 ℃ was selected as the reaction temperature for a reaction time of 1 h.

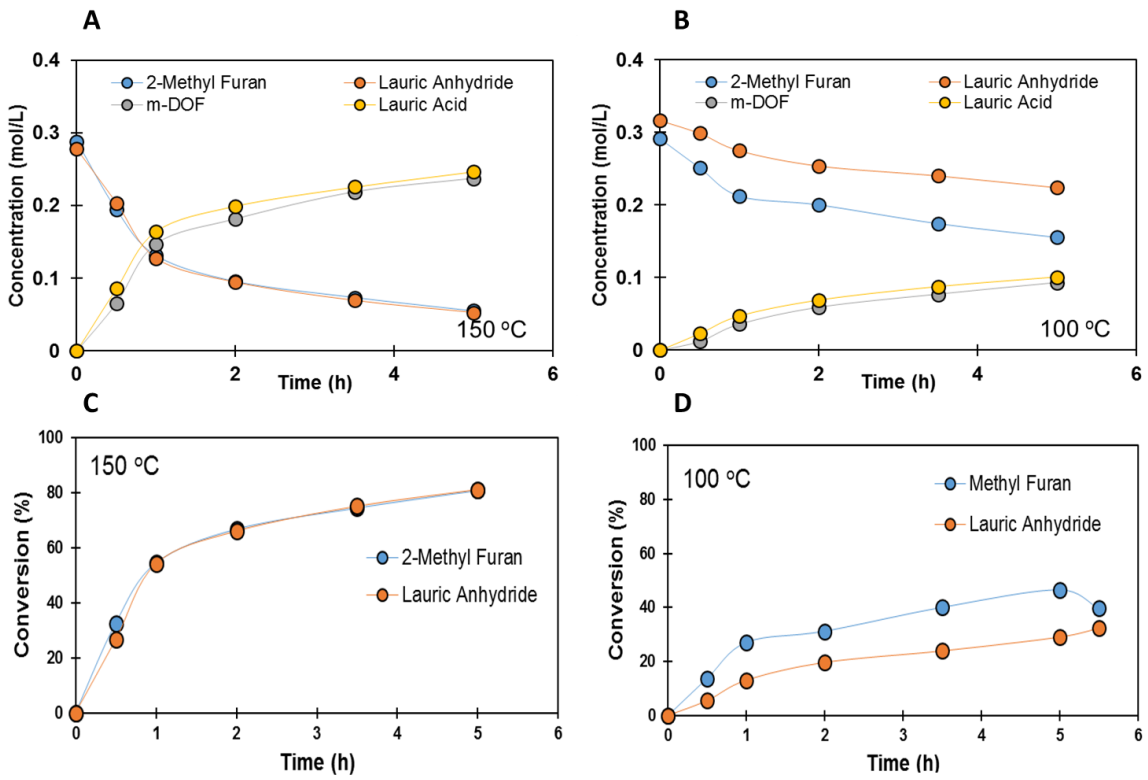

Figure 6-1. Concentration profiles of reactants, 2-methylfuran (blue) and lauric anhydride (orange) and products, m-DOF (grey) and lauric acid (yellow) **A.** 150 °C (95% carbon balance) and **B.** 100 °C (98% carbon balance). Conversion of reactants at **A.** 150 °Cand **B.** 100 °C. Reaction conditions: 200 psi N_2 at 25 °C, 5 h, 30 ml hexane, 0.2 g Al-MCM-41, 0.5 ml tridecane as internal standard.

During the reaction, one mole of lauric anhydride reacts to give one mole of lauric acid and the acylated product m-DOF. This was validated experimentally as shown in **Figure 6-2 A**. Lauric anhydride, thermally, in the presence of water and an acid catalyst can undergo hydrolysis to form two moles of lauric acid (**Scheme 6-2**).[137]

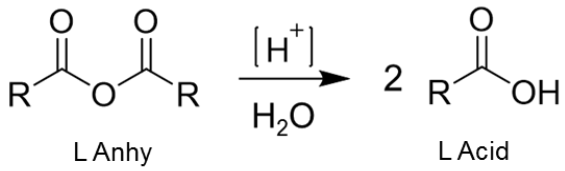

Scheme 6-2. Lauric anhydride (L Anhy) hydrolysis in the presence of an acid catalyst and water to form lauric acid (L Acid) (R=$C_{11}H_{23}$)

The results obtained from running a control experiment in the absence of 2-methylfuran verify that no hydrolysis of anhydride occurs and lauric acid produced during the reaction is solely from the acylation chemistry thereby indicating a *dry* system (**Figure 6-2 B**).

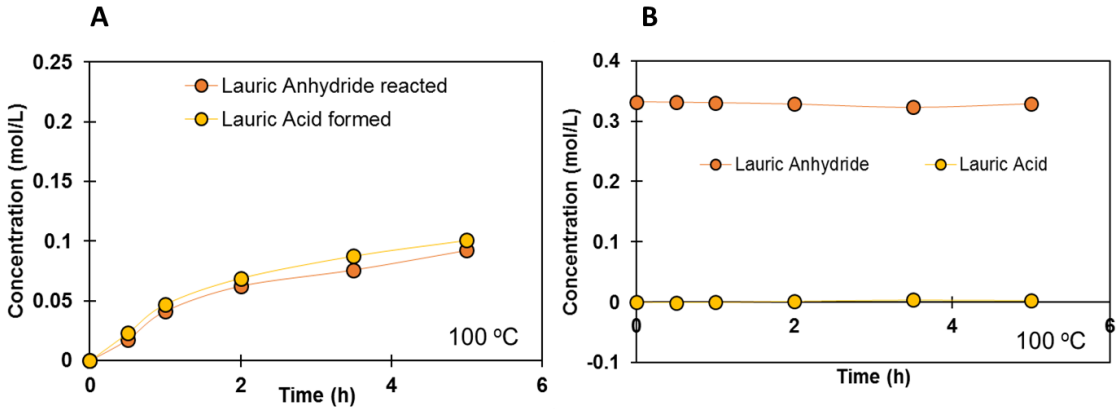

Figure 6-2. Concentration profile of **A.** Lauric acid (yellow) formed with respect to the amount of lauric anhydride (orange) reacted at 100 °C in the presence of 2-methylfuran and 0.1 g Al-MCM-41 and **B.** Lauric acid (yellow) formed in the absence of 2-methylfuran for a given concentration of lauric anhydride (orange) at 100 °C in the presence of 0.1 g Al-MCM-41 (97% carbon balance)

Reactions involving furan and its derivatives such as 2-methylfuran often report the formation of dimeric and trimeric species as well as coke on the surface of an acid catalyst.[83,138] A control experiment to assess the side reactions of 2-methylfuran was performed in the absence of lauric anhydride at 100 °C using 0.1 g Al-MCM-41 the results of which are shown in **Figure 6-3**.

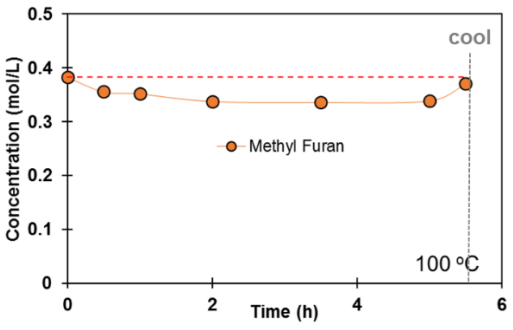

Figure 6-3. Control experiment for side reactions of 2-methylfuran. Reaction Conditions: 100 °C, 200 psi N_2 at 25 °C, 5 h, 0.014 mol 2-methylfuran, 30 ml hexane, 0.1 g Al-MCM-41, 0.5 ml tridecane internal standard

As reaction time progresses, we see a lowering of 2-methylfuran concentration which hits a plateau within 1 h of reaction time yielding a carbon balance of ~86%. Analysis of the final sample drawn

after cooling down the reaction mixture records a concentration roughly equivalent to that of the starting mixture with a carbon balance equal to 96%. Unlike other experiments, time zero here, is marked with respect to the original reactant mixture before heating. This potentially implies that the drop in the concentration during the reaction period is not due to side reactions but because of vapor liquid partitioning due to the high volatility of 2-methylfuran. A reaction temperature of 100 ℃ is sufficiently low to minimize significant loss of 2-methylfuran to oligomerization and coking reactions.

It was also verified that no reaction occurs in the absence of the catalyst Al-MCM-41 as shown in **Figure 6-4**.

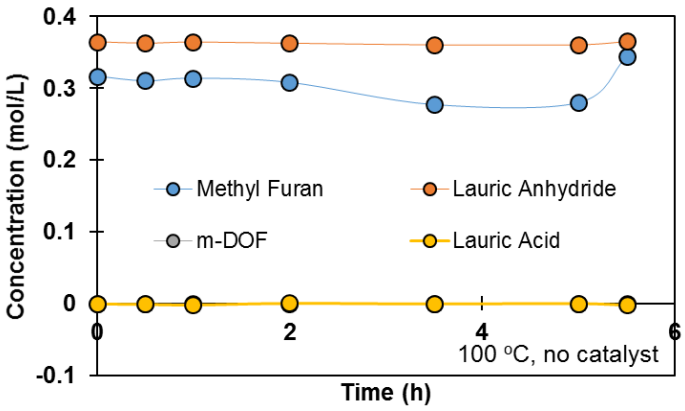

Figure 6-4. Concentration profile of reactants and products in an uncatalyzed system. Reaction conditions: 100 ℃, 200 psi N_2 at 25 ℃, 5 h, 30 ml hexane, 0.5 ml tridecane internal standard, no catalyst

6.3.1 Determination of Reaction Orders

The acylation reaction order estimation was performed in a batch reactor at 100 ℃ over a span of 1 h. Reactions conditions were maintained to ensure that the operation regime was under differential conditions i.e. less than 10% conversion of reactants.

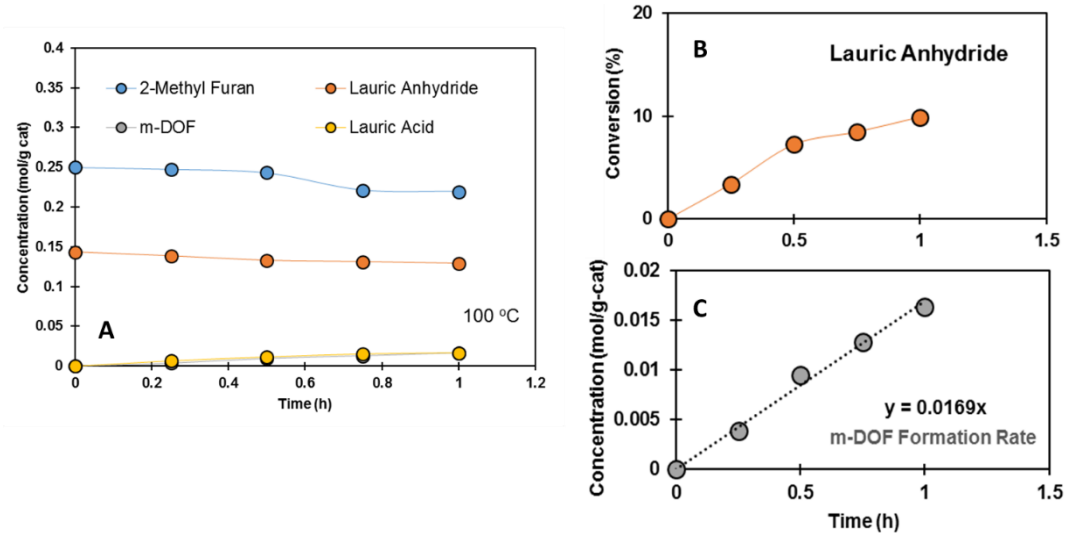

Figure 6-5. A. Concentration profile of reactants and products at 100 °C during 1 h for estimation of reaction orders (98% carbon balance). **B.** Conversion of lauric anhydride, **C.** Product formation rate utilized for evaluation of initial rates

Product (m-DOF) formation was used to determine initial rate of reaction in mol/(g catalyst-h). **Figure 6-6** shows data for determination of reaction orders for reactants and products.

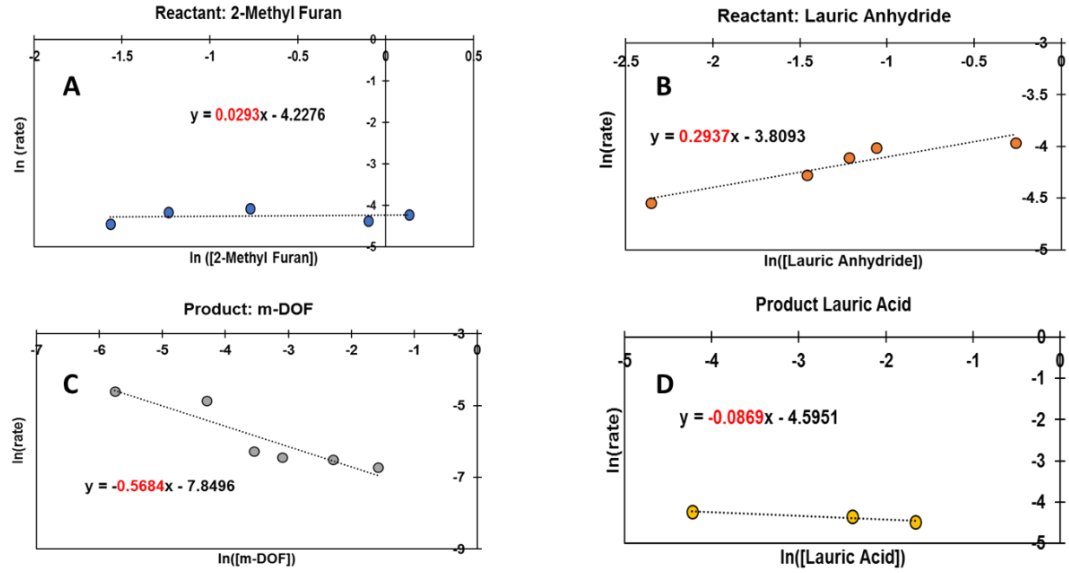

Figure 6-6. Reaction order determination. Natural log of reaction rate vs natural log of concentration of **A.** 2-methylfuran, **B.** lauric anhydride, **C.** m-DOF and **D.** lauric acid

The slope, highlighted in red, of the linear trend fitted to the data in the plot of ln(rate) vs ln(concentration) indicates the reaction order of the compound. As shown in **Figure 6-6**, the reaction has a partial order dependence (0.29) on the concentration of lauric anhydride and an almost zero order dependence on the concentration of 2-methylfuran (-0.029) and lauric acid (-0.087). Interestingly, the product m-DOF was found to inhibit the reaction exhibiting a negative reaction order of -0.57. With the data obtained, it is possible to propose a sequence of elementary reaction steps via a simplistic Eley-Rideal[139] approach for a surface reaction. Numerous possibilities exist for proposing a sequence and solid claims can be made towards a specific rate expression only after further detailed experimentation. One such sequence is listed below

$$\text{LAn} + * \rightleftharpoons \text{LAn}* \qquad (K_1)$$

$$\text{LAn}* \rightarrow \text{LAc} + \text{Ac}* \qquad (k_2)$$

$$\text{Ac}* + \text{MF} \rightleftharpoons \text{m-DOF}* \qquad (K_3)$$

$$\text{m-DOF}* \rightleftharpoons \text{m-DOF} + * \qquad (K_4)$$

where, LAn, MF, LAc and m-DOF represent lauric anhydride, 2-methylfuran, lauric acid and the acylated product 2-dodecanoyl-5-methylfuran respectively. * denotes an active acid site on the catalyst while Ac* is the adsorbed acyl species. Similarly, LAn* and m-DOF* represent the corresponding adsorbed species. K_1, K_3 and K_4 are equilibrium constants for steps 1, 3 and 4 while k_2 is the rate constant for step 2. The formation of the acyl species (marked by k_2) is assumed to be the rate determining step. For such a system, the following rate expression can be obtained.

$$r = K_1 k_2 [LAn] \frac{[*]_o}{1 + K_1[LAn] + \frac{[m-DOF]}{K_3 K_4 [MF]} + \frac{[m-DOF]}{K_4}}$$

$[*]_o$ denotes the total number of active acid sites present in the catalyst.

Since formation of acyl species is considered to be the rate determining step, the term $\frac{[m-DOF]}{K_3K_4[MF]}$ which represents the coverage of the acyl species (Ac*) can be neglected and the rate expression can be simplified to

$$r = K_1k_2[LAn]\frac{[*]_o}{1 + K_1[LAn] + \frac{[m-DOF]}{K_4}}$$

Using the above rate expression, we can potentially explain the partial order and zero order dependence of lauric anhydride and 2-methylfuran respectively as well as the inhibiting effect of the product m-DOF. Albeit, the aforementioned explanation can rationalize the observations in reaction order, it is important to remember that Eley-Rideal is a simplistic approach involving several assumptions to simplify rate expressions and the true expression could involve several other factors and elementary reactions. Mechanistically, acyl species have been observed by NMR[140] and FTIR,[141–143] and is proposed as a key surface reaction intermediate.[84,144] Brønsted acid zeolites aid in the formation of acylium ions and acyl species.[145] Meanwhile, ketenes have also been proposed as intermediates.[146–148] Acid sites activate the acyl intermediate for electrophilic attack from a base (e.g., furan, 2-methylfuran). Owing to the large number of unknown parameters, an accurate prediction of the reason behind the observation is not possible within the current experimental framework and would require additional detailed work including kinetic isotope effect (KIE) experiments.

6.4 Future Work and Conclusions

We have experimentally determined reaction orders of various reactants and products and assessed side reactions. It was found that the reaction rate has a zero-order dependence on the reactant 2-methylfuran and the product, lauric acid while exhibiting a partial order dependence on lauric

anhydride. Interestingly, the acylated product 2-dodecancoyl-5-methylfuran was found to have an inhibitive effect on the reaction rate thereby exhibiting a negative reaction order. In an acid catalyzed reaction, lauric acid was formed from lauric anhydride only via acylation, i.e. in the absence of 2-methylfuran, lauric anhydride did not undergo any substantial hydrolysis. Similarly, in the absence of lauric anhydride, 2-methylfuran was found to undergo minimal coking on the acid sites. It was also possible to conclude that the reaction occurs only when catalyzed. A simplistic Eley-Rideal model was applied to rationalize reaction orders and a rate expression was obtained. However, it is incorrect to form a conclusion regarding the rate expression without further experimentation.

Kinetic studies require differential conditions. However, operation of batch reactors under these conditions possess inherent problems.[149] The process of heating the reaction mixture to desired temperatures result in reactant conversion during the process which may result in significant conversion values when compared to differential conditions. Hence, sampling at low conversions becomes a problem. Furthermore, studies in a batch reactor involving temperature variation such as determination of activation energy do not account for on-stream catalyst deactivation which occurs at different rates at different temperatures. Flow reactors allow for catalyst deactivation prior to data collection and hence allows for the same original reference state for every data point. Future work will focus on performing kinetic experiments using a liquid phase flow reactor. Experimental determination of activation energy coupled with DFT simulations will further assist in determination of elementary reaction steps and identification of intermediates. Intermediate species can also be identified via transmission FT-IR via methods reported in literature. This technique can also be used to understand the accessibility of sites as the alkyl chain length of anhydrides varies and the stability of the corresponding intermediate in the relevant temperature range. Kinetics of acylation chemistry using furan as the substrate need to be evaluated and compared with the results

obtained for 2-methylfuran. The insight obtained from anhydride acylation could be extended to study direct acylation using fatty acids and triglycerides. The use of triglycerides as an acylating agent will cut down on the energy intensive step of converting acids obtained from hydrolysis of triglycerides to anhydrides making it viable for scale-up and process intensification.

Chapter 7 Conclusions

The primary innovation of the research undertaken is a tunable chemical pathway to make a new class of OFS surfactants from bio-renewable feedstock like furans and fatty acids. Properties of surfactants depend heavily on their molecular structure. However, alkylation chemistry used in commercial surfactant production has poor tunability which limits the application-specific engineering of surfactant molecules to achieve desired properties. We have shown the feasibility of OFS surfactants for detergency application. With the proposed chemistry, targeted surfactant molecules can be made with high selectivity. At the same time, these novel surfactants have enhanced performance and stability as compared to conventional surfactants which allows for lower concentrations of surfactant in consumer products. An important outcome of this innovation was the discovery that OFS were found to have order of magnitude higher hard water stability compared to commercial surfactants, thereby bypassing the need for toxic and expensive additives like chelants in formulations. While SLS and LAS can be used only in soft and hard water conditions respectively, OFS-12 can be used in conditions that are a hundred times worse without losing solution clarity and surfactant functionality. Environmentally benign OFS surfactants possess a dual in-built function of detergency and combating water hardness without compromising on surfactant performance at a potentially reduced cost. The improved surfactant properties can reduce the amount of surfactant used in consumer products reducing human exposure to harmful chemicals. At the same time, using structure-property relationships of surfactants, the tunable chemistry can allow us to engineer application-specific surfactant structures which will, if not eliminate, but certainly reduce the use of additives like chelating agents reducing the cost and improving sustainability. Coupling of reaction chemistries with acylation other than hydrogenation and aldol condensation enable expansion of the OFS platform. We looked at dehydration chemistries to synthesize potential branched and gemini surfactant precursors and observed effects

of pore confinement on unimolecular and bimolecular dehydration reactions of 2-DOF Alcohol. Investigation into kinetics of acylation reaction revealed preliminary data of reaction orders which can be utilized for proposing a reaction sequence consisting of elementary steps. Coupling of reaction chemistries, performance evaluation and kinetics allow for a comprehensive approach towards tuning the OFS platform to incorporate desired functionalities for specific surfactant properties to make a wide variety of OFS and opens the doors to explore the potential of furan-based surfactants for other applications.

Chapter 8 Bibliography

(1) Williams, C. L.; Chang, C.-C.; Do, P.; Nikbin, N.; Caratzoulas, S.; Vlachos, D. G.; Lobo, R. F.; Fan, W.; Dauenhauer, P. J. Cycloaddition of Biomass-Derived Furans for Catalytic Production of Renewable P-Xylene. *ACS Catal.* **2012**, *2* (6), 935–939.

(2) Dauenhauer, P. J.; Huber, G. W. Biomass at the Shale Gas Crossroads. *Green Chem.* **2014**, *16* (2), 382–383.

(3) *Bioenergy Technologies Office Multi-Year Program Plan: March 2015 Update*; 2015.

(4) Energy Inf. Adm. http://www.eia.gov/dnav/pet/pet_pnp_pct_dc_nus_pct.

(5) Mary J. Biddy; Kinchin, C. S. C. *Chemicals from Biomass: A Market Assessment of Bioproducts with Near-Term Potential*; 2016.

(6) Golden, J.; Handfield, R. B.; Daystar, J.; Mcconnell, T. E. *An Economic Impact Analysis of the U.S. Biobased Products Industry: A Report to the Congress of the United States of America*; 2015.

(7) Lange, K. R. *Surfactants : A Practical Handbook*; Hanser Publishers ; Hanser Gardner Publications: Munich; Cincinnati, 1999.

(8) Park, D. S.; Joseph, K. E.; Koehle, M.; Krumm, C.; Ren, L.; Damen, J. N.; Shete, M. H.; Lee, H. S.; Zuo, X.; Lee, B.; et al. Tunable Oleo-Furan Surfactants by Acylation of Renewable Furans. *ACS Cent. Sci.* **2016**, *2* (11), 820–824.

(9) Porter, M. R. *Handbook of Surfactants*, 2nd ed.; Springer Netherlands, 1994.

(10) *Handbook of Detergents, Part E: Applications*; Zoller, U., Ed.; CRC Press, 2008.

(11) Tsai, T.-C.; Wang, I.; Li, S.-J.; Liu, J.-Y. Development of a Green LAB Process: Alkylation of Benzene with 1-Dodecene over Mordenite. *Green Chem.* **2003**, *5* (4), 404–409.

(12) *Global Surfactant Market*, 4th ed.; Acmite Market Intelligence, 2016.

(13) Cross, J. *Anionic Surfactants : Analytical Chemistry*; CRC Press, 1998.

(14) *Linear Alkylbenzene Sulfonic Acid (LABSA)/Linear Alkylate Sulfonate (LAS)*; IHS Markit Chemical Economics Handbook, 2015.

(15) Linear Alkyl Benzene (LAB) Market Analysis By Application (Heavy Duty Laundry Liquids, Laundry Powders, Light Duty Dish Washing Liquids, Industrial Cleaners, Household Cleaners) And Segment Forecasts To 2020. *LAB Industry Report*. July 2015.

(16) *Green Household Cleaning Products in the U.S*, 3rd ed.; Packaged Facts, 2015.

(17) *Design and Selection of Performance Surfactants*; Karsa, D. R., Ed.; Taylor & Francis Inc: Bosa Roca, 1999.

(18) Roberts, D. W. Optimisation of the Linear Alkyl Benzene Sulfonation Process for Surfactant Manufacture. *Org. Process Res. Dev.* **2003**, *7* (2), 172–184.

(19) Vaughan, R. J. Sulfonation Process. 4,308,215, 1981.

(20) Modler, R. F.; Willhalm, R.; Yoshida, Y. Linear Alkylate Sulfonates. *CEH Marketing Research Report, SRI International*. 1996.

(21) Cao, Y.; Kessas, R.; Naccache, C.; Ben Taarit, Y. Alkylation of Benzene with Dodecene. The Activity and Selectivity of Zeolite Type Catalysts as a Function of the Porous Structure. *Appl. Catal. A Gen.* **1999**, *184* (2), 231–238.

(22) Kameoka, S.; Tanabe, T.; Tsai, A. P. Spinel CuFe2O4: A Precursor for Copper Catalyst with High Thermal Stability and Activity. *Catal. Letters* **2005**, *100* (1–2), 89–93.

(23) Kocal, J. A.; Vora, B. V; Imai, T. Production of Linear Alkylbenzenes. *Appl. Catal. A Gen.* **2001**, *221* (1), 295–301.

(24) A., S. E.; L., H. R.; C., A. R. An Evaluation of the River Die-away Technique for Studying Detergent Biodegradability. *J. Am. Oil Chem. Soc.* **2007**, *41* (12), 826–830.

(25) J., S. J. The Evolution of Anionic Surfactant Technology to Meet the Requirements of the Laundry Detergent Industry. *J. Surfactants Deterg.* **2015**, *7* (4), 319–328.

(26) Childres, I.; Jauregui, L.; Park, W.; Cao, H.; Chen, Y. Raman Spectroscopy of Graphene and Related Materials. *New Dev. Phot. Mater. Res.* **2013**, 1–20.

(27) Ma, J.-G.; Boyd, B. J.; Drummond, C. J. Positional Isomers of Linear Sodium Dodecyl Benzene Sulfonate: Solubility, Self-Assembly, and Air/Water Interfacial Activity. *Langmuir* **2006**, *22* (21), 8646–8654.

(28) Schramm, L. L.; Stasiuk, E. N.; Marangoni, D. G. 2 Surfactants and Their Applications. *Annu. Rep. Prog. Chem.{,} Sect. C Phys. Chem.* **2003**, *99* (0), 3–48.

(29) A Look at Hard Water Across the US. http://homewater101.com/look-hard-water-across-us.

(30) Lai, K.-Y. *Liquid Detergents*; CRC Press, 2005.

(31) Showell, M. *Handbook of Detergents, Part D: Formulation*; CRC Press Taylor & Francis Group: Boca Raton, FL, 2006.

(32) Boethling, R. S.; Sommer, E.; DiFiore, D. Designing Small Molecules for Biodegradability. *Chem. Rev.* **2007**, *107* (6), 2207–2227.

(33) Ragauskas, A. J.; Williams, C. K.; Davison, B. H.; Britovsek, G.; Cairney, J.; Eckert, C. A.; Frederick, W. J.; Hallett, J. P.; Leak, D. J.; Liotta, C. L.; et al. The Path Forward for Biofuels and Biomaterials. *Science (80-.).* **2006**, *311* (5760), 484–489.

(34) Bridgwater, A. V. Renewable Fuels and Chemicals by Thermal Processing of Biomass. *Chem. Eng. J.* **2003**, *91* (2), 87–102.

(35) Climent, M. J.; Corma, A.; Iborra, S. Converting Carbohydrates to Bulk Chemicals and Fine Chemicals over Heterogeneous Catalysts. *Green Chem.* **2011**, *13* (3), 520–540.

(36) Bognolo, G. The Surface Active Agents Market: Where Is It Going? A2 - Karsa, David R. BT - Industrial Applications of Surfactants IV; Woodhead Publishing, 1999; pp 40–49.

(37) *Green Household Cleaning Products in the U.S.*, 3rd ed.; 2015.

(38) Advances in Surfactants (Technical Insights). *Frost and Sullivan*. June 2014.

(39) Tropsch, J. *Sustainability for Bio-Based Products - Bio-Based Surfactant*; 2015.

(40) Johansson, I.; Strandberg, C.; Karlsson, B.; Karlsson, G.; Hammarstrand, K. Use of Mixtures of Alkyl Alkoxylates and Alkyl Glucosides in Strong Electrolytes and Highly Alkaline Systems A2 - Karsa, David R. BT - Industrial Applications of Surfactants IV; Woodhead Publishing, 1999; pp 88–107.

(41) Levey, M. E.; Revell, E. B.; Dahm, R.; Machowski, V. A New Surfactant Made from Kelp Seaweed A2 - Karsa, David R. BT - Industrial Applications of Surfactants IV; Woodhead Publishing, 1999; pp 108–116.

(42) Beck, R. Starch-Derived Products in Detergents A2 - Karsa, David R. BT - Industrial Applications of Surfactants IV; Woodhead Publishing, 1999; pp 117–129.

(43) Rust, D.; Wildes, S. Surfactants – A Market Opportunity Study Update. *United Soybean Board, Omni Tech International, LTD*. 2008.

(44) Beyond the Bottle: Ingredients http://methodhome.com/beyond-the-bottle/ingredients/.

(45) Ingredients + Science https://www.seventhgeneration.com/ingredients-glossary.

(46) Kraus, G. A.; Lee, J. J. A Direct Synthesis of Renewable Sulfonate-Based Surfactants. *J. Surfactants Deterg.* **2013**, *16* (3), 317–320.

(47) West, R. M.; Wu, R.; Silks III, L. A. Furan Based Composition. US20150150768A1, 2015.

(48) Gassama, A.; Ernenwein, C.; Youssef, A.; Agach, M.; Riguet, E.; Marinkovic, S.; Estrine, B.; Hoffmann, N. Sulfonated Surfactants Obtained from Furfural. *Green Chem.* **2013**, *15* (6), 1558–1566.

(49) Joseph, K. E.; Krumm, C. A Bio-Renewable Surfactant with a Trick up Its Sleeve. *AOCS Inf.* **2017**, *28* (5), 16–19.

(50) Augustin, M. A.; Hemar, Y. Nano- and Micro-Structured Assemblies for Encapsulation of Food Ingredients. *Chem. Soc. Rev.* **2009**, *38* (4), 902–912.

(51) *Surfactants in Consumer Products*, 1st ed.; Falbe, J., Ed.; Springer-Verlag Berlin Heidelberg, 1987.

(52) Fendler, J. H. Polymerized Surfactant Vesicles: Novel Membrane Mimetic Systems. *Science (80-.).* **1984**, *223* (4639), 888–894.

(53) Sorrenti, A.; Illa, O.; Ortuno, R. M. Amphiphiles in Aqueous Solution: Well beyond a Soap Bubble. *Chem. Soc. Rev.* **2013**, *42* (21), 8200–8219.

(54) Watry, M. R.; Richmond, G. L. Comparison of the Adsorption of Linear Alkanesulfonate and Linear Alkylbenzenesulfonate Surfactants at Liquid Interfaces. *J. Am. Chem. Soc.* **2000**, *122* (5), 875–883.

(55) Marinangeli, R. E.; Lawson, R. J.; Gaperin, L. B.; Fritsch, T. R. Process for Producing

Arylalkanes and Arylalkane Sulfonates, Compositions Produced Therefrom, and Uses Thereof. 6,187,981, 2011.

(56) Jordan, A.; Gathergood, N. Biodegradation of Ionic Liquids - a Critical Review. *Chem. Soc. Rev.* **2015**, *44* (22), 8200–8237.

(57) Bardach, J. E.; Fujiya, M.; Holl, A. Detergents: Effects on the Chemical Senses of the Fish Ictalurus Natalis (Le Sueur). *Science (80-.).* **1965**, *148* (3677), 1605 LP-1607.

(58) Park, D. S.; Krumm, C.; Koehle, M.; Joseph, K. E.; Vlachos, D. G.; Lobo, R. F.; Dauenhauer, P. J. Methods of Forming Aromatic Containing Compounds. Application WO2017079718A1, 2017.

(59) Krumm, C.; Joseph, K. E.; Park, D. S.; Mahanthappa, M.; Dauenhauer, P. J. Aromatic Surfactants. Application WO2017079719A1, 2017.

(60) Corma, A.; Iborra, S.; Velty, A. Chemical Routes for the Transformation of Biomass into Chemicals. *Chem. Rev.* **2007**, *107* (6), 2411–2502.

(61) Ursula, B.; Uwe, B.; R., M. M. A.; O., M. J.; J., S. H. Oils and Fats as Renewable Raw Materials in Chemistry. *Angew. Chemie Int. Ed.* **2011**, *50* (17), 3854–3871.

(62) Guo, Q.; Fan, F.; Pidko, E. A.; van der Graaff, W. N. P.; Feng, Z.; Li, C.; Hensen, E. J. M. Highly Active and Recyclable Sn-MWW Zeolite Catalyst for Sugar Conversion to Methyl Lactate and Lactic Acid. *ChemSusChem* **2013**, *6* (8), 1352–1356.

(63) Corma, A.; Fornés, V.; Martínez-Triguero, J.; Pergher, S. B. Delaminated Zeolites: Combining the Benefits of Zeolites and Mesoporous Materials for Catalytic Uses. *J. Catal.* **1999**, *186* (1), 57–63.

(64) Faba, L.; Díaz, E.; Ordóñez, S. Performance of Bifunctional Pd/MxNyO (M=Mg, Ca; N=Zr, Al) Catalysts for Aldolization–hydrogenation of Furfural–acetone Mixtures. *Catal. Today* **2011**, *164* (1), 451–456.

(65) Tago, T.; Konno, H.; Ikeda, S.; Yamazaki, S.; Ninomiya, W.; Nakasaka, Y.; Masuda, T. Selective Production of Isobutylene from Acetone over Alkali Metal Ion-Exchanged BEA Zeolites. *Catal. Today* **2011**, *164* (1), 158–162.

(66) SCULLY, J. F.; BROWN, E. V. THE SULFONATION OF FURAN AND FURAN HOMOLOGS. PREPARATION OF FURANSULFONAMIDES1. *J. Org. Chem.* **1954**, *19* (6), 894–901.

(67) Trummlitz, G.; Seeger, E.; Engel, W. 4-5-Dimethyl-thieno[3,2-d]ISO- Thiazolo-3(2H)-One-1,1- Dioxides, Compositions, and Methods of Use as a Sweetener. 4233333, 1980.

(68) Mohrig, J. R.; Hammond, C. N.; Schatz, P. F. *Techniques in Organic Chemistry*, 2nd ed.; W. H. Freeman and Company, 2006.

(69) Meloan, C. E. *Chemical Separations: Principles, Techniques and Experiments*; Wiley, 1999.

(70) Pretsch, E.; Bühlmann, P.; Badertscher, M. *Structure Determination of Organic Compounds*, 4th ed.; Springer-Verlag Berlin Heidelberg, 2009.

(71) Buehler, C. A.; Pearson, D. E. *Organic Synthesis*; Wiley: New York, 1974.

(72) Albertson, N. F. *Organic Reaction*; Cope, A. C., Ed.; Krieger Publishing, 1975.

(73) Fisher, J. W. Manufacture of Carboxylic Acids. 2,411,567, 1946.

(74) Goel, A. B.; Richards, H. J. Preparation of Carboxylic Acid Anhydrides. Google Patents 1984.

(75) Patai, S. *The Chemistry of Acid Derivatives Part I*; Wiley: New York, 1979.

(76) Heaney, H. 3.2 - The Bimolecular Aromatic Friedel–Crafts Reaction A2 - Trost, Barry M.; Fleming, I. B. T.-C. O. S., Ed.; Pergamon: Oxford, 1991; pp 733–752.

(77) Sartori, G.; Maggi, R. Update 1 of: Use of Solid Catalysts in Friedel−Crafts Acylation Reactions. *Chem. Rev.* **2011**, *111* (5), PR181-PR214.

(78) Opietnik, M.; Jungbauer, A.; Rosenau, K. M. and T. Mild Friedel-Crafts Acylation of Furan with Carboxylic Acids and the Heterogeneous Catalyst Couple AlPW12O40 / Mg(OH)2. *Current Organic Chemistry*. 2012, pp 2739–2744.

(79) Izumi, Y.; Ogawa, M.; Urabe, K. Alkali Metal Salts and Ammonium Salts of Keggin-Type Heteropolyacids as Solid Acid Catalysts for Liquid-Phase Friedel-Crafts Reactions. *Appl. Catal. A Gen.* **1995**, *132* (1), 127–140.

(80) Heidekum, A.; Harmer, M. A.; Hoelderich, W. F. Nafion/Silica Composite Material Reveals High Catalytic Potential in Acylation Reactions. *J. Catal.* **1999**, *188* (1), 230–232.

(81) Sheemol, V. N.; Tyagi, B.; Jasra, R. V. Acylation of Toluene Using Rare Earth Cation Exchanged Zeolite β as Solid Acid Catalyst. *J. Mol. Catal. A Chem.* **2004**, *215* (1), 201–208.

(82) Sandler, S. R.; Karo, W. *Organic Functional Group Preparation*; Academic Press: New York, 1989.

(83) Cheng, Y.-T.; Huber, G. W. Chemistry of Furan Conversion into Aromatics and Olefins over HZSM-5: A Model Biomass Conversion Reaction. *ACS Catal.* **2011**, *1* (6), 611–628.

(84) Koehle, M.; Saraçi, E.; Dauenhauer, P.; Lobo, R. F. Production of p-Methylstyrene and p-Divinylbenzene from Furanic Compounds. *ChemSusChem 10* (1), 91–98.

(85) Wade Jr., L. G. *Organic Chemistry*, 8th ed.; Pearson, 2013.

(86) Smyth, T. P.; Corby, B. W. Toward a Clean Alternative to Friedel−Crafts Acylation: In Situ Formation, Observation, and Reaction of an Acyl Bis(trifluoroacetyl)phosphate and Related Structures. *J. Org. Chem.* **1998**, *63* (24), 8946–8951.

(87) Tedder, J. M. The Use Of Trifluoroacetic Anhydride And Related Compounds In Organic Syntheses. *Chem. Rev.* **1955**, *55* (5), 787–827.

(88) Blaser, H.; Siegrist, U.; Steiner, H.; Studer, M.; Sheldon, R.; van Bekkum, H. *Fine Chemicals through Heterogeneous Catalysis*; Weinheim: Wiley/VCH, 2001.

(89) RYLANDER, P. N. 15 - Hydrogenation of Ketones; RYLANDER, P. N. B. T.-C. H. O. P. M., Ed.; Academic Press, 1967; pp 258–290.

(90) RYLANDER, P. N. 21 - Furans; RYLANDER, P. N. B. T.-C. H. O. P. M., Ed.; Academic

Press, 1967; pp 363–369.

(91) Faba, L.; Díaz, E.; Ordóñez, S. Aqueous-Phase Furfural-Acetone Aldol Condensation over Basic Mixed Oxides. *Appl. Catal. B Environ.* **2012**, *113–114*, 201–211.

(92) Mestres, R. A Green Look at the Aldol Reaction. *Green Chem.* **2004**, *6* (12), 583–603.

(93) Tago, T.; Konno, H.; Ikeda, S.; Yamazaki, S.; Ninomiya, W.; Nakasaka, Y.; Masuda, T. Selective Production of Isobutylene from Acetone over Alkali Metal Ion-Exchanged BEA Zeolites. *Catal. Today* **2011**, *164* (1), 158–162.

(94) Sanyal, S. N. *Reactions, Rearrangements and Reagents*, 4th ed.; Bharati Bhawan, 2015.

(95) Carruthers, W.; Coldham, I. *Modern Methods of Organic Synthesis*, 4th ed.; Cambridge University Press: Cambridge, 2004.

(96) Scott, M. J.; Jones, M. N. The Biodegradation of Surfactants in the Environment. *Biochim. Biophys. Acta - Biomembr.* **2000**, *1508* (1), 235–251.

(97) Bajpai, D.; Tyagi, V. K. Laundry Detergents: An Overview. *J. Oleo Sci.* **2007**, *56* (7), 327–340.

(98) J. Clayden; Greeves, N.; Warren, S. Electrophilic Aromatic Substitution. In *Organic Chemistry*; Oxford, New York, 2012; pp 493–494.

(99) Maneedaeng, A.; Flood, A. E.; Haller, K. J.; Grady, B. P. Modeling of Precipitation Phase Boundaries in Mixed Surfactant Systems Using an Improved Counterion Binding Model. *J. Surfactants Deterg.* **2012**, *15* (5), 523–531.

(100) Zimmerman, J. B.; Clarens, A. F.; Hayes, K. F.; Skerlos, S. J. Design of Hard Water Stable Emulsifier Systems for Petroleum- and Bio-Based Semi-Synthetic Metalworking Fluids. *Environ. Sci. Technol.* **2003**, *37* (23), 5278–5288.

(101) Shea, P. J.; Tupy, D. R. Reversal of Cation-Induced Reduction in Glyphosate Activity by EDTA. *Weed Sci.* **1984**, *32* (6), 802–806.

(102) Briggs, J. C.; Ficke, J. F. *Quality of Rivers of the United States, 1975 Water Year; Based on the National Stream Quality Accounting Network (NASQAN)*; Reston, VA, 1977.

(103) Nowack, B.; Kari, F. G.; Krüger, H. G. The Remobilization of Metals from Iron Oxides and Sediments by Metal-EDTA Complexes. *Water. Air. Soil Pollut.* **2001**, *125* (1), 243–257.

(104) NEWSAM, J. M. The Zeolite Cage Structure. *Science (80-.).* **1986**, *231* (4742), 1093 LP-1099.

(105) Analysis of Surfactants. Second Edition, Revised and Expanded By Thomas M. Schmitt (BASF Corp.). Marcel Dekker: New York. X + 638 Pp. $225.00. ISBN 0-8247-0449-5. *J. Am. Chem. Soc.* **2001**, *123* (34), 8446.

(106) Hummel, D. O.; Leach, R. G. *Handbook of Surfactant Analysis: Chemical, Physico-Chemical and Physical Methods*; John Wiley & Sons: Chichester, 2002.

(107) Vlachy, N.; Drechsler, M.; Verbavatz, J.-M.; Touraud, D.; Kunz, W. Role of the Surfactant Headgroup on the Counterion Specificity in the Micelle-to-Vesicle Transition

through Salt Addition. *J. Colloid Interface Sci.* **2008**, *319* (2), 542–548.

(108) Ž, M. J. The Krafft Temperature of Surfactant Solutions. *Therm. Sci.* **2012**, *16* (12), 631–640.

(109) Vautier-giongo, C.; Bales, B. L. Estimate of the Ionization Degree of Ionic Micelles Based on Krafft Temperature. **2003**, 5398–5403.

(110) Rosen, M. J. *Surfactants and Interfacial Phenomena*, 3rd ed.; Wiley-Interscience: New Jersey, 2004.

(111) Standard Test Method for Evaluation of Wetting Agents by the Skein Test. *ASTM D2281-10*; ASTM International, West Conshohocken, PA, 2010.

(112) Rodriguez, C. H.; Lowery, L. H.; Scamehorn, J. F.; Harwell, J. H. Kinetics of Precipitation of Surfactants. I. Anionic Surfactants with Calcium and with Cationic Surfactants. *J. Surfactants Deterg.* **2001**, *4* (1), 1–14.

(113) Rodriguez, C. H.; Chintanasathien, C.; Scamehorn, J. F.; Saiwan, C.; Chavadej, S. Precipitation in Solutions Containing Mixtures of Synthetic Anionic Surfactant and Soap. I. Effect of Sodium Octanoate on Hardness Tolerance of Sodium Dodecyl Sulfate. *J. Surfactants Deterg.* **1998**, *1* (3), 321–328.

(114) H., R. C.; F., S. J. Kinetics of Precipitation of Surfactants. II. Anionic Surfactant Mixtures. *J. Surfactants Deterg.* **2001**, *4* (1), 15–26.

(115) Mihelj, T.; Tomašić, V.; Biliškov, N.; Liu, F. Temperature-Dependent IR Spectroscopic and Structural Study of 18-Crown-6 Chelating Ligand in the Complexation with Sodium Surfactant Salts and Potassium Picrate. *Spectrochim. Acta Part A Mol. Biomol. Spectrosc.* **2014**, *124*, 12–20.

(116) Barnes, G.; Gentle, I. *Interfacial Science: An Introduction*, 2nd ed.; Oxford University Press, 2011.

(117) Reduction of Surface and Interfacial Tension by Surfactants. In *Surfactants and Interfacial Phenomena*; Wiley-Blackwell, 2004; pp 208–242.

(118) Micelle Formation by Surfactants. In *Surfactants and Interfacial Phenomena*; Wiley-Blackwell, 2004; pp 105–177.

(119) Itri, R.; Amaral, L. Q. Distance Distribution Function of Sodium Dodecyl Sulfate Micelles by X-Ray Scattering. *J. Phys. Chem.* **1991**, *95* (1), 423–427.

(120) V., S. A.; I., S. D. GNOM– a Program Package for Small-angle Scattering Data Processing. *J. Appl. Crystallogr.* **2007**, *24* (5), 537–540.

(121) Gemini Surfactants. In *Surfactants and Interfacial Phenomena*; Wiley-Blackwell, 2004; pp 415–427.

(122) Holmberg, K. *Novel Surfactants: Preparation Applications And Biodegradability, Second Edition, Revised And Expanded*; CRC Press, 2003.

(123) J., B. K. Surfactant Biodegradation, Surfactant Science Series Vol. 3. Von R. D. Swisher. Marcel Dekker, Inc., New York 1970. XXIII, 496 S., Geb. $ 33.50. *Angew. Chemie 83* (8), 300.

(124) Paulo, A. M. S.; Aydin, R.; Dimitrov, M. R.; Vreeling, H.; Cavaleiro, A. J.; García-Encina, P. A.; Stams, A. J. M.; Plugge, C. M. Sodium Lauryl Ether Sulfate (SLES) Degradation by Nitrate-Reducing Bacteria. *Appl. Microbiol. Biotechnol.* **2017**, *101* (12), 5163–5173.

(125) Kamal, M. S. A Review of Gemini Surfactants: Potential Application in Enhanced Oil Recovery. *J. Surfactants Deterg.* **2016**, *19* (2), 223–236.

(126) Menger, F. M.; Littau, C. A. Gemini Surfactants: A New Class of Self-Assembling Molecules. *J. Am. Chem. Soc.* **1993**, *115* (22), 10083–10090.

(127) SHUKLA, D.; TYAGI, V. K. ANIONIC GEMINI SURFACTANTS: SYNTHESIS AND SURFACE ACTIVE PROPERTIES. *Surf. Rev. Lett.* **2007**, *14* (5), 991–997.

(128) Kumar, N.; Tyagi, R. Industrial Applications of Dimeric Surfactants: A Review. *J. Dispers. Sci. Technol.* **2014**, *35* (2), 205–214.

(129) J., K. M.; J., B. D.; J., H. C. The Power of Thiol-ene Chemistry. *J. Polym. Sci. Part A Polym. Chem. 48* (4), 743–750.

(130) E., H. C.; N., B. C. Thiol–Ene Click Chemistry. *Angew. Chemie Int. Ed. 49* (9), 1540–1573.

(131) Li, Y.; Su, H.; Feng, X.; Wang, Z.; Guo, K.; Wesdemiotis, C.; Fu, Q.; Cheng, S. Z. D.; Zhang, W.-B. Thiol-Michael "click" chemistry: Another Efficient Tool for Head Functionalization of Giant Surfactants. *Polym. Chem.* **2014**, *5* (21), 6151–6162.

(132) Procházková, D.; Zámostný, P.; Bejblová, M.; Červený, L.; Čejka, J. Hydrodeoxygenation of Aldehydes Catalyzed by Supported Palladium Catalysts. *Appl. Catal. A Gen.* **2007**, *332* (1), 56–64.

(133) Mingming, L.; Jiang, D.; Yikai, L.; Yong, W. Efficient Catalytic Hydrodeoxygenation of Aromatic Carbonyls over a Nitrogen-Doped Hierarchical Porous Carbon Supported Nickel Catalyst. *ChemistrySelect* **2017**, *2* (27), 8486–8492.

(134) Database of Zeolite Structures http://www.iza-structure.org/databases/.

(135) Roberts, R. M.; Khalaf, A. A. *Friedel-Crafts Alkylation Chemistry : A Century of Discovery*; M. Dekker: New York, 1984.

(136) Friedel-Crafts Alkylation. In *Comprehensive Organic Name Reactions and Reagents*; American Cancer Society, 2010; pp 1131–1136.

(137) Gold, V. The Hydrolysis of Acetic Anhydride. *Trans. Faraday Soc.* **1948**, *44* (0), 506–518.

(138) Yati, I.; Yeom, M.; Choi, J.-W.; Choo, H.; Suh, D. J.; Ha, J.-M. Water-Promoted Selective Heterogeneous Catalytic Trimerization of Xylose-Derived 2-Methylfuran to Diesel Precursors. *Appl. Catal. A Gen.* **2015**, *495*, 200–205.

(139) McKee, C. Catalytic Mechanisms. II. Eley, Rideal et Al. *Appl. Catal. A Gen.* **1995**, *122* (1), N2–N3.

(140) Kresnawahjuesa, O.; Gorte, R. J.; White, D. Characterization of Acylating Intermediates Formed on H-ZSM-5. *J. Mol. Catal. A Chem.* **2004**, *208* (1), 175–185.

(141) Cheung, P.; Bhan, A.; Sunley, G. J.; Law, D. J.; Iglesia, E. Site Requirements and Elementary Steps in Dimethyl Ether Carbonylation Catalyzed by Acidic Zeolites. *J. Catal.* **2007**, *245* (1), 110–123.

(142) Gumidyala, A.; Sooknoi, T.; Crossley, S. Selective Ketonization of Acetic Acid over HZSM-5: The Importance of Acyl Species and the Influence of Water. *J. Catal.* **2016**, *340*, 76–84.

(143) Gumidyala, A.; Wang, B.; Crossley, S. Direct Carbon-Carbon Coupling of Furanics with Acetic Acid over Brønsted Zeolites. *Sci. Adv.* **2016**, *2* (9).

(144) Corma, A.; JoséCliment, M.; García, H.; Primo, J. Design of Synthetic Zeolites as Catalysts in Organic Reactions: Acylation of Anisole by Acyl Chlorides or Carboxylic Acids Over Acid Zeolites. *Appl. Catal.* **1989**, *49* (1), 109–123.

(145) Corma, A. Inorganic Solid Acids and Their Use in Acid-Catalyzed Hydrocarbon Reactions. *Chem. Rev.* **1995**, *95* (3), 559–614.

(146) Bonati, M. L. M.; Joyner, R. W.; Stockenhuber, M. A Temperature Programmed Desorption Study of the Interaction of Acetic Anhydride with Zeolite Beta (BEA). *Catal. Today* **2003**, *81* (4), 653–658.

(147) Bonati, M. L. M.; Joyner, R. W.; Paine, G. S.; Stockenhuber, M. Adsorption Studies of Acylation Reagents and Products on Zeolite Beta Catalysts. In *Recent Advances in the Science and Technology of Zeolites and Related Materials*; van Steen, E., Claeys, M., Callanan, L. H. B. T.-S. in S. S. and C., Eds.; Elsevier, 2004; Vol. 154, pp 2724–2730.

(148) Bonati, M. L. M.; Joyner, R. W.; Stockenhuber, M. On the Mechanism of Aromatic Acylation over Zeolites. *Microporous Mesoporous Mater.* **2007**, *104* (1), 217–224.

(149) Wojciechowski, B. W.; Rice, N. M. 1 - Reactor Types and Their Characteristics BT - Experimental Methods in Kinetic Studies; Elsevier Science: Amsterdam, 2003; pp 5–19.